國 立 交 通 大 學

機械工程學系

碩士論文

Ge-Ku-van der Pol 系統及 Sprott 22 系統

的渾沌與渾沌同步

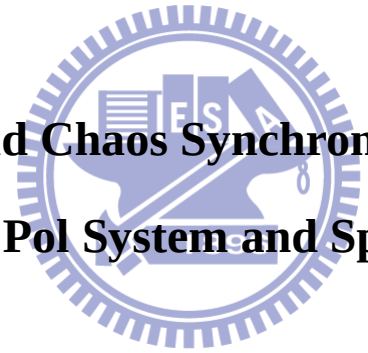

Chaos and Chaos Synchronization of

Ge-Ku-van der Pol System and Sprott 22 Systems

研 究 生：蔡尚恩

指導教授：戈正銘　教授

中華民國九十九年六月

Ge-Ku-van der Pol 系統及 Sprott 22 系統的渾沌與渾沌同步

Chaos and Chaos Synchronization of Ge-Ku-van der Pol System and Sprott 22 Systems

研究生：蔡尚恩　　Student: Shang-En Tsai

指導教授：戈正銘　　Advisor: Zheng-Ming Ge

國 立 交 通 大 學

機 械 工 程 學 系

碩 士 論 文

A Thesis

Submitted to Department of Mechanical Engineering

College of Engineering

National Chiao Tung University

In Partial Fulfillment of the Requirement

For the Degree of master of science

In

Mechanical Engineering

June 2010

Hsinchu, Taiwan, Republic of China

中華民國九十九年六月

Ge-Ku-van der Pol 系統及 Sprott 22 系統的渾沌與渾沌同步

學生：蔡尚恩　　指導教授：戈正銘

國 立 交 通 大 學

機 械 工 程 學 系

摘要

本篇論文以相圖、龐卡萊映射圖、李亞普洛夫指數以及分歧圖等數值方法研究新 Ge-Ku-van der Pol 系統的渾沌現象。對此系統應用部分區域穩定性理論和實用漸進穩定理論來達成廣義同步；應用主動控制獲得雙重及多重渾沌交織同步。更進一步使用新模糊模型來研究 Sprott 22 系統的模糊模型化和渾沌同步。此外，將探討新模糊邏輯常數控制器應用在投影同步及含有不確定度的渾沌系統。在以上研究中，皆可由相圖和時間歷程圖得到驗證。

Chaos and Chaos Synchronization of Ge-Ku-van der Pol System and Sprott 22 Systems

Student：Shang- En Tsai **Advisor：Zheng-Ming Ge**

Department of Mechanical Engineering

National Chiao Tung University

Abstract

In this thesis, the chaotic behavior in new Ge-Ku-van der Pol system is studied by phase portraits, time history, Poincaré maps, Lyapunov exponent and bifurcation diagrams. A new kind of chaotic generalized synchronization, *different translation pragmatical generalized synchronization*, is obtained by pragmatical asymptotical stability theorem and partial region stability theory. Second new type for chaotic synchronization, *double and multiple symplectic synchronization*, are obtained by active control. A new method, using new fuzzy model, is studied for fuzzy modeling and synchronization of Sprott 22 systems. Moreover, the new fuzzy logic constant controller is studied for projective synchronization and chaotic system with uncertainty. Numerical analyses, such as phase portraits and time histories can be provided to verify the effectiveness in all above studies.

誌　謝

本篇碩士論文得以順利完成，首先感謝在研究過程中不斷給予耐心指導的老師　戈正銘榮譽教授。老師是我遇過最學識淵博、智慧超群的學者，不但在動力學、渾沌力學等等科學貢獻許多，在文學與哲學方面也有所鑽研。在詩詞方面註有「文革以來詩詞選及注解」之詩集，內有教授坎坷的過去與豐富的人生紀錄。在此碩士論文研究過程中，老師不但給予研究方向與專業領域的知識，而且當遇到困難時，也會適時的給予寶貴的意見，教導我作研究應有的態度，讓我學習到如何克服及解決問題的能力。此外，感謝老師不厭其煩的修改論文，才能使此碩士論文得以完整。

兩年的碩士研究生涯，感謝博士班的張晉銘與李士宇學長的細心指導，兩位學長不斷的將他們的研究經驗傳授給我，也在耐心且仔細的為我解答許多疑問，讓我在此研究領域的知識更為精進。碩士班的陳聰文、徐瑜韓、張育銘、陳志銘學長，在研究過程中，給予我珍貴的意見與鼓勵。同時也要感謝同學李泳厚、江振賓、王翔平不但在課業上幫忙許多，在這兩年的碩士班的互相扶持與成長，更是讓我留下許多難忘的記憶。

最終要感謝我的家人，感謝兩位優秀的哥哥成為我追逐的目標，也讓我在求學過程中有正確的方向。感謝親愛的老爸，在你眼裡不愛動頭腦的我，您依然呵護倍至，讓我在求學過程沒有擔憂。感謝親愛的老媽，在我研究所推甄失敗，鼓勵我重考且再次挑戰自己，過程中也不斷的一旁照料我的身體，讓我如願考上交通大學機械所。還有寶貝的大姊，感謝你總是那樣疼愛我，體諒我的忙碌，幫我照顧好家鄉的父母，十分的感謝。最後，感謝一位親密的朋友，在我推甄研究所失敗、重考與繁忙的碩士班研究日子裡，對我不離不棄，陪伴在我身邊鼓勵我，非常感謝。

Contents

List of Tables

List of Figures

Chapter 1

Introduction

Since Pecora and Carroll proposed the concept of chaotic synchronization [1] in 1990, chaos synchronization has become a hot subject in the field of nonlinear science due to its wide-spread potential application in various disciplines. The various types of synchronization, such as generalized synchronization [2-4], phase synchronization [5-7], lag synchronization [8-10], inverse synchronization [11-12], partially synchronization [13-14], Q-S synchronization [15-17], LMI-based synchronization [18], extended backstepping sliding mode controlling technique [19] and , projective synchronization [20-23] are investigated extensively in the past years.

In Chapter 2, we give the dynamic equations of a new Ge-Ku-van der Pol (GKv) [24] system and its chaotic behaviors are studied.

In Chapter 3, the symplectic synchronization [25] is expressed as $y = F(x, y, t)$, where x, y are the state vectors of the "master" and of the "slave", respectively. The final desired state y of the "slave" system not only depends upon the "master" system state x but also depends upon the "slave" system state y itself. Therefore the "slave" system is not a traditional pure "slave" obeying the "master" system completely but plays a role to determine the final desired state of the "slave" system. Since the "slave" y plays an interwined role, this type of synchronization is called symplectic synchronization, and call the "master" system Partner A, the slave system Partner B. We propose a new type of double symplectic synchronization, $G(x, y, t) = F(x, y, t)$. This idea is an extension of symplectic synchronization, $y = F(x, y, t)$. Due to the complexity of the form of the double symplectic synchronization, it may be applied to increase the security of secret communication. The Gkv system is used as an example system for double symplectic scheme, while the synchronization is

derived based on Barbalat's lemma [26] and active control.

Chaos generalized synchronization is a very important methodology, which has been studied to date extensively on chaotic dynamical systems described by real variables [27-29]. However, there also are many interesting cases involving complex variables which are scarcely explored. In Chapter 4 design different complex conjugate form to couple with Ge-Ku real variable nonlinear system [30-31], different chaotic behaviors appear. Chaos generalized synchronization is accomplished by applying pragmatical active control.

In current scheme of adaptive control of chaotic motion [32-37], the Babalat's lemma [26] is used to prove the error vector approaches zero, as time approaches infinity. But the question, why the estimated parameters also approach to the uncertain parameters, remains no answer.

In Chapter 5, a new chaos generalized synchronization strategy by different shift pragmatical synchronization [38-40] and stability theory of partial region [41-43] is proposed. By using the different shift pragmatical synchronization and stability theory of partial region, the Lyapunov function is a simple linear homogeneous function of error states and the controllers are more simple and have less simulation error because they are in lower degree than that of traditional controllers, for which the Lyapunov function is a quadratic form of error states, and the question of that why the estimated parameters also approach uncertain parameters can be answered strictly.

In Chapter 6, we propose a new strategy [44] to design simplest constant number controllers which achieve projective synchronization of uncertainty chaotic systems. Furthermore, in chaos synchronization, most publications often assume that the synchronization system is without external disturbances. However, in practical applications, it is hard to avoid external disturbances due to uncontrollable environmental conditions. The implementation of control inputs of practical systems

is frequently subject to uncertainties as a result of physical limitations. Thus, the derivation of a robust synchronization controller to resist the disturbance is an important problem.

In recent years, some chaos synchronizations based on fuzzy systems have been proposed since the fuzzy set theory was initiated by Zadeh [45]. The fuzzy logic control (FLC) scheme has been widely developed and successfully applied to many applications [44]. Yau and Shieh [46] proposed an amazing new idea in designing fuzzy logic controllers. The constructed fuzzy rules subject to a common Lyapunov function such that the master-slave chaos systems satisfy stability in the Lyapunov sense. In [46], there are two main controllers in their slave system. One is used in elimination of nonlinear terms and the another is built by fuzzy rules subjected to a common Lyapunov function. Therefore the resulting controllers are in nonlinear form. In [46], the regular form is necessary. In order to carry out the new method, the original system must to be transformed into their regular form.

In this Chapter, a simplest fuzzy logic constant controller (FLCC) which is derived via fuzzy logic design and Lyapunov direct method is presented for projective synchronization of non-autonomous chaotic systems with uncertain and stochastic disturbances. The constant numbers in controllers are decided by the upper bound and the lower bound of the error derivatives. Use this fuzzy logic constant controller (FLCC) approach, a simplest controller, i.e. constant controller, can be obtained and the difficulty in realization of complicated controllers in chaos synchronization by Lyapunov direct method can be also coped. Different form conventional approaches, the resulting control law has less maximum magnitude of the instantaneous control command and it can reduce the actuator saturation phenomenon in real physical system.

In Chapter 7, a newfangled fuzzy model is used to simulate and synchronize

GKv system, extended GKv system and Ge-Ku-Mathieu (GKM) system. In recent years, fuzzy logic proposed by L. A. Zadeh [45] has received much attention as a powerful tool for the nonlinear control. Among various kinds of fuzzy methods, Takagi-Sugeno fuzzy (T-S fuzzy) system is widely accepted as a useful tool for design and analysis of fuzzy control system [47-51]. Currently, some chaos control and synchronization based on T-S fuzzy systems have been proposed, such as fuzzy sliding mode controlling technique [52-54], LMI-based synchronization [55-57] and robust control [58]. These researches all focus on two identical nonlinear systems. Furthermore, two different nonlinear systems may have different numbers of nonlinear terms. It causes different numbers of linear subsystems. For synchronization of two different nonlinear systems, the traditional method using the idea of PDC to design the fuzzy control law for stabilization of the error dynamics can not be used here, since the number of subsystems becomes very large.

In this Chapter, the newfangled fuzzy model is proposed. In traditional Takagi-Sugeno fuzzy model (T-S fuzzy model) [47], the process of fuzzy modeling focus on the whole system. Therefore, there will be linear subsystems (according to fuzzy rules) and equations in the T-S fuzzy system, where N is the number of nonlinear terms and m is the order of the system. If N is large, the number of linear subsystems in T-S fuzzy system is huge. It becomes more inefficient and complicated.

In Ge-Li fuzzy model (G-L fuzzy model) [59], we focus on each equation of the system. The numbers of fuzzy rules can be reduced from 2^N to $2\times N$. The fuzzy equations become much simpler. However, the limitation of G-L fuzzy model is that there should be one nonlinear terms in each equation. Consequently, the newfangled fuzzy model is proposed to solve this defect—all nonlinear terms in each equation will be treated as one nonlinear term. It can be used to model various kinds of complex nonlinear systems, even if the nonlinear terms are copious and complicated.

Ge-Ku-van der Pol (GKv) systems and Ge-Ku-Mathieu (GKM) system are illustrated in numerical simulations to show the effectiveness and feasibility of new model. And in Chapter 8, conclusions are drawn.

Chapter 2

Chaos of a New Ge-Ku-van der Pol System

2.1 Preliminary

In this Chapter, the chaotic behaviors of a new Ge-Ku-van der Pol (GKv) system is studied numerically by phase portraits, time histories, Poincaré maps, Lyapunov exponents, and bifurcation diagrams.

2.2 Description of New GKv System

Ge and Ku [24] gave a chaotic system formed by simple pendulum with its pivot rotating about an axis as Fig 2.1. This chaotic system is

$$\begin{cases} \dot{x}_1 = x_2 \\ \dot{x}_2 = -a_1 x_2 - \sin x_1 (b_1 (c_1 + \cos x_1) + d_1 \sin \omega t) \end{cases} \tag{2.1}$$

where a_1, b_1, c_1, d_1 are parameters. After simplification $\sin(x_1) = x_1$, $\cos(x_1) = 1 - \frac{x_1^2}{2}$ addition of coupling terms, combining with van-der-Pol equation

$$\begin{cases} \dot{x}_3 = x_4 \\ \dot{x}_4 = -g_1 x_3 - h_1 (1 - x_3^2) x_4 - l_1 \sin(\Omega t) \end{cases} \tag{2.2}$$

where g_1, h_1, l_1 are parameters and $\sin(\Omega t)$ is substuted by x_3, we get the Gkv system

$$\begin{cases} \dot{x}_1 = x_2 \\ \dot{x}_2 = -a x_2 - x_3 (b(c - x_1^2) + d x_3) \\ \dot{x}_3 = -g x_3 + h(1 - x_3^2) x_2 + l x_1 \end{cases} \tag{2.3}$$

where a, b, c, d, g, h, l are parameters.

2.3 Computational Analysis of a New GKv System

For numerical analysis of computation, this system exhibits chaos when the parameters of system are $a = 0.08, b = -0.35, c = 100.56, d = -1000.02, g = 0.61, h = 0.08, l = 0.01$ and the initial states of system are $x_1(0) = 0.01, x_2(0) = 0.01, x_3(0) = 0.01$. The bifurcation diagram by changing damping parameter a is shown in Fig. 2.2. Its

corresponding Lyapunov exponents are shown in Fig. 2.3. The phase portraits, time histories, and Poincaré maps of the systems are showed in Fig. 2.4~Fig. 2.8.When a=0.206572, period 1 phenomena are shown in Fig. 2.4. When a=0.216232, period 2 phenomena are shown in Fig. 2.5. When a=0.218164, period 4 phenomena are shown in Fig. 2.6. When a=0.21913, period 8 phenomena are shown in Fig. 2.7.When a=0.08, the chaotic behaviors and time histories are given in Fig. 2.8 and Fig. 2.9.

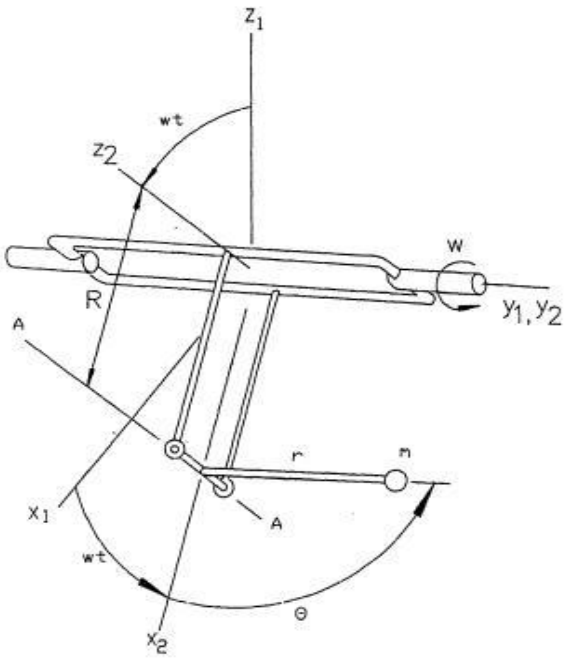

Fig 2.1. The pendulum on rotating arm.

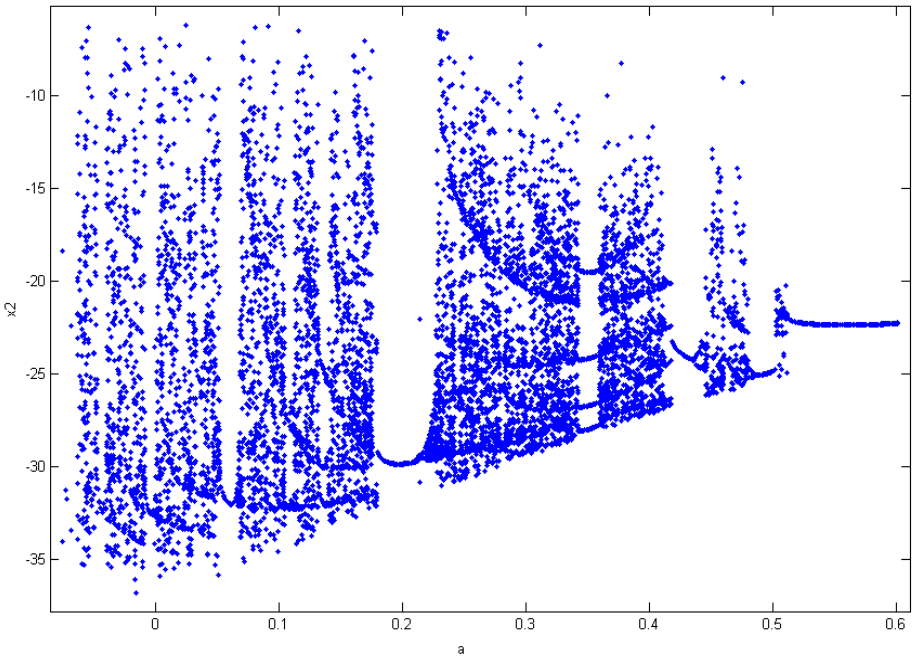

Fig. 2.2 The bifurcation diagram for new GKv system.

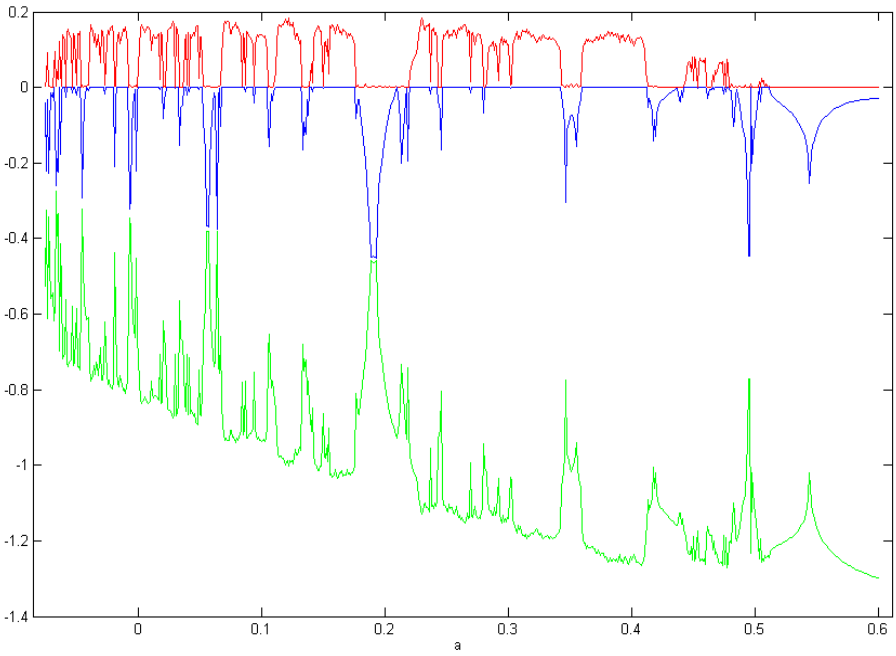

Fig. 2.3 The Lyapunov exponents for new GKv system.

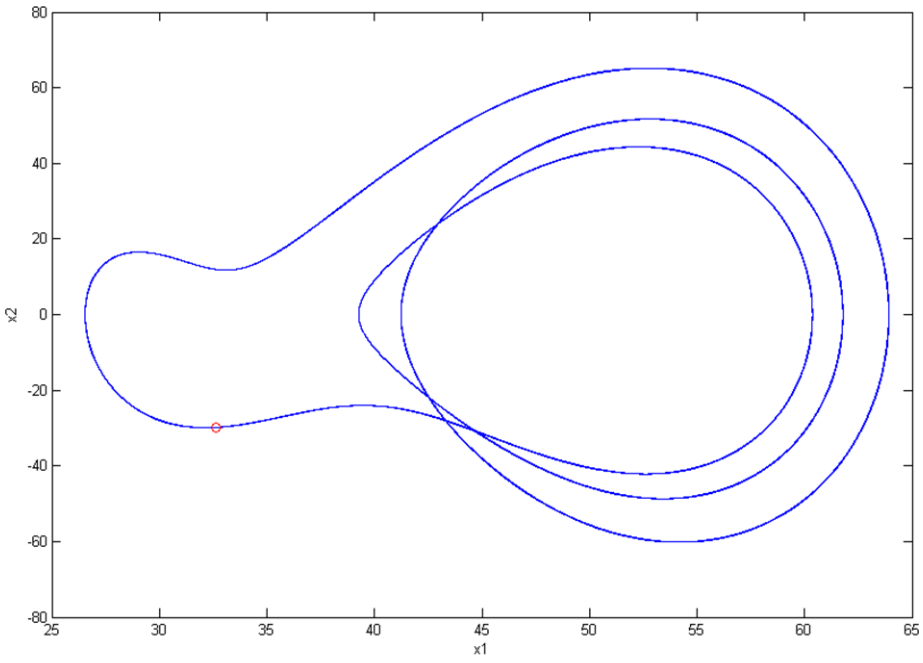

Fig. 2.4 Phase portrait and Poincaré maps for new GKv system with a=0.206572 (period 1).

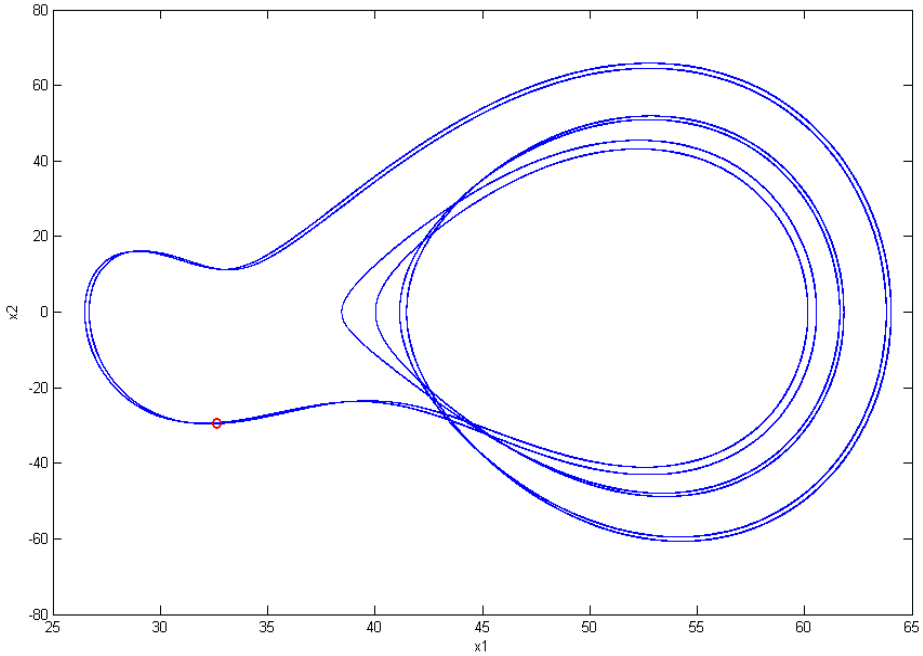

Fig. 2.5 Phase portrait and Poincaré maps for new GKv system with a=0.216232 (period 2).

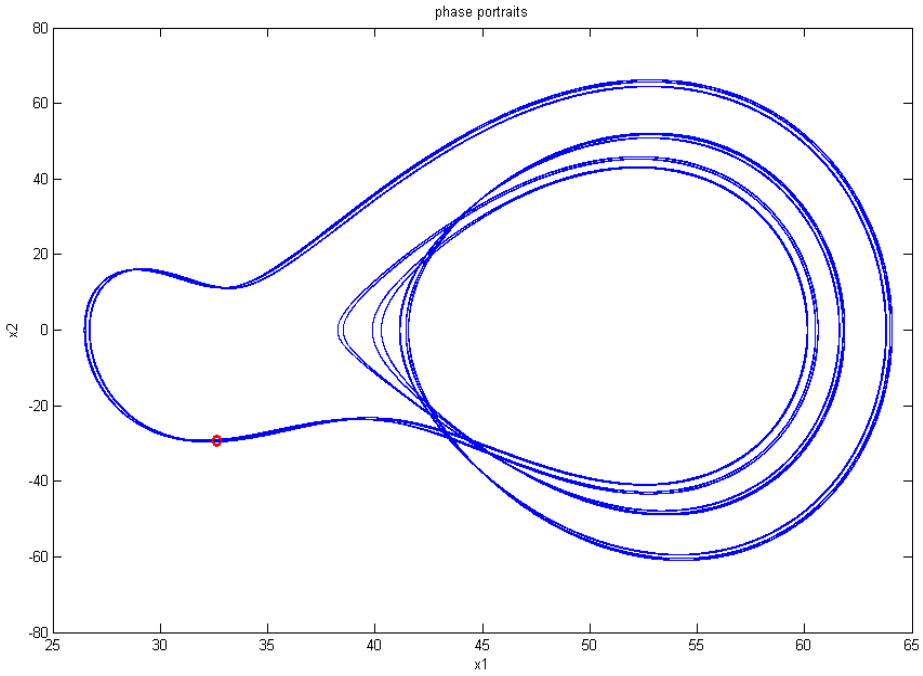

Fig. 2.6 Phase portrait and Poincaré maps for new GKv system with a=0.218164 (period 4).

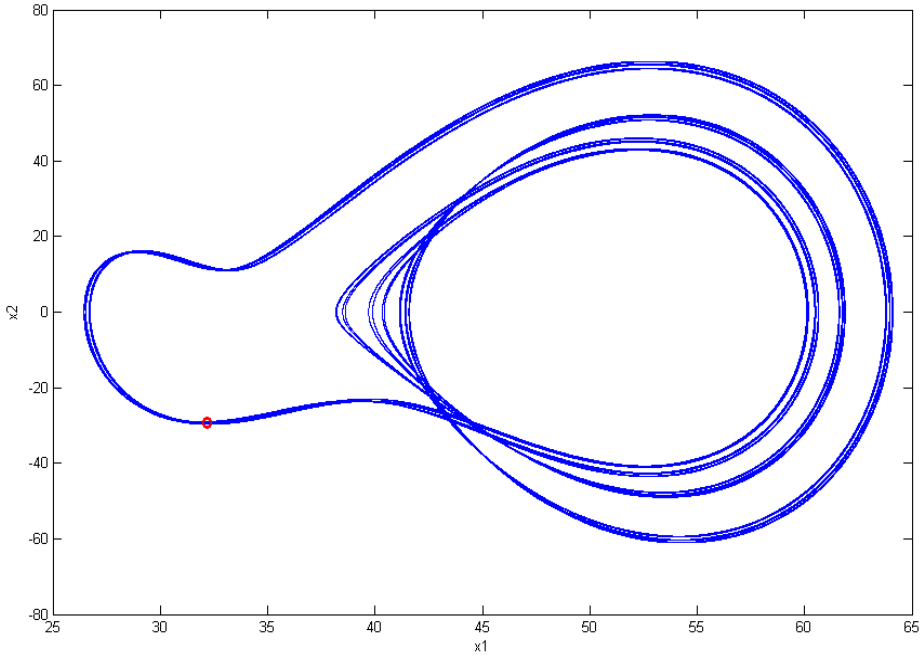

Fig. 2.7 Phase portrait and Poincaré maps for new GKv system with a=0.21913 (period 8).

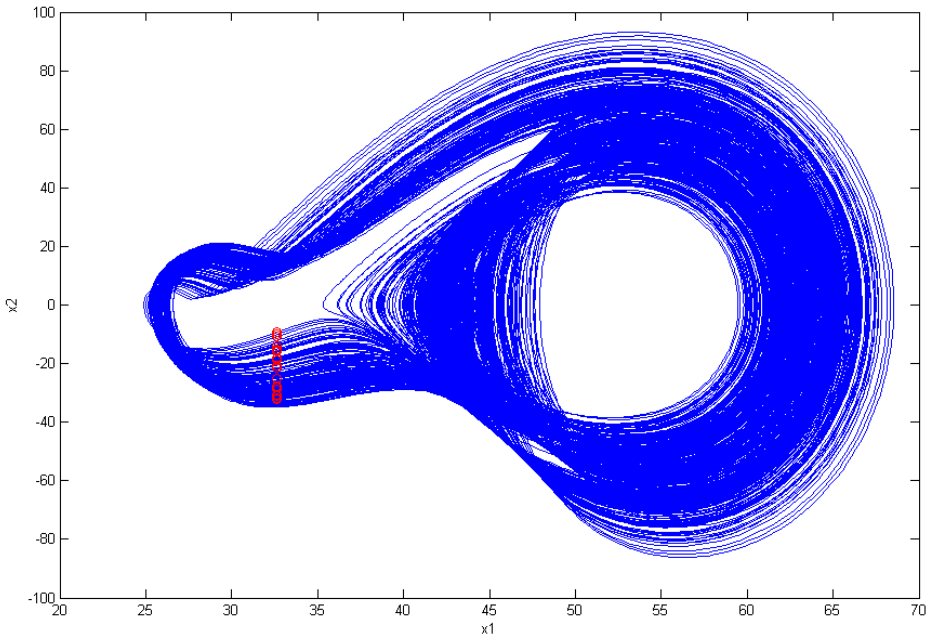

Fig. 2.8 Phase portrait and Poincaré maps for new GKv system with a=0.08 (chaos).

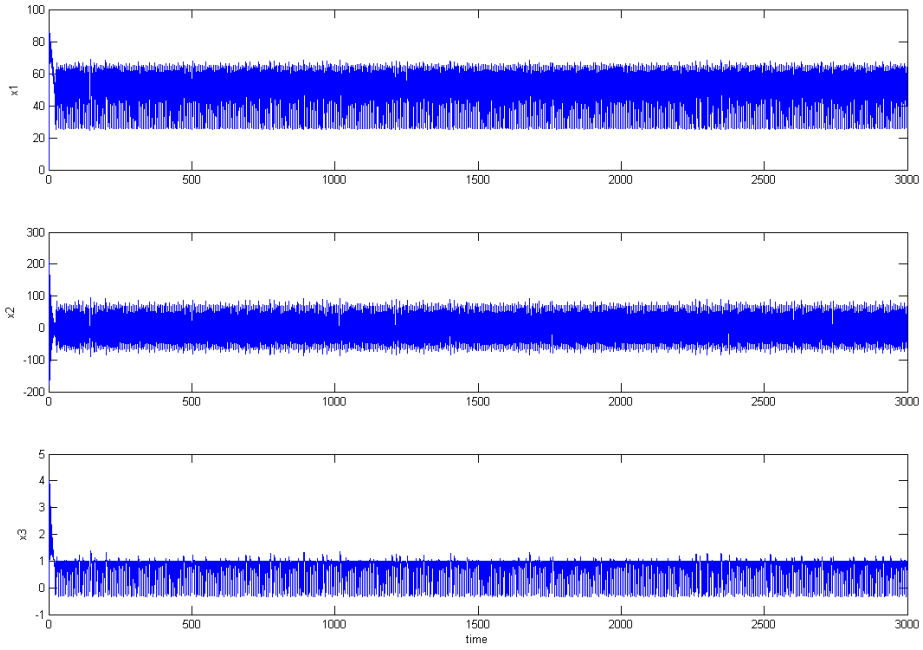

Fig. 2.9 Time histories for new GKv system with a=0.08 (chaos).

Chapter 3

Double Symplectic Synchronization for Ge-Ku-van-der-Pol system

3.1 Preliminary

In this Chapter, a new double symplectic synchronization of chaotic system is studied. The chaotic system studied is a new GKv system. Double symplectic synchronization is an extension of symplectic synchronization, $\mathbf{y} = \mathbf{F}(\mathbf{x}, \mathbf{y}, t)$. Since the symplectic functions are presented at both sides of the equality, it is called double symplectic synchronization $\mathbf{G}(\mathbf{x}, \mathbf{y}, t) = \mathbf{F}(\mathbf{x}, \mathbf{y}, t)$. The double symplectic synchronization is accomplished based on Barbalat's lemma and active control. Numerical simulations are given to show that the proposed scheme is applied successfully to both autonomous and non-autonomous chaotic systems.

3.2 Double Symplectic Synchronization Scheme

Consider two different nonlinear chaotic systems, Partner A and Partner B, described by

$$\dot{\mathbf{x}} = \mathbf{f}(\mathbf{x}, t), \tag{3.1}$$

$$\dot{\mathbf{y}} = \mathbf{C}(t)\mathbf{y} + \mathbf{g}(\mathbf{y}, t) + \mathbf{u}, \tag{3.2}$$

where $\mathbf{x} = [x_1, x_2, \ldots, x_n]^{\mathrm{T}} \in R^n$ and $\mathbf{y} = [y_1, y_2, \ldots, y_n]^{\mathrm{T}} \in R^n$ are the state vectors of Partner A and Partner B, $\mathbf{C} \in R^{n \times n}$ is a give matrix, $\mathbf{f}$ and $\mathbf{g}$ are continuous nonlinear vector functions, and $\mathbf{u}$ is the controller. Our goal is to design the controller $\mathbf{u}$ such that $\mathbf{G}(\mathbf{x}, \mathbf{y}, t)$ asymptotically approaches $\mathbf{F}(\mathbf{x}, \mathbf{y}, t)$, where $\mathbf{G}(\mathbf{x}, \mathbf{y}, t)$ and $\mathbf{F}(\mathbf{x}, \mathbf{y}, t)$ are two given functions. For simplicity we take $\mathbf{G}(\mathbf{x}, \mathbf{y}, t) = \mathbf{x} + \mathbf{y}$ and $\mathbf{F}$ is a continuous nonlinear vector function.

Property [24]: An $m \times n$ matrix A of real elements defines a linear mapping $y = Ax$ from R^n into R^m, and the induced p-norm of A for $p = 1, 2,$ and ∞ is given by

$$\|A\|_1 = \max_j \sum_{i=1}^{m} |a_{ij}|, \quad \|A\|_2 = \left[\lambda_{\max}(A^{\mathrm{T}}A)\right]^{1/2}, \quad \|A\|_\infty = \max_i \sum_{j=1}^{n} |a_{ij}|. \tag{3.3}$$

The useful property of induced matrix norms for real matrix A is as follow:

$$\|A\|_2 \le \sqrt{\|A\|_1 \|A\|_\infty} \tag{3.4}$$

Theorem 1 : For chaotic systems of Partner A (3.1) and of Partner B (3.2), if the controller $\mathbf{u}$ is designed as

$$\begin{aligned} \mathbf{u} = (\mathbf{I} - \mathbf{D}_{\mathbf{y}}\mathbf{F})^{-1} [& \mathbf{D}_{\mathbf{x}}\mathbf{F}(\mathbf{f}(\mathbf{x}, t) + \mathbf{C}(t)(\mathbf{x} - \mathbf{F})) + \mathbf{D}_{\mathbf{y}}\mathbf{F}(\mathbf{g}(\mathbf{y}, t) + \mathbf{C}(t)(\mathbf{y} - \mathbf{F})) - \mathbf{D}_t\mathbf{F} - (\mathbf{f}(\mathbf{x}, t) \\ & + \mathbf{C}(t)(\mathbf{x} - \mathbf{F})) - \mathbf{K}(\mathbf{x} - \mathbf{y} - \mathbf{F})], \end{aligned} \tag{3.5}$$

where $\mathbf{D}_{\mathbf{x}}\mathbf{F}$, $\mathbf{D}_{\mathbf{y}}\mathbf{F}$, $\mathbf{D}_t\mathbf{F}$ are the Jacobian matrices of $\mathbf{F}(\mathbf{x}, \mathbf{y}, t)$, $\mathbf{K} = \mathrm{diag}(k_1, k_2, \ldots, k_m)$, and satisfies

$$\frac{\min(k_i)}{\|\mathbf{C}(t)\|} > 1, \tag{3.6}$$

then the double symplectic synchronization will be achieved.

Proof: Define the error vectors as

$$\mathbf{e} = \mathbf{x} + \mathbf{y} - \mathbf{F}(\mathbf{x}, t, \mathbf{y}), \tag{3.7}$$

then the following error dynamics can be obtained by introducing the designed controller

$$\begin{aligned} \frac{d\mathbf{e}}{dt} = \dot{\mathbf{e}} &= \dot{\mathbf{x}} + \dot{\mathbf{y}} - \mathbf{D}_{\mathbf{x}}\mathbf{F}\dot{\mathbf{x}} - \mathbf{D}_{\mathbf{y}}\mathbf{F}\dot{\mathbf{y}} - \mathbf{D}_t\mathbf{F} \\ &= \mathbf{f}(\mathbf{x}, t) + \mathbf{C}(t)(\mathbf{y}) + \mathbf{g}(\mathbf{y}, t) - \mathbf{D}_{\mathbf{x}}\mathbf{F}(\mathbf{f}(\mathbf{x}, t) + \mathbf{C}(t)(\mathbf{y})) - \mathbf{D}_{\mathbf{y}}\mathbf{F}(\mathbf{g}(\mathbf{y}, t) + \mathbf{C}(t)(\mathbf{y})) - \mathbf{D}_t\mathbf{F}, \\ &\quad + (\mathbf{I} - \mathbf{D}_{\mathbf{y}}\mathbf{F})\mathbf{u} \\ &= (\mathbf{C}(t) - \mathbf{K})\mathbf{e} \end{aligned} \tag{3.8}$$

Choose a positive definite Lyapunov function of the form

$$V(t)=\frac{1}{2}\mathbf{e}^{\mathrm{T}}\mathbf{e} \tag{3.9}$$

Taking the time derivative of $V(t)$ along the trajectory of Eq. (3.8), we have

$$\begin{aligned}\dot{V}(t)&=\mathbf{e}^{\mathrm{T}}\dot{\mathbf{e}}\\&=\mathbf{e}^{\mathrm{T}}\mathbf{C}(t)\mathbf{e}-\mathbf{e}^{\mathrm{T}}\mathbf{K}\mathbf{e}\\&\le\|\mathbf{C}(t)\|\cdot\|\mathbf{e}\|^{2}-\min(k_i)\|\mathbf{e}\|^{2}\\&=(\|\mathbf{C}(t)\|-\min(k_i))\|\mathbf{e}\|^{2}\end{aligned} \tag{3.10}$$

Since $M=\min(k_i)-\|\mathbf{C}(t)\|>0$, then $\dot{V}(t)\le -M\|\mathbf{e}\|^{2}=-2MV(t)$. Therefore, it can be obtained that

$$V(t)\le V(0)e^{-2Mt} \tag{3.11}$$

and $\lim_{t\to\infty}\int_0^t|V(\xi)|d\xi$ is bounded. Besides, $V(t)$ is uniformly continuous. According to Barbalat's lemma [26], the conclusion can be drawn that $\lim_{t\to\infty}V(t)=0$, i.e. $\lim_{t\to\infty}\|\mathbf{e}(t)\|=0$. Thus, the double symplectic synchronization can be achieved asymptotically.

3.3 Synchronization of Two Different New Chaotic Systems

Case 1.

Consider a new Ge-Ku-Duffing(GKD) system as Partner A described by

$$\begin{cases}\dot{x}_1=x_2\\ \dot{x}_2=-ax_2-x_1\left[b\ \ c-x_1^{\ 2}\ +dx_3\right]\\ \dot{x}_3=-x_3-x_3^{\ 3}-fx_2+gx_1\end{cases} \tag{3.12}$$

where $a=0.1, b=1, c=40, d=54, f=6, g=30$ and the initial conditions are $x_1(0)=2,\ x_2(0)=2.4,\ x_3(0)=5$. Eq. (3.12) can be rewritten in the form of Eq. (3.1),

where $\mathbf{f}(x,t)=\begin{bmatrix} x_2 \\ -ax_2 - x_1\left[b\ \ c-x_1^{\ 2}\ +dx_3\right] \\ -x_3 - x_3^{\ 3} - fx_2 + gx_1 \end{bmatrix}$.

The chaotic attractor of the new GKD system is shown in Fig. 3.1.

The controlled GKv system is considered as Partner B described by

$$\begin{cases} \dot{y}_1 = y_2 + u_1 \\ \dot{y}_2 = -my_2 - y_3\left[n\ \ v-y_1^{\ 2}\ + py_3\right] + u_2 \\ \dot{y}_3 = -qy_3 + r\ \ 1-y_3^{\ 2}\ \ y_2 + sy_1 + u_3 \end{cases} \tag{3.13}$$

where $m=0.08, n=-0.35, v=100.56, p=-1000.02, q=0.61, r=0.08, s=0.01$, $\mathbf{u}=u_1,u_2,u_3^{\ \mathrm{T}}$ is the controller, and the initial conditions are $y_1(0)=5.2$, $y_2(0)=50$, $y_3(0)=4.5$. The chaotic attractor of uncontrolled new GKv system is shown in Fig. 3.2. The Eq. (3.13) can be rewritten in the form of Eq. (3.2), where $\mathbf{C}(t)=\begin{bmatrix} 0 & 1 & 0 \\ 0 & -m & -nv \\ s & r & -q \end{bmatrix}$ and $\mathbf{g}(y,t)=\begin{bmatrix} 0 \\ ny_1^{\ 2}y_3 - yx_3^{\ 2} \\ -ry_2y_3^{\ 2} \end{bmatrix}$.

By applying **Property 1**, it is derived that $\|\mathbf{C}(t)\|_1=-nv-q$, $\|\mathbf{C}(t)\|_\infty=-m-nv$, and $\|\mathbf{C}(t)\|_2 \le \sqrt{-nv-q\ \ (-m-nv)}=\sqrt{1214.52}$. Then $\|\mathbf{C}(t)\|=34$ is estimated.

Define $\mathbf{F}(\mathbf{x},\mathbf{y},t)=\begin{bmatrix} x_1\sin y_1 \\ x_2\sin y_2 \\ x_3\sin y_3 \end{bmatrix}$, and our goal is to achieve the double symplectic synchronization $\mathbf{x}+\mathbf{y}=\mathbf{F}(\mathbf{x},\mathbf{y},t)$. According to Theorem, the inequality $\frac{\min(k_i)}{\|\mathbf{C}(t)\|}>1$ must be satisfied. It can be obtained that $\min(k_i)>34$. Thus we choose $\mathbf{K}=\begin{bmatrix} k_1 & 0 & 0 \\ 0 & k_2 & 0 \\ 0 & 0 & k_3 \end{bmatrix}=\begin{bmatrix} 35 & 0 & 0 \\ 0 & 36 & 0 \\ 0 & 0 & 37 \end{bmatrix}$ and design the controller as

$$\begin{cases} u_1 = x_2 \sin y_1 + x_1 y_2 \cos y_1 - x_2 - y_2 + x_1 \sin y_1 - x_1 - y_1 \\ u_2 = \ -ax_2 - x_1\left[b\ \ c - x_1^{\ 2}\ + dx_3\right]\ (\sin y_2 - 1) + x_2 \cos(y_2) \\ \qquad -my_2 - y_3\left[n\ \ v - y_1^{\ 2}\ + py_3\right]\ -\ -my_2 - y_3\left[n\ \ v - y_1^{\ 2}\ + py_3\right] \\ \qquad + x_2 \sin y_2 - x_2 - y_2 \\ u_3 = (-x_3 - x_3^{\ 3} - fx_2 + gx_1)(\sin y_3 - 1) + x_3 \cos(y_3) \\ \qquad \left[-qy_3 - r(1 - y_3^{\ 2})y_2 + sy_1\right] - \left[-qy_3 - r(1 - y_3^{\ 2})y_2 + sy_1\right] \\ \qquad + x_3 \sin y_3 - x_3 - y_3 \end{cases} \tag{3.14}$$

The theorem is satisfied and the double symplectic synchronization is achieved. The chaotic attractor of the controlled GKv system is shown in Fig. 3.3, the time histories of double symplectic synchronization and the time histories of the state errors are shown in Fig. 3.4 and Fig. 3.5 respectively.

Case 2.

Consider a new Double Ge-Ku(DGK) system as Partner A described by

$$\begin{cases} \dot{x}_1 = x_2 \\ \dot{x}_2 = -ax_2 - x_1\left[b\ \ c - x_1^{\ 2}\ + dx_3\right] \\ \dot{x}_3 = -ax_3 - x_3\left[b\ \ c - x_3^{\ 2}\ + ex_1\right] \end{cases} \tag{3.15}$$

where $a = -0.5, b = -1.4, c = 1.9, d = -4.5, e = 6.2$ and the initial conditions are $x_1(0) = 0.01,\ x_2(0) = 0.01,\ x_3(0) = 0.01$. Eq. (3.15) can be rewritten in the form of Eq. (3.1), where $\mathbf{f}(x,t) = \begin{bmatrix} x_2 \\ -ax_2 - x_1\left[b\ \ c - x_1^{\ 2}\ + dx_3\right] \\ -ax_3 - x_3\left[b\ \ c - x_3^{\ 2}\ + ex_1\right] \end{bmatrix}$. The chaotic attractor of the new DGK system is shown in Fig. 3.6.

The controlled GKv system is considered as Partner B described by

$$\begin{cases} \dot{y}_1 = y_2 + u_1 \\ \dot{y}_2 = -my_2 - y_3\left[n\ \ v - y_1^{\ 2}\ \ + py_3\right] + u_2 \\ \dot{y}_3 = -qy_3 + r\ \ 1 - y_3^{\ 2}\ \ y_2 + sy_1 + u_3 \end{cases} \tag{3.16}$$

where $m = 0.08, n = -0.35, v = 100.56, p = -1000.02, q = 0.61, r = 0.08, s = 0.01$, $\mathbf{u} = u_1, u_2, u_3^{\ \mathrm{T}}$ is the controller, and the initial conditions are $y_1(0) = 10$, $y_2(0) = 7$, $y_3(0) = 10$. Eq. (3.16) can be rewritten in the form of Eq. (3.2), where $\mathbf{C}(t) = \begin{bmatrix} 0 & 1 & 0 \\ 0 & -m & -nv \\ s & r & -q \end{bmatrix}$ and $\mathbf{g}(y,t) = \begin{bmatrix} 0 \\ ny_1^{\ 2}y_3 - yx_3^{\ 2} \\ -ry_2y_3^{\ 2} \end{bmatrix}$.

By applying **Property 1**, it can be derived that $\|\mathbf{C}(t)\|_1 = -nv - q$, $\|\mathbf{C}(t)\|_\infty = -m - nv$, and $\|\mathbf{C}(t)\|_2 \le \sqrt{-nv - q\ \ (-m - nv)} = \sqrt{1214.52}$. Then $\|\mathbf{C}(t)\| = 34$ is estimated.

Define $\mathbf{F}(\mathbf{x},\mathbf{y},t) = \begin{bmatrix} x_1 \sin y_1 \\ x_2 \sin y_2 \\ x_3 \sin y_3 \end{bmatrix}$, and our goal is to achieve the double symplectic synchronization $\mathbf{x} + \mathbf{y} = \mathbf{F}(\mathbf{x},\mathbf{y},t)$. According to Theorem, the inequality $\frac{\min(k_i)}{\|\mathbf{C}(t)\|} > 1$ must be satisfied. It can be obtained that $\min(k_i) > 34$. Thus we choose $\mathbf{K} = \begin{bmatrix} k_1 & 0 & 0 \\ 0 & k_2 & 0 \\ 0 & 0 & k_3 \end{bmatrix} = \begin{bmatrix} 35 & 0 & 0 \\ 0 & 36 & 0 \\ 0 & 0 & 37 \end{bmatrix}$ and design the controller as

$$\begin{cases} u_1 = x_2 \sin y_1 + x_1 y_2 \cos y_1 - x_2 - y_2 + x_1 \sin y_1 - x_1 - y_1 \\ u_2 = \ -ax_2 - x_1\left[b\ \ c - x_1^{\ 2}\ + dx_3\right]\ (\sin y_2 - 1) + x_2 \cos(y_2) \\ \qquad -my_2 - y_3\left[n\ \ v - y_1^{\ 2}\ + py_3\right]\ -\ -my_2 - y_3\left[n\ \ v - y_1^{\ 2}\ + py_3\right] \\ \qquad + x_2 \sin y_2 - x_2 - y_2 \\ u_3 = \ -ax_3 - x_3\left[b\ \ c - x_3^{\ 2}\ + ex_1\right]\ (\sin y_3 - 1) + x_3 \cos(y_3) \\ \qquad \left[-qy_3 - r(1 - y_3^{\ 2})y_2 + sy_1\right] - \left[-qy_3 - r(1 - y_3^{\ 2})y_2 + sy_1\right] \\ \qquad + x_3 \sin y_3 - x_3 - y_3 \end{cases} \tag{3.17}$$

The theorem is satisfied and the double symplectic synchronization is achieved. The chaotic attractor of the controlled GKv system is shown in Fig. 3.7, the time histories of double symplectic synchronization and the time histories of the state errors are shown in Fig. 3.8 and Fig. 3.9, respectively.

Case 3.

Consider a new Ge-Ku-Mathieu(GKM) system as Partner A described by

$$\begin{cases} \dot{x}_1 = x_2 \\ \dot{x}_2 = -ax_2 - x_1\left[b\ \ c - x_1^{\ 2}\ + dx_2 x_3\right] \\ \dot{x}_3 = -\ \ g + hx_1\ \ x_3 + lx_2 + ex_1 x_3 \end{cases} \tag{3.18}$$

where $a = -0.6, b = 5, c = 11, d = 0.3, g = 8, h = 10, l = 0.5, e = 0.2$ and the initial condition is $x_1(0) = 0.01,\ x_2(0) = 0.01,\ x_3(0) = 0.01$. Eq. (18) can be rewritten in the form of Eq. (3.1), where $\mathbf{f}(x,t) = \begin{bmatrix} x_2 \\ -ax_2 - x_1\left[b\ \ c - x_1^{\ 2}\ + dx_2 x_3\right] \\ -\ \ g + hx_1\ \ x_3 + lx_2 + ex_1 x_3 \end{bmatrix}$. The chaotic attractor of the new GKM system is shown in Fig. 3.10.

The controlled GKv system is considered as Partner B described by

$$\begin{cases} \dot{y}_1 = y_2 + u_1 \\ \dot{y}_2 = -my_2 - y_3\left[n\ \ v - y_1^{\ 2}\ + py_3\right] + u_2 \\ \dot{y}_3 = -qy_3 + r\ \ 1 - y_3^{\ 2}\ \ y_2 + sy_1 + u_3 \end{cases} \tag{3.19}$$

where $m = 0.08, n = -0.35, v = 100.56, p = -1000.02, q = 0.61, r = 0.08, s = 0.01$,

$\mathbf{u} = u_1, u_2, u_3{}^{\mathrm{T}}$ is the controller, and the initial conditions are $y_1(0) = -1.5$, $y_2(0) = 20$, $y_3(0) = 15.2$. Eq. (3.19) can be rewritten in the form of Eq. (3.2), where

$$\mathbf{C}(t) = \begin{bmatrix} 0 & 1 & 0 \\ 0 & -m & -nv \\ s & r & -q \end{bmatrix} \text{ and } \mathbf{g}(y,t) = \begin{bmatrix} 0 \\ ny_1{}^2 y_3 - yx_3{}^2 \\ -ry_2 y_3{}^2 \end{bmatrix}.$$

By applying **Property 1**, it is derived that $\|\mathbf{C}(t)\|_1 = -no - q$, $\|\mathbf{C}(t)\|_\infty = -m - nv$, and $\|\mathbf{C}(t)\|_2 \le \sqrt{-nv - q\ (-m - nv)} = \sqrt{1214.52}$. Then $\|\mathbf{C}(t)\| = 34$ is estimated.

Define $\mathbf{F}(\mathbf{x}, \mathbf{y}, t) = \begin{bmatrix} x_1 \sin y_1 \\ x_2 \sin y_2 \\ x_3 \sin y_3 \end{bmatrix}$, and our goal is to achieve the double symplectic synchronization $\mathbf{x} + \mathbf{y} = \mathbf{F}(\mathbf{x}, \mathbf{y}, t)$. According to Theorem, the inequality $\frac{\min(k_i)}{\|\mathbf{C}(t)\|} > 1$ must be satisfied. It can be obtained that $\min(k_i) > 34$. Thus we choose

$$\mathbf{K} = \begin{bmatrix} k_1 & 0 & 0 \\ 0 & k_2 & 0 \\ 0 & 0 & k_3 \end{bmatrix} = \begin{bmatrix} 35 & 0 & 0 \\ 0 & 36 & 0 \\ 0 & 0 & 37 \end{bmatrix}$$ and design the controller as

$$\begin{cases} u_1 = x_2 \sin y_1 + x_1 y_2 \cos y_1 - x_2 - y_2 + x_1 \sin y_1 - x_1 - y_1 \\ u_2 = -ax_2 - x_1 \left[b\ c - x_1{}^2 + dx_2 x_3 \right] (\sin y_2 - 1) + x_2 \cos(y_2) \\ \qquad -my_2 - y_3 \left[n\ v - y_1{}^2 + py_3 \right] - \left[-my_2 - y_3 \left[n\ v - y_1{}^2 + py_3 \right] \right] \\ \qquad + x_2 \sin y_2 - x_2 - y_2 \\ u_3 = -g + hx_1\ x_3 + lx_2 + ex_1 x_3\ (\sin y_3 - 1) + x_3 \cos(y_3) \\ \qquad \left[-qy_3 - r(1 - y_3{}^2) y_2 + sy_1 \right] - \left[-qy_3 - r(1 - y_3{}^2) y_2 + sy_1 \right] \\ \qquad + x_3 \sin y_3 - x_3 - y_3 \end{cases} \tag{3.20}$$

The theorem is satisfied and the double symplectic synchronization is achieved. The chaotic attractor of the controlled GKv system is shown in Fig. 3.11, the time histories of double symplectic synchronization and the time histories of the state errors are shown in Fig. 3.12 and Fig. 3.13, respectively.

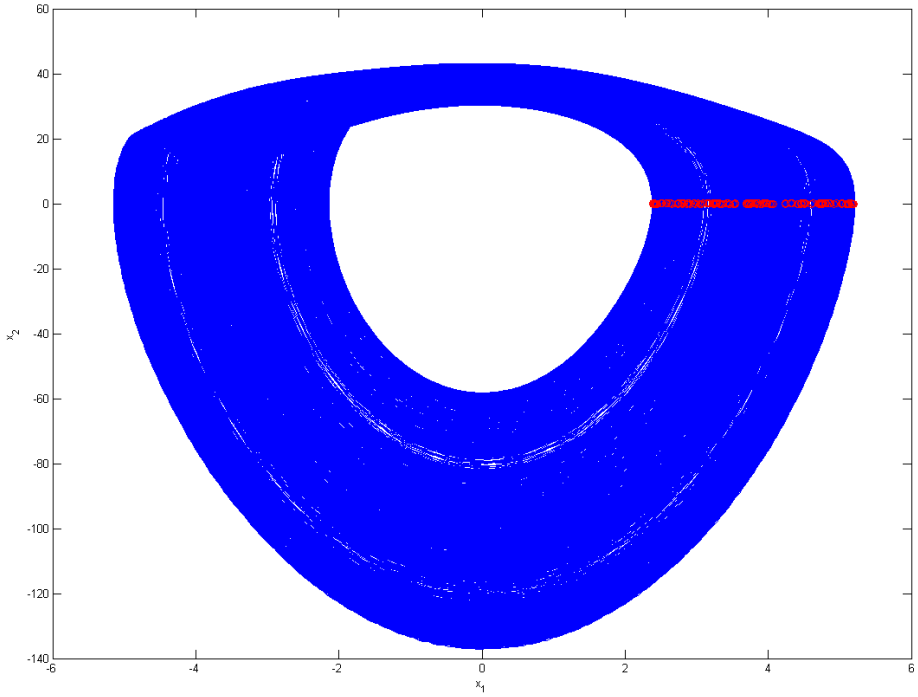

Fig. 3.1 The chaotic attractor of a new GKD system.

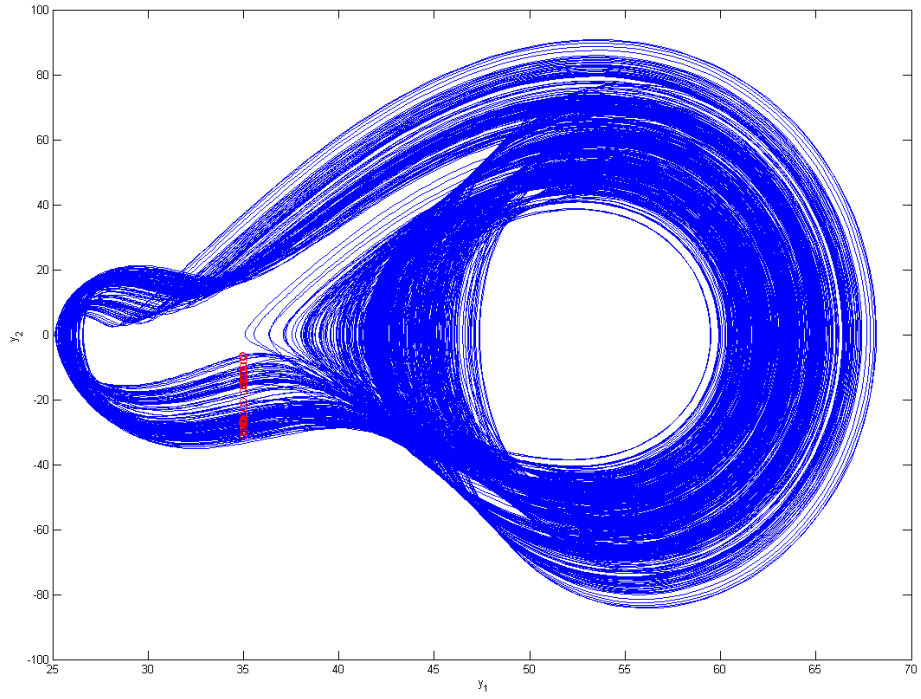

Fig. 3.2 The chaotic attractor of uncontrolled new GKv system.

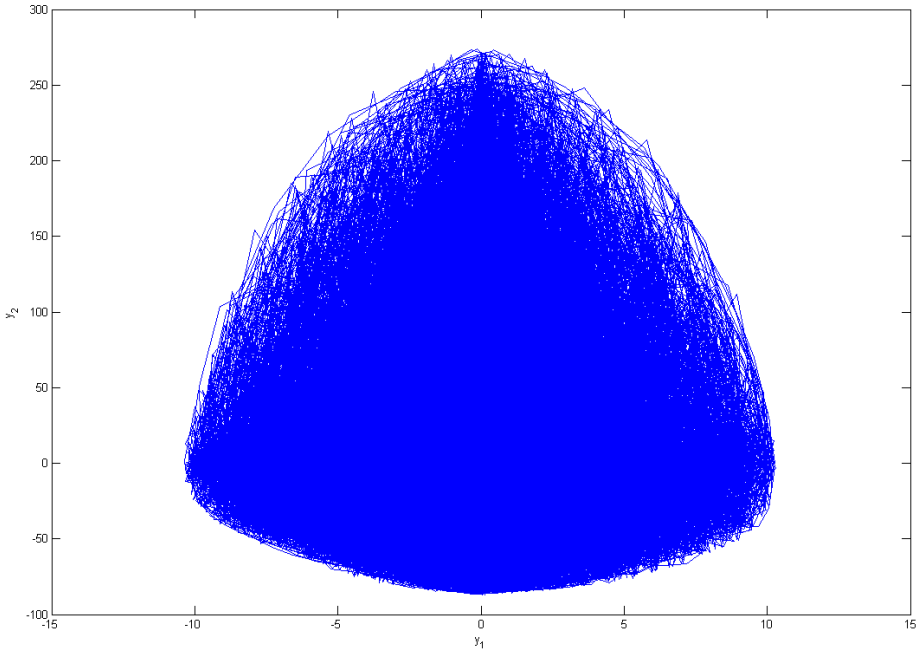

Fig. 3.3 The chaotic attractor of the controlled new GKv system for Case1.

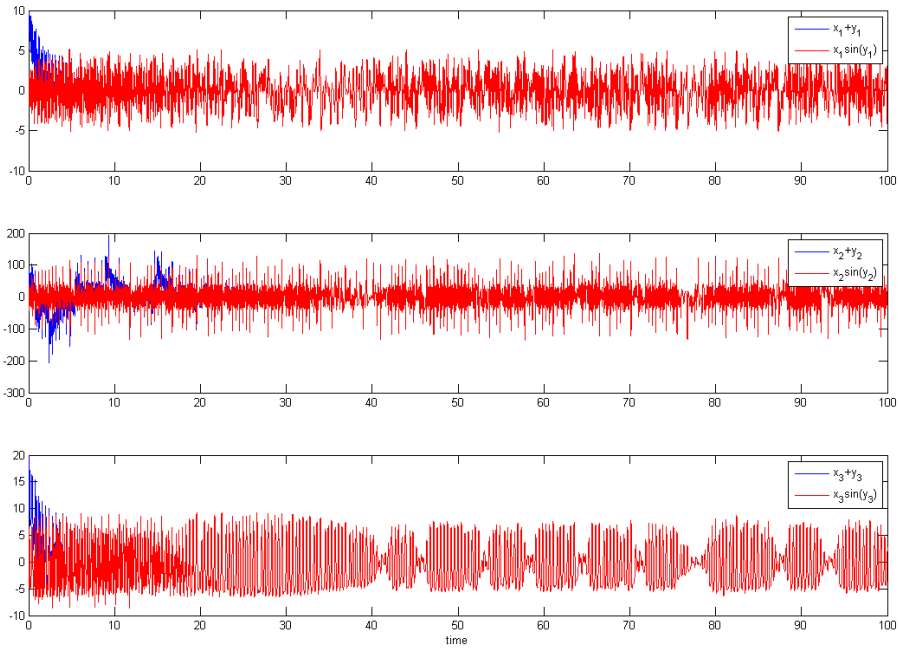

Fig. 3.4 Time histories of $x_i + y_i$ and $x_i \sin y_i$ for Case 1.

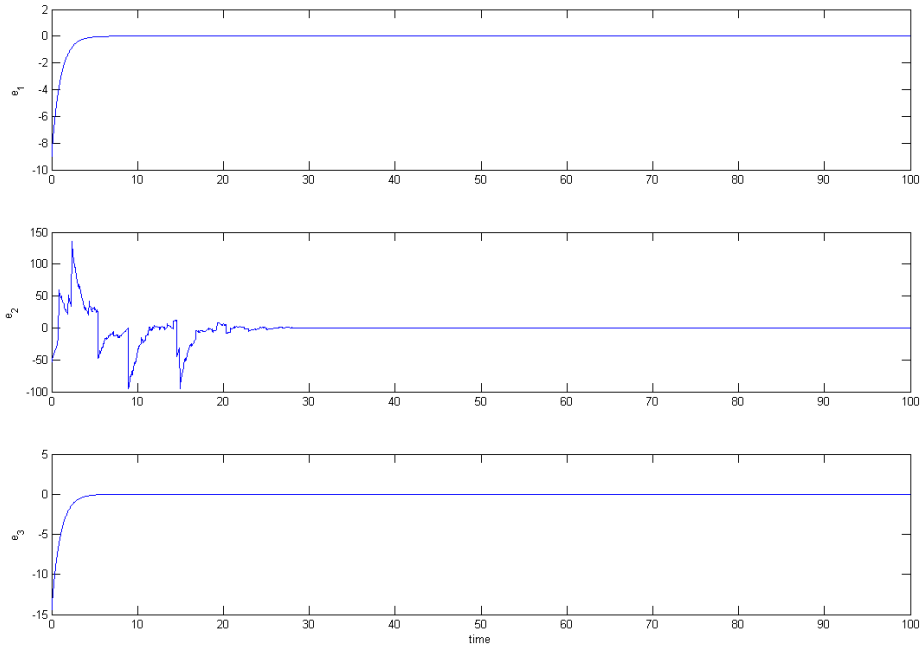

Fig. 3.5 Time histories of the state errors for Case 1.

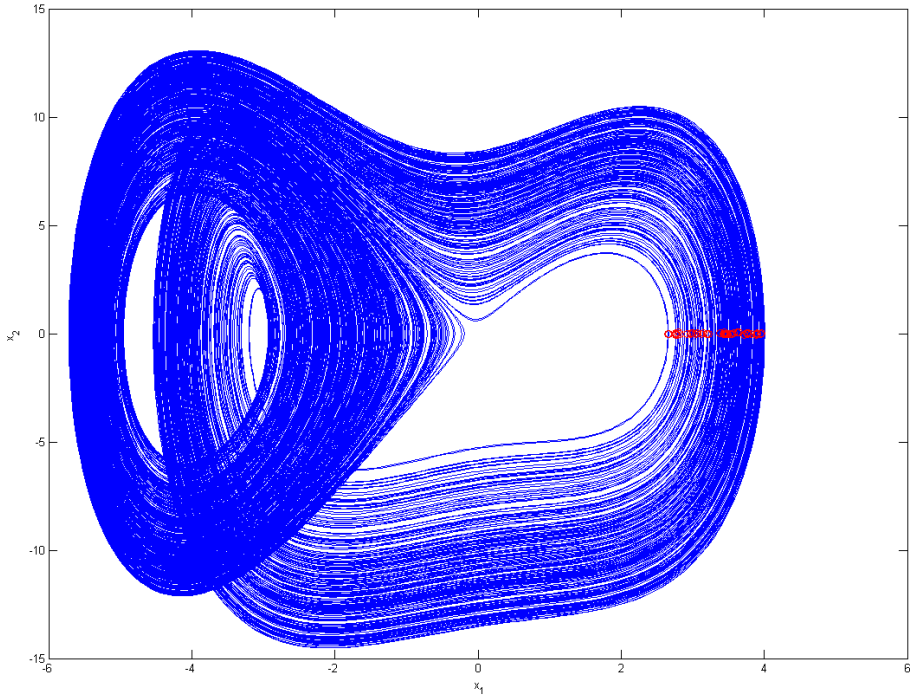

Fig. 3.6 The chaotic attractor of a new DGK system.

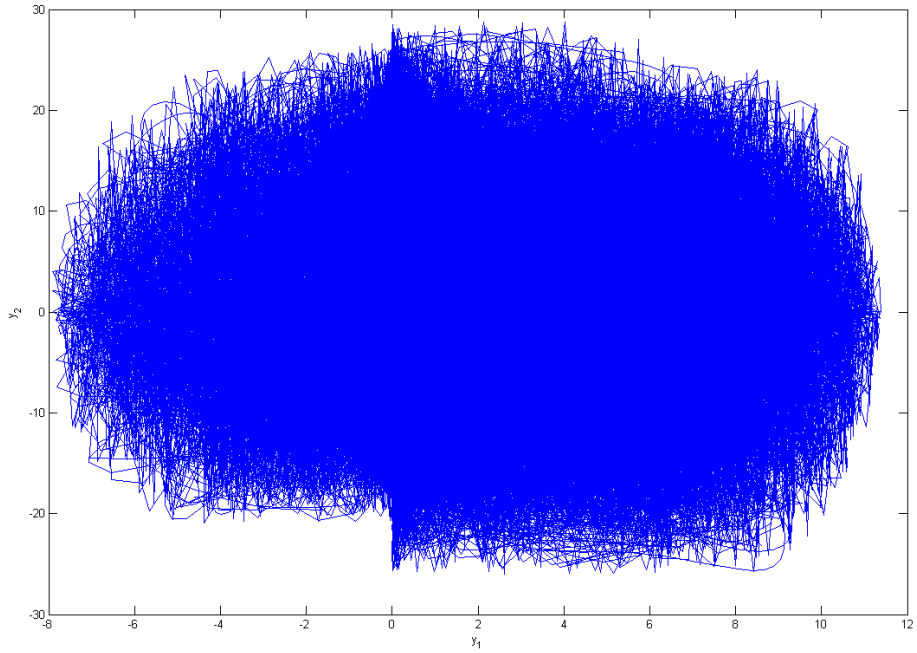

Fig. 3.7 The chaotic attractor of the controlled new GKv system for Case 2.

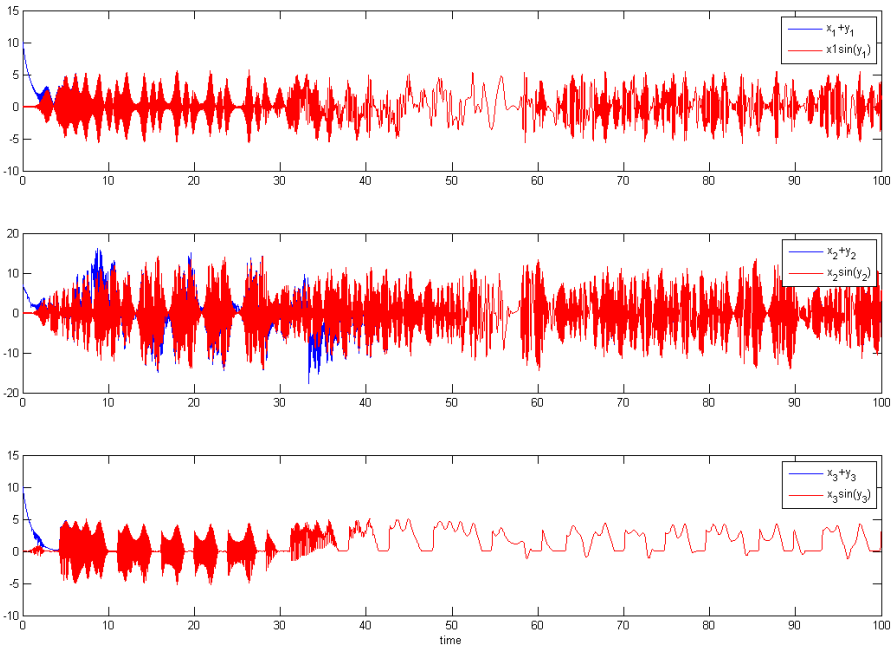

Fig. 3.8 Time histories of $x_i + y_i$ and $x_i \sin y_i$ for Case 2.

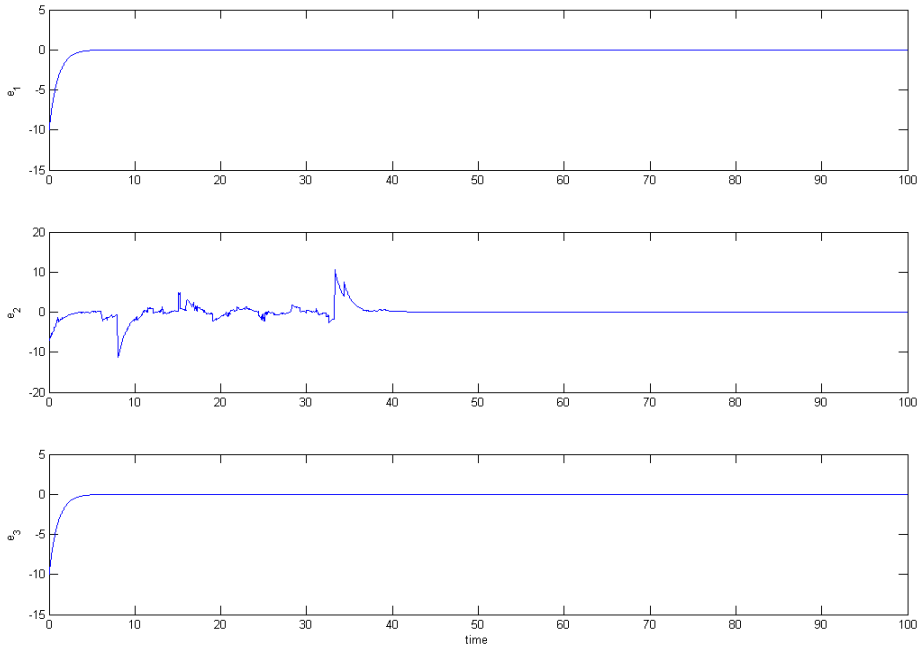

Fig. 3.9 Time histories of the state errors for Case 2.

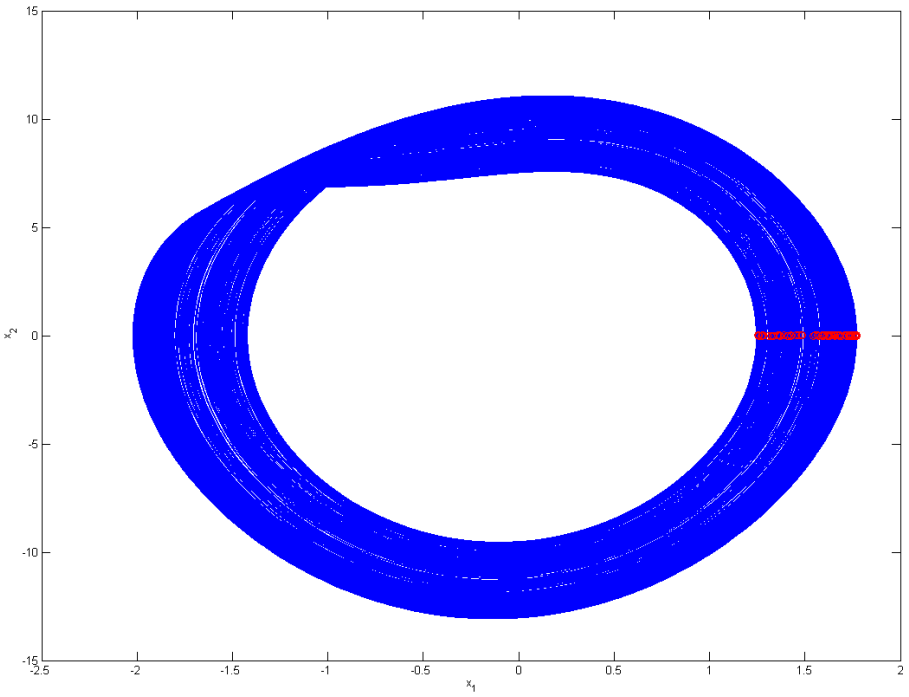

Fig. 3.10 The chaotic attractor of a new GKM system.

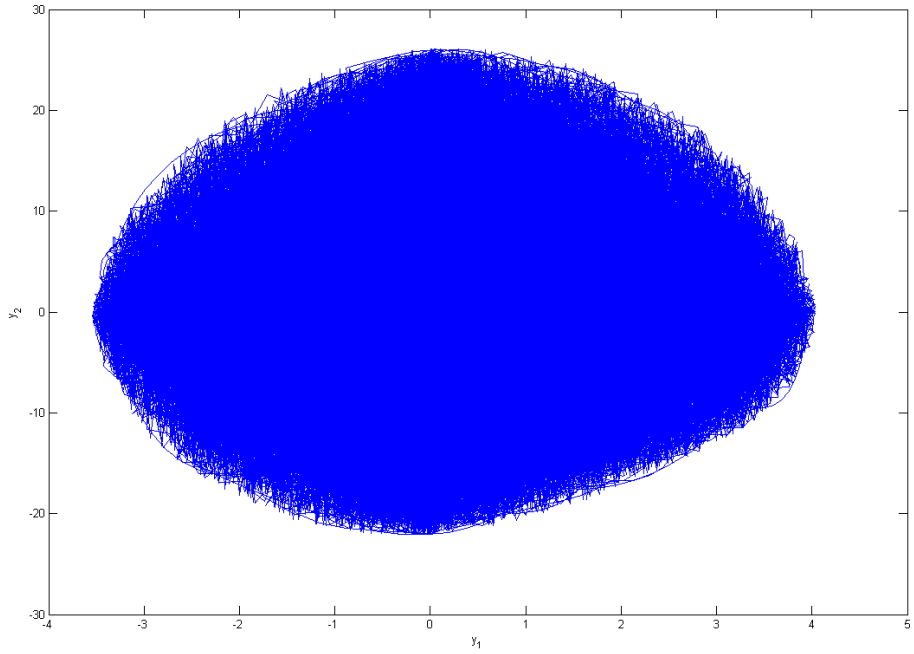

Fig. 3.11 The chaotic attractor of the controlled new GKv system for Case3.

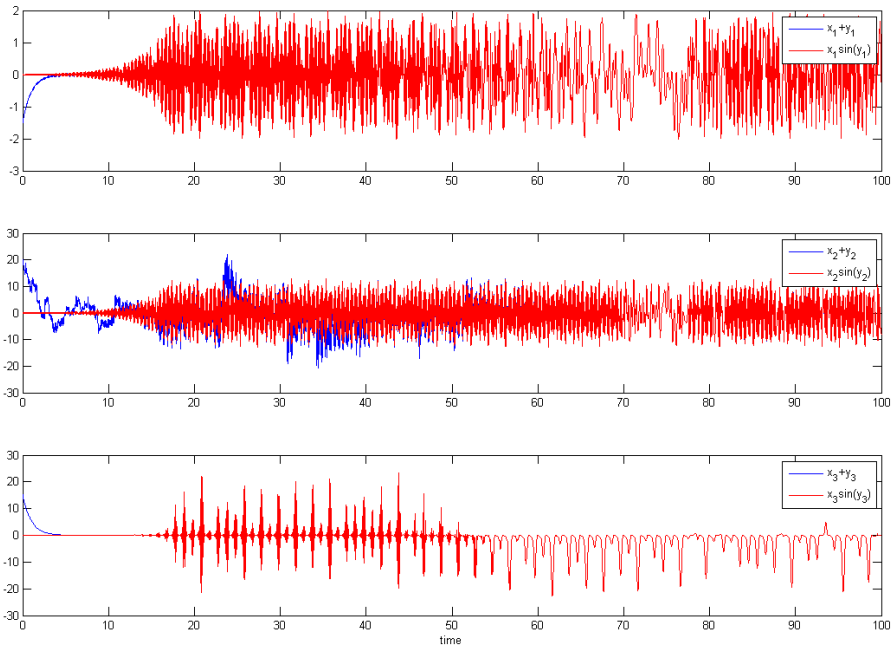

Fig. 3.12 Time histories of $x_i + y_i$ and $x_i \sin y_i$ for Case 3.

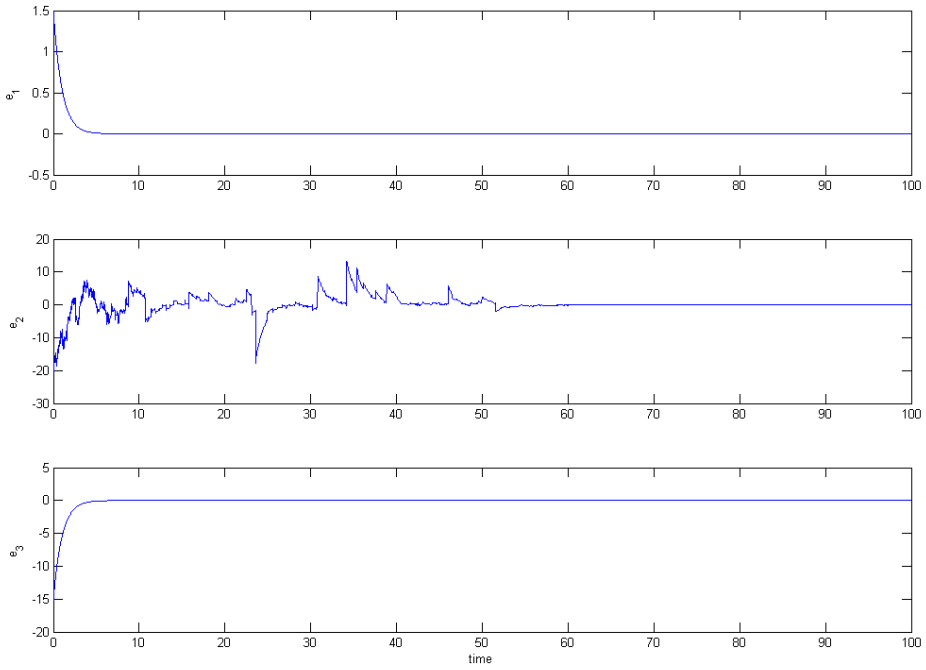

Fig. 3.13 Time histories of the state errors for Case 3.

Chapter 4

Complex State Chaotic System with Pragmatical Adaptive Synchronization

4.1 Preliminary

In this Chapter, the main objective of this work is to investigate the chaotic behavior and chaos generalized synchronization of two identical three creative complex state dynamic systems. This three complex state system consists of a second-order Ge-Ku complex system and one of three different single complex systems respectively. We reduce the three complex state systems to five real state systems by pragmatical stability theory. Chaos is found for them and generalized synchronizations are accomplished for these five real state systems. Since three complex dynamic systems are creative, the security is highly increased if they are used for secret communication. Numerical simulations are given to show that the proposed scheme is applied successfully.

4.2 The Scheme of Pragmatical Generalized Synchronization by Adaptive Control

There are two identical nonlinear dynamical systems, and the master system controls the slave system. The master system is given by

$$\dot{\mathbf{x}} = \mathbf{A}\mathbf{x} + f(\mathbf{x}, \mathbf{B}), \tag{4.1}$$

where $\mathbf{x} = [x_1, x_2, ..., x_n]^T \in R_n$ denotes a state vector, $\mathbf{A}$ is an $n \times n$ uncertain constant coefficient matrix, f is a nonlinear vector function, and $\mathbf{B}$ is a vector of uncertain constant coefficients in f.

The slave system is given by

$$\dot{\mathbf{y}} = \hat{\mathbf{A}}\mathbf{y} + f(\mathbf{y}, \hat{\mathbf{B}}) + \mathbf{u}(t), \tag{4.2}$$

where $\mathbf{y} = [y_1, y_2, ..., y_n]^T \in R_n$ denotes a state vector, $\hat{\mathbf{A}}$ is an $n \times n$ estimated coefficient matrix, $\hat{\mathbf{B}}$ is a vector of estimated coefficients in f, and $\mathbf{u}(t) = [u_1(t), u_2(t), ..., u_n(t)]^T \in R^n$ is a control input vector.

Our goal is to design a controller $\mathbf{u}(t)$ so that the state vector of the slave system Eq. (4.2) asymptotically approaches the state vector of the master system Eq. (4.1) plus a given chaotic vector function $\mathbf{F}(t) = [F_1(t), F_2(t), ..., F_n(t)]^T$. This is a special kind of generalized synchronization. y is a given function of x:

$$\mathbf{y} = \mathbf{G}(x) = \mathbf{x} + \mathbf{F}(t). \tag{4.3}$$

The synchronization can be accomplished when $t \to \infty$, the limit of the error vector $\mathbf{e}(t) = [e_1(t), e_2(t), ..., e_n(t)]^T$ approaches zero:

$$\lim_{t \to \infty} \mathbf{e} = \quad , \tag{4.4}$$

where

$$\mathbf{e} = \mathbf{x} - \mathbf{y} + \mathbf{F}(t). \tag{4.5}$$

From Eq. (4.5) we have

$$\dot{\mathbf{e}} = \dot{\mathbf{x}} - \dot{\mathbf{y}} + \dot{\mathbf{F}}(t), \tag{4.6}$$

$$\dot{\mathbf{e}} = \mathbf{A}\mathbf{x} - \hat{\mathbf{A}}\mathbf{y} + f(\mathbf{x}, \mathbf{B}) - f(\mathbf{y}, \hat{\mathbf{B}}) + \dot{\mathbf{F}}(t) - \mathbf{u}(t). \tag{4.7}$$

A Lyapunov function $V(\mathbf{e}, \tilde{\mathbf{A}}, \tilde{\mathbf{B}})$ is chosen as a positive definite function

$$V(\mathbf{e}, \tilde{\mathbf{A}}, \tilde{\mathbf{B}}) = \frac{1}{2} e^T e + \frac{1}{2} \tilde{\mathbf{A}} \tilde{\mathbf{A}}^T + \frac{1}{2} \tilde{\mathbf{B}} \tilde{\mathbf{B}}^T, \tag{4.8}$$

where $\tilde{\mathbf{A}} = \mathbf{A} - \hat{\mathbf{A}}$, $\tilde{\mathbf{B}} = \mathbf{B} - \hat{\mathbf{B}}$, $\tilde{\mathbf{A}}$ and $\tilde{\mathbf{B}}$ are two column matrices whose elements are all the elements of matrix $\tilde{\mathbf{A}}$ and of matrix $\tilde{\mathbf{B}}$ respectively.

Its derivative along any solution of the differential equation system consisting of Eq. (4.7) and update parameter differential equations for $\tilde{\mathbf{A}}$ and $\tilde{\mathbf{B}}$ is

$$\dot{V}(\mathbf{e},\tilde{\mathbf{A}},\tilde{\mathbf{B}}) = \mathbf{e}^T[\mathbf{A}\mathbf{x} - \hat{\mathbf{A}}\mathbf{y} + f(\mathbf{x},\mathbf{B}) - f(\mathbf{y},\hat{\mathbf{B}}) + \dot{\mathbf{F}}(t) - \mathbf{u}(t)] + \tilde{\mathbf{A}}\dot{\tilde{\mathbf{A}}} + \tilde{\mathbf{B}}\dot{\tilde{\mathbf{B}}}, \quad (4.9)$$

where $\mathbf{u}(t)$, $\dot{\tilde{\mathbf{A}}}$ and $\dot{\tilde{\mathbf{B}}}$ are chosen so that $\dot{V} = \mathbf{e}^T\mathbf{C}\mathbf{e}$, $\mathbf{C}$ is a diagonal negative definite matrix, and $\dot{V}$ is a negative semi-definite function of e and parameter differences $\tilde{\mathbf{A}}$ and $\tilde{\mathbf{B}}$. In the current scheme of adaptive synchronization [32-34], the traditional Lyapunov stability theorem and Babalat's lemma [26] are used to prove that the error vector approaches zero, as time approaches infinity. But the question of why the estimated parameters also approach uncertain parameters remains unanswered. By the pragmatical asymptotical stability theorem, the question can be answered strictly as shown in Appendix B.

4.3 Chaotic Behaviors and Pragmatical Generalized Synchronization of Three Complex State Ge-Ku Systems

Ge and Ku [24] gave a chaotic system formed by a simple pendulum with its pivct rotating about an axis as Fig. 2.1. The equation of motion can be written as

$$\ddot{x} + a\dot{x} + \sin(x)(b(c + \cos(x)) + d\sin(\omega t)) = 0, \quad (4.13)$$

where a, b, c, d are parameters. After simplification $\sin(x) = x$, $\cos(x) = 1 - x_1^2$, $\sin(\omega t) = x$ and addition of gx_1^2. After simplification we get the new Ge-Ku system

$$\begin{cases} \dot{x}_1 = x_2 \\ \dot{x}_2 = -ax_2 - x_1(b(c - x_1^2) + dx_1) + gx_1^2 \end{cases}, \quad (4.14)$$

where a, b, c, d, g are parameters.

Case 1.

A new complex state system consists of Ge-Ku system coupling with a particularly designed complex conjugate system

$$\begin{cases} \dot{x}_1 = x_2 \\ \dot{x}_2 = -ax_2 - x_3(b(c - x_1^2) + dx_3) + gx_1^2 \\ \dot{x}_3 = \frac{1}{2}(\bar{x}_1\bar{x}_2 + x_1x_2) - h\sin(x_3) \end{cases}, \tag{4.15}$$

where $x_1 = u_{11} + iu_{21}$, $x_2 = u_{31} + iu_{41}$ and $x_3 = u_{51}$.

Equating real and imaginary parts of both sides of Eq. (4.15), we can get dynamic equations of real u_{i1}. The complex system Eq. (4.15) can thus be written in the form of five real first order ODEs:

$$\begin{cases} \dot{u}_{11} = u_{31} \\ \dot{u}_{21} = u_{41} \\ \dot{u}_{31} = -au_{31} - u_{51}(b(c - u_{11}^{\ 2} + u_{21}^{\ 2}) + du_{51}) + g(u_{11}^{\ 2} - u_{21}^{\ 2}), \\ \dot{u}_{41} = -au_{41} + 2u_{11}u_{21}(bu_{51} + 1) \\ \dot{u}_{51} = u_{11}u_{31} - u_{21}u_{41} - h\sin(u_{51}) \end{cases} \tag{4.16}$$

After exhaustive search, we find that when system parameters $a = 1.15$, $b = -0.76$, $c = 1.76$, $d = 1.95$, $g = 7.67$, $h = 0.91$ are system parameters and initial conditions $u_{11}(0) = 0.01$, $u_{21}(0) = 0.01$, $u_{31}(0) = 0.01$, $u_{41}(0) = 0.01$ and $u_{51}(0) = 0.01$, chaos of the system are found and illustrated by phase portraits Fig. 4.1. The bifurcation diagram and the Lyapunov exponents are shown in Fig. 4.2 and Fig. 4.3 respectively.

The slave system is described by

$$\begin{cases} \dot{y}_1 = y_2 \\ \dot{y}_2 = -\hat{a}y_2 - y_3(\hat{b}(\hat{c} - y_1^2) + \hat{d}y_3) + \hat{g}y_1^2, \\ \dot{y}_3 = \frac{1}{2}(\bar{y}_1\bar{y}_2 + y_1y_2) - \hat{h}\sin(y_3) \end{cases} \tag{4.17}$$

where $y_1 = u_{12} + iu_{22}$, $y_2 = u_{32} + iu_{42}$ and $y_3 = u_{52}$.

Equating real and imaginary parts of both sides of Eq. (4.17) and leading $(u_{12}, u_{22}, u_{32}, u_{42}, u_{52})$ to $(u_{11} + F_1(t),\ u_{21} + F_2(t),\ u_{31} + F_3(t),\ u_{41} + F_4(t),\ u_{51} + F_5(t))$, we add real and complex control functions $v_1 + iv_2$, $v_3 + iv_4$ and v_5 to each equation respectively, we can get dynamic equation of all real variables u_{i2} and v_j.

The complex system Eq. (4.17) can thus be written in the form of five real first order ODEs:

$$\begin{cases} \dot{u}_{12} = u_{32} + v_1 \\ \dot{u}_{22} = u_{42} + v_2 \\ \dot{u}_{32} = -\hat{a}u_{32} - u_{52}(\hat{b}(\hat{c} - {u_{12}}^2 + {u_{22}}^2) + \hat{d}u_{52}) + \hat{g}({u_{12}}^2 - {u_{22}}^2) + v_3 \\ \dot{u}_{42} = -\hat{a}u_{42} + 2u_{12}u_{22}(\hat{b}u_{52} + 1) + v_4 \\ \dot{u}_{52} = u_{12}u_{32} - u_{22}u_{42} - h\sin(u_{52}) + v_5 \end{cases}, \quad (4.18)$$

when initial states be $u_{12}(0) = 10$, $u_{22}(0) = 10$, $u_{32}(0) = 10$, $u_{42}(0) = 10$ and $u_{52}(0) = 10$.

In order to obtain the active control signals, we define the errors between the drive and the response states as $e_{ui} = u_{i1} - u_{i2} + F(t)$ where $F(t) = z = (z_1, z_2, z_3, z_4, z_5)$, where z_1, z_2, z_3 are the states of Lorenz chaotic system and z_4, z_5 are the states of Duffing chaotic system respectively:

$$\begin{cases} \dot{z}_1 = f(z_2 - z_1) \\ \dot{z}_2 = z_1(k - z_3) - z_2 \\ \dot{z}_3 = z_1 z_2 - l z_3 \\ \dot{z}_4 = z_5 \\ \dot{z}_5 = -r z_5 - s z_4 - z_4^3 + o\cos(qt) \end{cases}, \quad (4.19)$$

where $f = 10$, $k = 28$, $l = \frac{3}{8}$, $r = 0.25$, $s = -1$, $o = 0.3$, $q = 1$ and initial states are $z_1(0) = 0.01$, $z_2(0) = 0.01$, $z_3(0) = 0.01$, $z_4(0) = 2$, $z_5(0) = 2$.

We obtain the errors as

$$\begin{cases} e_{u1} + ie_{u2} = x_1 - y_1 + (z_1 + iz_2) = (u_{11} - u_{12} + z_1) + i(u_{21} - u_{22} + z_2) \\ e_{u3} + ie_{u4} = x_2 - y_2 + (z_3 + iz_4) = (u_{31} - u_{32} + z_3) + i(u_{41} - u_{42} + z_4) \\ e_{u5} = x_5 - y_5 - z_5 = (u_{51} - u_{52} + z_5) \end{cases}, \quad (4.20)$$

and our aim is $\lim_{t\to\infty} \mathbf{e} = 0$, i.e.

$$\lim_{t\to\infty} e_{ui} = \lim_{t\to\infty} u_{i1} - u_{i2} + z_i = 0, \ i = 1, 2, 3, 4, 5. \quad (4.21)$$

However,

$$\begin{cases} \dot{e}_{u1} + i\dot{e}_{u2} = \dot{x}_1 - \dot{y}_1 + (\dot{z}_1 + i\dot{z}_2) = (\dot{u}_{11} - \dot{u}_{12} + \dot{z}_1) + i(\dot{u}_{21} - \dot{u}_{22} + \dot{z}_2) \\ \dot{e}_{u3} + i\dot{e}_{u4} = \dot{x}_2 - \dot{y}_2 + (\dot{z}_3 + i\dot{z}_4) = (\dot{u}_{31} - \dot{u}_{32} + \dot{z}_3) + i(\dot{u}_{41} - \dot{u}_{42} + \dot{z}_4), \\ \dot{e}_{u5} = \dot{x}_5 - \dot{y}_5 - \dot{z}_5 = (\dot{u}_{51} - \dot{u}_{52} + \dot{z}_5) \end{cases} \quad (4.22)$$

Eq. (4.22) describes a dynamical system where the e_{ui} evolve in time and its ODEs.

When equating real and imaginary parts of both sides of Eq. (4.22), we get

$$\begin{cases} \dot{e}_{u1} = \dot{u}_{11} - \dot{u}_{12} + \dot{z}_1 = u_{31} - u_{32} - v_1 + \dot{z}_1 \\ \dot{e}_{u2} = \dot{u}_{21} - \dot{u}_{22} + \dot{z}_2 = u_{41} - u_{42} - v_2 + \dot{z}_2 \\ \dot{e}_{u3} = \dot{u}_{31} - \dot{u}_{32} + \dot{z}_3 = -au_{31} - u_{51}(b(c - {u_{11}}^2 + {u_{21}}^2) + du_{51}) + g({u_{11}}^2 - {u_{21}}^2) \\ \qquad\qquad + \hat{a}u_{32} + u_{52}(\hat{b}(\hat{c} - {u_{12}}^2 + {u_{22}}^2) + \hat{d}u_{52}) - \hat{g}({u_{12}}^2 - {u_{22}}^2) \\ \qquad\qquad - v_3 + \dot{z}_3 \\ \dot{e}_{u4} = \dot{u}_{41} - \dot{u}_{42} + \dot{z}_4 = -au_{41} + 2u_{11}u_{21}(bu_{51} + 1) + \hat{a}u_{42} - 2u_{12}u_{22}(\hat{b}u_{52} + 1) \\ \qquad\qquad - v_4 + \dot{z}_4 \\ \dot{e}_{u5} = \dot{u}_{51} - \dot{u}_{52} + \dot{z}_5 = u_{11}u_{31} - u_{21}u_{41} - h\sin(u_{51}) - u_{12}u_{32} + u_{22}u_{42} + \hat{h}\sin(u_{52}) \\ \qquad\qquad - v_5 + \dot{z}_5 \end{cases}, \quad (4.23)$$

where $\tilde{a} = a - \hat{a}$, $\tilde{b} = b - \hat{b}$, $\tilde{c} = c - \hat{c}$, $\tilde{d} = d - \hat{d}$, $\tilde{g} = g - \hat{g}$, $\tilde{h} = h - \hat{h}$ and $\hat{a}$, $\hat{b}$, $\hat{c}$, $\hat{d}$, $\hat{g}$, $\hat{h}$ are estimates of uncertain parameters a, b, c, d, g and h respectively.

Choose a Lyapunov function in the form of a positive definite function:

$$\begin{aligned} &V(e_{u1}, e_{u2}, e_{u3}, e_{u4}, e_{u5}, \tilde{a}, \tilde{b}, \tilde{c}, \tilde{d}, \tilde{g}, \tilde{h}) \\ &\quad = \tfrac{1}{2}({e_{u1}}^2 + {e_{u2}}^2 + {e_{u3}}^2 + {e_{u4}}^2 + {e_{u5}}^2 + \tilde{a}^2 + \tilde{b}^2 + \tilde{c}^2 + \tilde{d}^2 + \tilde{g}^2 + \tilde{h}^2) > 0 \end{aligned}. \quad (4.24)$$

Choose parameter dynamics as

$$\begin{cases} \dot{\tilde{a}} = -\dot{\hat{a}} = -\tilde{a}(e_{u3} + e_{u4}) \\ \dot{\tilde{b}} = -\dot{\hat{b}} = -\tilde{b}(e_{u3} + e_{u4}) \\ \dot{\tilde{c}} = -\dot{\hat{c}} = -\tilde{c}(e_{u3} + e_{u4}) \\ \dot{\tilde{d}} = -\dot{\hat{d}} = -\tilde{d}(e_{u3} + e_{u4}) \\ \dot{\tilde{g}} = -\dot{\hat{g}} = -\tilde{g}(e_{u3} + e_{u4}) \\ \dot{\tilde{h}} = -\dot{\hat{h}} = -\tilde{h}e_{u5} \end{cases}, \quad (4.25)$$

Time derivative of V along any solution of Eq. (4.24) and parameter dynamics

is

$$\begin{aligned}\dot{V} = {} & e_{u1}(u_{31} - u_{32} - v_1 + \dot{z}_1) + e_{u2}(u_{41} - u_{42} - v_2 + \dot{z}_2) + e_{u3} \\ & (-au_{31} - u_{51}(b(c - u_{11}^{\ 2} + u_{21}^{\ 2}) + du_{51}) + g(u_{11}^{\ 2} - u_{21}^{\ 2}) \\ & + \hat{a}u_{32} + u_{52}(\hat{b}(\hat{c} - u_{12}^{\ 2} + u_{22}^{\ 2}) + \hat{d}u_{52}) - \hat{g}(u_{12}^{\ 2} - u_{22}^{\ 2}) \\ & - v_3 + \dot{z}_3) + e_{u4}(-au_{41} + 2u_{11}u_{21}(bu_{51} + 1) + \hat{a}u_{42} - 2u_{12} \\ & u_{22}(\hat{b}u_{52} + 1) - v_4 + \dot{z}_4) + e_{u5}(u_{11}u_{31} - u_{21}u_{41} - h\sin(u_{51}) \\ & - u_{12}u_{32} + u_{22}u_{42} + \hat{h}\sin(u_{52}) - v_5 + \dot{z}_5) + \tilde{a}(-\dot{\hat{a}}) + \tilde{b}(-\dot{\hat{b}}) \\ & + \tilde{c}(-\dot{\hat{c}}) + \tilde{d}(-\dot{\hat{d}}) + \tilde{g}(-\dot{\hat{g}}) + \tilde{h}(-\dot{\hat{h}})\end{aligned} \quad . \tag{4.26}$$

Choose

$$\begin{cases} v_1 = u_{31} - u_{32} + \dot{z}_1 + e_{u1} \\ v_2 = u_{41} - u_{42} + \dot{z}_2 + e_{u2} \\ v_3 = -au_{31} - u_{51}(b(c - u_{11}^{\ 2} + u_{21}^{\ 2}) + du_{51}) + g(u_{11}^{\ 2} - u_{21}^{\ 2}) \\ \qquad + \hat{a}u_{32} + u_{52}(\hat{b}(\hat{c} - u_{12}^{\ 2} + u_{22}^{\ 2}) + \hat{d}u_{52}) - \hat{g}(u_{12}^{\ 2} - u_{22}^{\ 2}) \\ \qquad + \dot{z}_3 - (\tilde{a}^2 + \tilde{b}^2 + \tilde{c}^2 + \tilde{d}^2 + \tilde{g}^2) + e_{u4} \\ v_4 = -au_{41} + 2u_{11}u_{21}(bu_{51} + 1) + \hat{a}u_{42} - 2u_{12}u_{22}(\hat{b}u_{52} + 1) + \dot{z}_4 \\ \qquad - (\tilde{a}^2 + \tilde{b}^2 + \tilde{c}^2 + \tilde{d}^2 + \tilde{g}^2) + e_{u4} \\ v_5 = u_{11}u_{31} - u_{21}u_{41} - h\sin(u_{51}) - u_{12}u_{32} + u_{22}u_{42} + \hat{h}\sin(u_{52}) \\ \qquad + \dot{z}_5 - \tilde{h}^2 + e_{u5} \end{cases} \quad . \tag{4.27}$$

Substituting Eqs. (4.25) and (4.27) into Eq. (4.26), we obtain

$$\dot{V} = -(e_{u1}^{\ 2} + e_{u2}^{\ 2} + e_{u3}^{\ 2} + e_{u4}^{\ 2} + e_{u5}^{\ 2}) < 0\,, \tag{4.28}$$

which is a negative semi-definite function of e_{u1}, e_{u2}, e_{u3}, e_{u4}, e_{u5}, $\tilde{a}$, $\tilde{b}$, $\tilde{c}$, $\tilde{d}$, $\tilde{g}$, $\tilde{h}$. The Lyapunov asymptotical stability theorem is not satisfied. We can not obtain that common origin of error dynamics Eq. (4.23) and parameter dynamics Eq. (4.25) are asymptotically stable. However, By pragmatical asymptotically stability theorem, $\mathbf{D}$ is a *n*-manifold, *n*=11 and the number of error state variables $p = 5$.

When $e_{u1} = e_{u2} = e_{u3} = e_{u4} = e_{u5} = 0$ and $\tilde{a}$, $\tilde{b}$, $\tilde{c}$, $\tilde{d}$, $\tilde{g}$, $\tilde{h}$ take arbitrary values, $\dot{V} < 0$, so $\mathbf{X}$ is 5-manifold, $m = n - p = 11 - 5 = 6$. $m + 1 < n$ is satisfied.

By pragmatical asymptotical stability theorem, error vector e approaches zero and the estimated parameters also approach the uncertain parameters. The pragmatical generalized synchronization is obtained. Under the assumption of equal probability, it is actually asymptotically stable. The simulation results are shown in Figs. 4.4-4.6.

Case 2.

A new system, i.e. one of the three complex state Ge-Ku systems, studied in this part consists of Ge-Ku system coupling with a particularly designed complex conjugate system

$$\begin{cases} \dot{x}_1 = x_2 \\ \dot{x}_2 = -ax_2 - x_3(b(c - x_1^2) + dx_3) + gx_1^2 \\ \dot{x}_3 = \frac{1}{2}(\bar{x}_1 x_2 + x_1 \bar{x}_2) - h\sin(x_3) \end{cases}, \tag{4.29}$$

where $x_1 = u_{11} + iu_{21}$, $x_2 = u_{31} + iu_{41}$ and $x_3 = u_{51}$.

Equating real and imaginary parts of both sides of Eq. (4.29), we can get dynamic equations of all real u_{i1}. The complex system Eq. (4.29) can thus be written in the form of five real first order ODEs:

$$\begin{cases} \dot{u}_{11} = u_{31} \\ \dot{u}_{21} = u_{41} \\ \dot{u}_{31} = -au_{31} - u_{51}(b(c - {u_{11}}^2 + {u_{21}}^2) + du_{51}) + g({u_{11}}^2 - {u_{21}}^2), \\ \dot{u}_{41} = -au_{41} + 2u_{11}u_{21}(bu_{51} + 1) \\ \dot{u}_{51} = u_{11}u_{31} + u_{21}u_{41} - h\sin(u_{51}) \end{cases} \tag{4.30}$$

After exhaustive search, we find that when system parameters $a = 1.21$, $b = -0.87$, $c = 1.75$, $d = 2.2$, $g = 9.3$, $h = 1.01$ and initial conditions $u_{11}(0) = 0.01$, $u_{21}(0) = 0.01$, $u_{31}(0) = 0.01$, $u_{41}(0) = 0.01$ and $u_{51}(0) = 0.01$, chaos of the system are found and illustrated by phase portraits Fig. 4.7.

The slave system is described by

$$\begin{cases} \dot{y}_1 = y_2 \\ \dot{y}_2 = -\hat{a}y_2 - y_3(\hat{b}(\hat{c} - y_1^2) + \hat{d}y_3) + \hat{g}y_1^2 \\ \dot{y}_3 = \frac{1}{2}(\overline{y}_1 y_2 + y_1 \overline{y}_2) - \hat{h}\sin(y_3) \end{cases}, \tag{4.31}$$

where $y_1 = u_{12} + iu_{22}$, $y_2 = u_{32} + iu_{42}$ and $y_3 = u_{52}$.

Equating real and imaginary parts of both sides of Eq. (4.31) and leading $(u_{12}, u_{22}, u_{32}, u_{42}, u_{52})$ to $(u_{11} + F_1(t),\ u_{21} + F_2(t),\ u_{31} + F_3(t),\ u_{41} + F_4(t),\ u_{51} + F_5(t))$, we add real and complex control functions $v_1 + iv_2$, $v_3 + iv_4$ and v_5 to each equation respectively, we can get dynamic equation of all real variables u_{i2} and v_j. The complex system Eq. (4.31) can thus be written in the form of five real first order ODEs:

$$\begin{cases} \dot{u}_{12} = u_{32} + v_1 \\ \dot{u}_{22} = u_{42} + v_2 \\ \dot{u}_{32} = -\hat{a}u_{32} - u_{52}(\hat{b}(\hat{c} - u_{12}^2 + u_{22}^2) + \hat{d}u_{52}) + \hat{g}(u_{12}^2 - u_{22}^2) + v_3 \\ \dot{u}_{42} = -\hat{a}u_{42} + 2u_{12}u_{22}(\hat{b}u_{52} + 1) + v_4 \\ \dot{u}_{52} = u_{12}u_{32} - u_{22}u_{42} - h\sin(u_{52}) + v_5 \end{cases}, \tag{4.32}$$

when initial states be $u_{12}(0) = 20$, $u_{22}(0) = -20$, $u_{32}(0) = 20$, $u_{42}(0) = -20$ and $u_{52}(0) = 20$.

In order to obtain the active control signals, we define the errors between the master and the slave states as $e_{ui} = u_{i1} - u_{i2} + F(t)$ where $F(t) = z = (z_1, z_2, z_3, z_4, z_5)$, where z_1, z_2, z_3 are the states of Lorenz chaotic system and z_4, z_5 are the states of Duffing chaotic system respectively:

$$\begin{cases} \dot{z}_1 = f(z_2 - z_1) \\ \dot{z}_2 = z_1(k - z_3) - z_2 \\ \dot{z}_3 = z_1 z_2 - lz_3 \\ \dot{z}_4 = z_5 \\ \dot{z}_5 = -rz_5 - sz_4 - z_4^3 + o\cos(qt) \end{cases}, \tag{4.33}$$

where $f = 10$, $k = 28$, $l = \frac{3}{8}$, $r = 0.25$, $s = -1$, $o = 0.3$, $q = 1$ and initial states are

$z_1(0)=0.01,\ \ z_2(0)=0.01, z_3(0)=0.01, z_4(0)=2, z_5(0)=2$.

We obtain the errors as

$$\begin{cases} e_{u1}+ie_{u2}=x_1-y_1+(z_1+iz_2)=(u_{11}-u_{12}+z_1)+i(u_{21}-u_{22}+z_2) \\ e_{u3}+ie_{u4}=x_2-y_2+(z_3+iz_4)=(u_{31}-u_{32}+z_3)+i(u_{41}-u_{42}+z_4), \\ e_{u5}=x_5-y_5-z_5=(u_{51}-u_{52}+z_5) \end{cases} \tag{4.34}$$

and our aim is $\lim_{t\to\infty}\mathbf{e}=0$, i.e.

$$\lim_{t\to\infty}e_{ui}=\lim_{t\to\infty}u_{i1}-u_{i2}+z_i=0,\ \ i=1,2,3,4,5. \tag{4.35}$$

However,

$$\begin{cases} \dot{e}_{u1}+i\dot{e}_{u2}=\dot{x}_1-\dot{y}_1+(\dot{z}_1+i\dot{z}_2)=(\dot{u}_{11}-\dot{u}_{12}+\dot{z}_1)+i(\dot{u}_{21}-\dot{u}_{22}+\dot{z}_2) \\ \dot{e}_{u3}+i\dot{e}_{u4}=\dot{x}_2-\dot{y}_2+(\dot{z}_3+i\dot{z}_4)=(\dot{u}_{31}-\dot{u}_{32}+\dot{z}_3)+i(\dot{u}_{41}-\dot{u}_{42}+\dot{z}_4), \\ \dot{e}_{u5}=\dot{x}_5-\dot{y}_5-\dot{z}_5=(\dot{u}_{51}-\dot{u}_{52}+\dot{z}_5) \end{cases} \tag{4.36}$$

Eq. (4.36) describes a dynamical system which the e_{ui} evolve in time and its ODEs.

When equating real and imaginary parts of both sides of Eq. (4.36), we get

$$\begin{cases} \dot{e}_{u1}=\dot{u}_{11}-\dot{u}_{12}+\dot{z}_1=u_{31}-u_{32}-v_1+\dot{z}_1 \\ \dot{e}_{u2}=\dot{u}_{21}-\dot{u}_{22}+\dot{z}_2=u_{41}-u_{42}-v_2+\dot{z}_2 \\ \dot{e}_{u3}=\dot{u}_{31}-\dot{u}_{32}+\dot{z}_3=-au_{31}-u_{51}(b(c-u_{11}^{\ 2}+u_{21}^{\ 2})+du_{51})+g(u_{11}^{\ 2}-u_{21}^{\ 2}) \\ \qquad\qquad +\hat{a}u_{32}+u_{52}(\hat{b}(\hat{c}-u_{12}^{\ 2}+u_{22}^{\ 2})+\hat{d}u_{52})-\hat{g}(u_{12}^{\ 2}-u_{22}^{\ 2}) \\ \qquad\qquad -v_3+\dot{z}_3 \\ \dot{e}_{u4}=\dot{u}_{41}-\dot{u}_{42}+\dot{z}_4=-au_{41}+2u_{11}u_{21}(bu_{51}+1)+\hat{a}u_{42}-2u_{12}u_{22}(\hat{b}u_{52}+1) \\ \qquad\qquad -v_4+\dot{z}_4 \\ \dot{e}_{u5}=\dot{u}_{51}-\dot{u}_{52}+\dot{z}_5=u_{11}u_{31}+u_{21}u_{41}-h\sin(u_{51})-u_{12}u_{32}-u_{22}u_{42}+\hat{h}\sin(u_{52}) \\ \qquad\qquad -v_5+\dot{z}_5 \end{cases}, \tag{4.37}$$

where $\tilde{a}=a-\hat{a}$, $\tilde{b}=b-\hat{b}$, $\tilde{c}=c-\hat{c}$, $\tilde{d}=d-\hat{d}$, $\tilde{g}=g-\hat{g}$, $\tilde{h}=h-\hat{h}$ and $\hat{a}$, $\hat{b}$, $\hat{c}$, $\hat{d}$, $\hat{g}$, $\hat{h}$ are estimates of uncertain parameters a, b, c, d, g and h respectively.

Choose a Lyapunov function in the form of a positive definite function:

$$V(e_{u1}, e_{u2}, e_{u3}, e_{u4}, e_{u5}, \tilde{a}, \tilde{b}, \tilde{c}, \tilde{d}, \tilde{g}, \tilde{h}) = \tfrac{1}{2}({e_{u1}}^2 + {e_{u2}}^2 + {e_{u3}}^2 + {e_{u4}}^2 + {e_{u5}}^2 + \tilde{a}^2 + \tilde{b}^2 + \tilde{c}^2 + \tilde{d}^2 + \tilde{g}^2 + \tilde{h}^2) > 0 \quad . \tag{4.38}$$

Choose parameter dynamics as

$$\begin{cases} \dot{\tilde{a}} = -\dot{\hat{a}} = -\tilde{a}(e_{u3} + e_{u4}) \\ \dot{\tilde{b}} = -\dot{\hat{b}} = -\tilde{b}(e_{u3} + e_{u4}) \\ \dot{\tilde{c}} = -\dot{\hat{c}} = -\tilde{c}(e_{u3} + e_{u4}) \\ \dot{\tilde{d}} = -\dot{\hat{d}} = -\tilde{d}(e_{u3} + e_{u4}) \\ \dot{\tilde{g}} = -\dot{\hat{g}} = -\tilde{g}(e_{u3} + e_{u4}) \\ \dot{\tilde{h}} = -\dot{\hat{h}} = -\tilde{h}e_{u5} \end{cases}, \tag{4.39}$$

Time derivative along any solution of Eq. (3.38) and parameter dynamics is

$$\begin{aligned} \dot{V} = {} & e_{u1}(u_{31} - u_{32} - v_1 + \dot{z}_1) + e_{u2}(u_{41} - u_{42} - v_2 + \dot{z}_2) + e_{u3} \\ & (-au_{31} - u_{51}(b(c - {u_{11}}^2 + {u_{21}}^2) + du_{51}) + g({u_{11}}^2 - {u_{21}}^2) \\ & + \hat{a}u_{32} + u_{52}(\hat{b}(\hat{c} - {u_{12}}^2 + {u_{22}}^2) + \hat{d}u_{52}) - \hat{g}({u_{12}}^2 - {u_{22}}^2) \\ & - v_3 + \dot{z}_3) + e_{u4}(-au_{41} + 2u_{11}u_{21}(bu_{51} + 1) + \hat{a}u_{42} - 2u_{12} \\ & u_{22}(\hat{b}u_{52} + 1) - v_4 + \dot{z}_4) + e_{u5}(u_{11}u_{31} + u_{21}u_{41} - h\sin(u_{51}) \\ & - u_{12}u_{32} - u_{22}u_{42} + \hat{h}\sin(u_{52}) - v_5 + \dot{z}_5) + \tilde{a}(-\dot{\hat{a}}) + \tilde{b}(-\dot{\hat{b}}) \\ & + \tilde{c}(-\dot{\hat{c}}) + \tilde{d}(-\dot{\hat{d}}) + \tilde{g}(-\dot{\hat{g}}) + \tilde{h}(-\dot{\hat{h}}) \end{aligned} \quad . \tag{4.40}$$

Choose

$$\begin{cases} v_1 = u_{31} - u_{32} + \dot{z}_1 + e_{u1} \\ v_2 = u_{41} - u_{42} + \dot{z}_2 + e_{u2} \\ v_3 = -au_{31} - u_{51}(b(c - {u_{11}}^2 + {u_{21}}^2) + du_{51}) + g({u_{11}}^2 - {u_{21}}^2) \\ \qquad + \hat{a}u_{32} + u_{52}(\hat{b}(\hat{c} - {u_{12}}^2 + {u_{22}}^2) + \hat{d}u_{52}) - \hat{g}({u_{12}}^2 - {u_{22}}^2) \\ \qquad + \dot{z}_3 - (\tilde{a}^2 + \tilde{b}^2 + \tilde{c}^2 + \tilde{d}^2 + \tilde{g}^2) + e_{u4} \\ v_4 = -au_{41} + 2u_{11}u_{21}(bu_{51} + 1) + \hat{a}u_{42} - 2u_{12}u_{22}(\hat{b}u_{52} + 1) + \dot{z}_4 \\ \qquad - (\tilde{a}^2 + \tilde{b}^2 + \tilde{c}^2 + \tilde{d}^2 + \tilde{g}^2) + e_{u4} \\ v_5 = u_{11}u_{31} + u_{21}u_{41} - h\sin(u_{51}) - u_{12}u_{32} - u_{22}u_{42} + \hat{h}\sin(u_{52}) \\ \qquad + \dot{z}_5 - \tilde{h}^2 + e_{u5} \end{cases} \quad . \tag{4.41}$$

Substituting Eqs. (4.39) and (4.41) into Eq. (4.40), we obtain

$$\dot{V} = -({e_{u1}}^2 + {e_{u2}}^2 + {e_{u3}}^2 + {e_{u4}}^2 + {e_{u5}}^2) < 0 \,, \tag{4.42}$$

which is a negative semi-definite function of e_{u1}, e_{u2}, e_{u3}, e_{u4}, e_{u5}, $\tilde{a}$, $\tilde{b}$, $\tilde{c}$, $\tilde{d}$, $\tilde{g}$, $\tilde{h}$. The Lyapunov asymptotical stability theorem is not satisfied. We can not obtain that common origin of error dynamics Eq. (4.37) and parameter dynamics Eq. (4.39) are asymptotically stable. However, By pragmatical asymptotically stability theorem, $\mathbf{D}$ is a *n*-manifold, $n = 11$ and the number of error state variables $p = 5$.

When $e_{u1} = e_{u2} = e_{u3} = e_{u4} = e_{u5} = 0$ and $\tilde{a}$, $\tilde{b}$, $\tilde{c}$, $\tilde{d}$, $\tilde{g}$, $\tilde{h}$ take arbitrary values, $\dot{V} < 0$, so $\mathbf{X}$ is 5-manifold, $m = n - p = 11 - 5 = 6$. $m+1 < n$ is satisfied. By pragmatical asymptotical stability theorem, error vector e approaches zero and the estimated parameters also approach the uncertain parameters. The pragmatical generalized synchronization is obtained. Under the assumption of equal probability, it is actually asymptotically stable. The simulation results are shown in Figs. 4.8-4.10.

Case 3.

A new system, i.e. one of the three complex state Ge-Ku systems, studied in this part consists of Ge-Ku system couples with a particularly designed complex conjugate system

$$\begin{cases} \dot{x}_1 = x_2 \\ \dot{x}_2 = -ax_2 - x_3(b(c - x_1^2) + dx_3) + gx_1^2 \\ \dot{x}_3 = \frac{1}{2}(\overline{x}_1 x_1 + \overline{x}_2 x_2) - h\sin(x_3) \end{cases}, \tag{4.43}$$

where $x_1 = u_{11} + iu_{21}$, $x_2 = u_{31} + iu_{41}$ and $x_3 = u_{51}$.

Equating real and imaginary parts of both sides of Eq. (4.43), we can get dynamic equations of all real u_{i1}. The complex system Eq. (4.43) can thus be written in the form of five real first order ODEs:

$$\begin{cases} \dot{u}_{11} = u_{31} \\ \dot{u}_{21} = u_{41} \\ \dot{u}_{31} = -au_{31} - u_{51}(b(c - {u_{11}}^2 + {u_{21}}^2) + du_{51}) + g({u_{11}}^2 - {u_{21}}^2), \\ \dot{u}_{41} = -au_{41} + 2u_{11}u_{21}(bu_{51} + 1) \\ \dot{u}_{51} = {u_{11}}^2 + {u_{21}}^2 + {u_{31}}^2 + {u_{41}}^2 - h\sin(u_{51}) \end{cases} \tag{4.44}$$

After exhaustive search, we find that when system parameters $a = 2.48$, $b = -1.51$, $c = 1.79$, $d = 30.95$, $g = -1.67$, $h = 115$ and initial conditions are $u_{11}(0) = 0.01$, $u_{21}(0) = 0.01$, $u_{31}(0) = 0.01$, $u_{41}(0) = 0.01$ and $u_{51}(0) = 0.01$, chaos of the system are found and illustrated by phase portraits Fig. 4.11.

The slave system is described by

$$\begin{cases} \dot{y}_1 = y_2 \\ \dot{y}_2 = -\hat{a}y_2 - y_3(\hat{b}(\hat{c} - y_1^2) + \hat{d}y_3) + \hat{g}y_1^2, \\ \dot{y}_3 = \frac{1}{2}(\bar{y}_1 y_1 + \bar{y}_2 y_2) - \hat{h}\sin(y_3) \end{cases} \tag{4.45}$$

where $y_1 = u_{12} + iu_{22}$, $y_2 = u_{32} + iu_{42}$ and $y_3 = u_{52}$.

Equating real and imaginary parts of both sides of Eq. (4.45) and leading $(u_{12}, u_{22}, u_{32}, u_{42}, u_{52})$ to $(u_{11} + F_1(t),\ u_{21} + F_2(t),\ u_{31} + F_3(t),\ u_{41} + F_4(t),\ u_{51} + F_5(t))$, we add real and complex control functions $v_1 + iv_2$, $v_3 + iv_4$ and v_5 to each equation respectively, we can get dynamic equation of all real variables u_{i2} and v_j. The complex system Eq. (4.45) can thus be written in the form of five real first order ODEs:

$$\begin{cases} \dot{u}_{12} = u_{32} + v_1 \\ \dot{u}_{22} = u_{42} + v_2 \\ \dot{u}_{32} = -\hat{a}u_{32} - u_{52}(\hat{b}(\hat{c} - {u_{12}}^2 + {u_{22}}^2) + \hat{d}u_{52}) + \hat{g}({u_{12}}^2 - {u_{22}}^2) + v_3, \\ \dot{u}_{42} = -\hat{a}u_{42} + 2u_{12}u_{22}(\hat{b}u_{52} + 1) + v_4 \\ \dot{u}_{52} = {u_{12}}^2 + {u_{22}}^2 + {u_{32}}^2 + {u_{42}}^2 - h\sin(u_{52}) + v_5 \end{cases} \tag{4.46}$$

when initial states be $u_{12}(0) = 10$, $u_{22}(0) = 10$, $u_{32}(0) = 10$, $u_{42}(0) = 10$ and $u_{52}(0) = 10$.

In order to obtain the active control signals, we define the errors between the

drive and the response states as $e_{ui} = u_{i1} - u_{i2} + F(t)$ where $F(t) = z = (z_1, z_2, z_3, z_4, z_5)$, where z_1, z_2, z_3 are the states of Lorenz chaotic system and z_4, z_5 are the states of Duffing chaotic system respectively:

$$\begin{cases} \dot{z}_1 = f(z_2 - z_1) \\ \dot{z}_2 = z_1(k - z_3) - z_2 \\ \dot{z}_3 = z_1 z_2 - l z_3 \\ \dot{z}_4 = z_5 \\ \dot{z}_5 = -r z_5 - s z_4 - z_4^3 + o\cos(qt) \end{cases}, \tag{4.47}$$

where $f = 10$, $k = 28$, $l = \frac{3}{8}$, $r = 0.25$, $s = -1$, $o = 0.3$, $q = 1$ and initial states are $z_1(0) = 0.01$, $z_2(0) = 0.01, z_3(0) = 0.01, z_4(0) = 2, z_5(0) = 2$.

We obtain the errors as

$$\begin{cases} e_{u1} + ie_{u2} = x_1 - y_1 + (z_1 + iz_2) = (u_{11} - u_{12} + z_1) + i(u_{21} - u_{22} + z_2) \\ e_{u3} + ie_{u4} = x_2 - y_2 + (z_3 + iz_4) = (u_{31} - u_{32} + z_3) + i(u_{41} - u_{42} + z_4), \\ e_{u5} = x_5 - y_5 - z_5 = (u_{51} - u_{52} + z_5) \end{cases} \tag{4.48}$$

and our aim is $\lim_{t\to\infty} \mathbf{e} = 0$, i.e.

$$\lim_{t\to\infty} e_{ui} = \lim_{t\to\infty} u_{i1} - u_{i2} + z_i = 0, \; i = 1, 2, 3, 4, 5. \tag{4.49}$$

However,

$$\begin{cases} \dot{e}_{u1} + i\dot{e}_{u2} = \dot{x}_1 - \dot{y}_1 + (\dot{z}_1 + i\dot{z}_2) = (\dot{u}_{11} - \dot{u}_{12} + \dot{z}_1) + i(\dot{u}_{21} - \dot{u}_{22} + \dot{z}_2) \\ \dot{e}_{u3} + i\dot{e}_{u4} = \dot{x}_2 - \dot{y}_2 + (\dot{z}_3 + i\dot{z}_4) = (\dot{u}_{31} - \dot{u}_{32} + \dot{z}_3) + i(\dot{u}_{41} - \dot{u}_{42} + \dot{z}_4), \\ \dot{e}_{u5} = \dot{x}_5 - \dot{y}_5 - \dot{z}_5 = (\dot{u}_{51} - \dot{u}_{52} + \dot{z}_5) \end{cases} \tag{4.50}$$

Eq. (4.50) describes a dynamical system which the e_{ui} evolve in time and its ODEs.

When equating real and imaginary parts of both sides of Eq. (4.50), we get

$$\begin{cases} \dot{e}_{u1} = \dot{u}_{11} - \dot{u}_{12} + \dot{z}_1 = \mu_{11} - \mu_{12} - v_1 + \dot{z}_1 \\ \dot{e}_{u2} = \dot{u}_{21} - \dot{u}_{22} + \dot{z}_2 = \mu_{21} - \mu_{22} - v_2 + \dot{z}_2 \\ \dot{e}_{u3} = \dot{u}_{31} - \dot{u}_{32} + \dot{z}_3 = -au_{31} - \mu_{31}(b(c_{31} - u_{11}^2 + u_{21}^2) + du_{21}) + g(u_{51}^2 - u_{31}^2) \\ \qquad + \hat{a}u_{32} + u_{52}(\hat{b}(\hat{c} - u_{12}^2 + u_{22}^2) + \hat{d}u_{52}) - \hat{g}(u_{12}^2 - u_{22}^2) \\ \qquad - v_3 + \dot{z}_3 \\ \dot{e}_{u4} = \dot{u}_{41} - \dot{u}_{42} + \dot{z}_4 = -au_{41} + 2u_{11}u_{21}(bu_{51} + 1) + \hat{a}u_{42} - 2u_{12}u_{22}(\hat{b}u_{52} + 1) \\ \qquad - v_4 + \dot{z}_4 \\ \dot{e}_{u5} = \dot{u}_{51} - \dot{u}_{52} + \dot{z}_5 = u_{11}^2 + u_{21}^2 + u_{31}^2 + u_{41}^2 - h\sin(u_{51}) - u_{12}^2 - u_{22}^2 - u_{32}^2 \\ \qquad - u_{42}^2 + \hat{h}\sin(u_{52}) - v_5 + \dot{z}_5 \end{cases}, \quad (4.51)$$

where $\tilde{a} = a - \hat{a}$, $\tilde{b} = b - \hat{b}$, $\tilde{c} = c - \hat{c}$, $\tilde{d} = d - \hat{d}$, $\tilde{g} = g - \hat{g}$, $\tilde{h} = h - \hat{h}$ and $\hat{a}$, $\hat{b}$, $\hat{c}$, $\hat{d}$, $\hat{g}$, $\hat{h}$ are estimates of uncertain parameters a, b, c, d, g and h respectively.

Choose a Lyapunov function in the form of a positive definite function:

$$\begin{aligned} &V(e_{u1}, e_{u2}, e_{u3}, e_{u4}, e_{u5}, \tilde{a}, \tilde{b}, \tilde{c}, \tilde{d}, \tilde{g}, \tilde{h}) \\ &= \tfrac{1}{2}(e_{u1}^2 + e_{u2}^2 + e_{u3}^2 + e_{u4}^2 + e_{u5}^2 + \tilde{a}^2 + \tilde{b}^2 + \tilde{c}^2 + \tilde{d}^2 + \tilde{g}^2 + \tilde{h}^2) > 0 \end{aligned}. \quad (4.52)$$

Choose parameter dynamics as

$$\begin{cases} \dot{\tilde{a}} = -\dot{\hat{a}} = -\tilde{a}(e_{u3} + e_{u4}) \\ \dot{\tilde{b}} = -\dot{\hat{b}} = -\tilde{b}(e_{u3} + e_{u4}) \\ \dot{\tilde{c}} = -\dot{\hat{c}} = -\tilde{c}(e_{u3} + e_{u4}) \\ \dot{\tilde{d}} = -\dot{\hat{d}} = -\tilde{d}(e_{u3} + e_{u4}) \\ \dot{\tilde{g}} = -\dot{\hat{g}} = -\tilde{g}(e_{u3} + e_{u4}) \\ \dot{\tilde{h}} = -\dot{\hat{h}} = -\tilde{h}e_{u5} \end{cases}, \quad (4.53)$$

Time derivative of V along any solution of Eq. (4.52) and parameter dynamics is

$$
\begin{aligned}
\dot{V} = {} & e_{u1}(u_{31} - u_{32} - v_1 + \dot{z}_1) + e_{u2}(u_{41} - u_{42} - v_2 + \dot{z}_2) + e_{u3} \\
& (-au_{31} - u_{51}(b(c - u_{11}^{\ 2} + u_{21}^{\ 2}) + du_{51}) + g(u_{11}^{\ 2} - u_{21}^{\ 2}) \\
& + \hat{a}u_{32} + u_{52}(\hat{b}(\hat{c} - u_{12}^{\ 2} + u_{22}^{\ 2}) + \hat{d}u_{52}) - \hat{g}(u_{12}^{\ 2} - u_{22}^{\ 2}) \\
& - v_3 + \dot{z}_3) + e_{u4}(-au_{41} + 2u_{11}u_{21}(bu_{51} + 1) + \hat{a}u_{42} - 2u_{12} \\
& u_{22}(\hat{b}u_{52} + 1) - v_4 + \dot{z}_4) + e_{u5}(u_{11}^{\ 2} + u_{21}^{\ 2} + u_{31}^{\ 2} + u_{41}^{\ 2} \\
& - h\sin(u_{51}) - u_{12}^{\ 2} - u_{22}^{\ 2} - u_{32}^{\ 2} - u_{42}^{\ 2} + \hat{h}\sin(u_{52}) - v_5 \\
& + \dot{z}_5) + \tilde{a}(-\dot{\hat{a}}) + \tilde{b}(-\dot{\hat{b}}) + \tilde{c}(-\dot{\hat{c}}) + \tilde{d}(-\dot{\hat{d}}) + \tilde{g}(-\dot{\hat{g}}) + \tilde{h}(-\dot{\hat{h}})
\end{aligned}
\quad . \tag{4.54}
$$

Choose

$$
\begin{cases}
v_1 = u_{31} - u_{32} + \dot{z}_1 + e_{u1} \\
v_2 = u_{41} - u_{42} + \dot{z}_2 + e_{u2} \\
v_3 = -au_{31} - u_{51}(b(c - u_{11}^{\ 2} + u_{21}^{\ 2}) + du_{51}) + g(u_{11}^{\ 2} - u_{21}^{\ 2}) \\
\qquad + \hat{a}u_{32} + u_{52}(\hat{b}(\hat{c} - u_{12}^{\ 2} + u_{22}^{\ 2}) + \hat{d}u_{52}) - \hat{g}(u_{12}^{\ 2} - u_{22}^{\ 2}) \\
\qquad + \dot{z}_3 - (\tilde{a}^2 + \tilde{b}^2 + \tilde{c}^2 + \tilde{d}^2 + \tilde{g}^2) + e_{u4} \\
v_4 = -au_{41} + 2u_{11}u_{21}(bu_{51} + 1) + \hat{a}u_{42} - 2u_{12}u_{22}(\hat{b}u_{52} + 1) + \dot{z}_4 \\
\qquad - (\tilde{a}^2 + \tilde{b}^2 + \tilde{c}^2 + \tilde{d}^2 + \tilde{g}^2) + e_{u4} \\
v_5 = u_{11}^{\ 2} + u_{21}^{\ 2} + u_{31}^{\ 2} + u_{41}^{\ 2} - h\sin(u_{51}) - u_{12}^{\ 2} - u_{22}^{\ 2} - u_{32}^{\ 2} - u_{42}^{\ 2} \\
\qquad + \hat{h}\sin(u_{52}) + \dot{z}_5 - \tilde{h}^2 + e_{u5}
\end{cases}
\quad . \tag{4.55}
$$

Substituting Eqs. (3.53) and (3.55) into Eq. (3.54), we obtain

$$
\dot{V} = -(e_{u1}^{\ 2} + e_{u2}^{\ 2} + e_{u3}^{\ 2} + e_{u4}^{\ 2} + e_{u5}^{\ 2}) < 0 , \tag{4.56}
$$

which is a negative semi-definite function of e_{u1}, e_{u2}, e_{u3}, e_{u4}, e_{u5}, $\tilde{a}$, $\tilde{b}$, $\tilde{c}$, $\tilde{d}$, $\tilde{g}$, $\tilde{h}$. The Lyapunov asymptotical stability theorem is not satisfied. We can't obtain that common origin of error dynamics Eq. (4.51) and parameter dynamics Eq. (4.53) are asymptotically stable. However, By pragmatical asymptotically stability theorem, $\mathbf{D}$ is a *n*-manifold, *n*=11 and the number of error state variables $p = 5$.

When $e_{u1} = e_{u2} = e_{u3} = e_{u4} = e_{u5} = 0$ and $\tilde{a}$, $\tilde{b}$, $\tilde{c}$, $\tilde{d}$, $\tilde{g}$, $\tilde{h}$ take arbitrary values, $\dot{V} < 0$, so $\mathbf{X}$ is 5-manifold, $m = n - p = 11 - 5 = 6$. $m+1 < n$ is satisfied. By pragmatical asymptotical stability theorem, error vector e approaches zero and the

estimated parameters also approach the uncertain parameters. The pragmatical generalized synchronization is obtained. Under the assumption of equal probability, it is actually asymptotically stable. The simulation results are shown in Figs. 4.12-4.14.

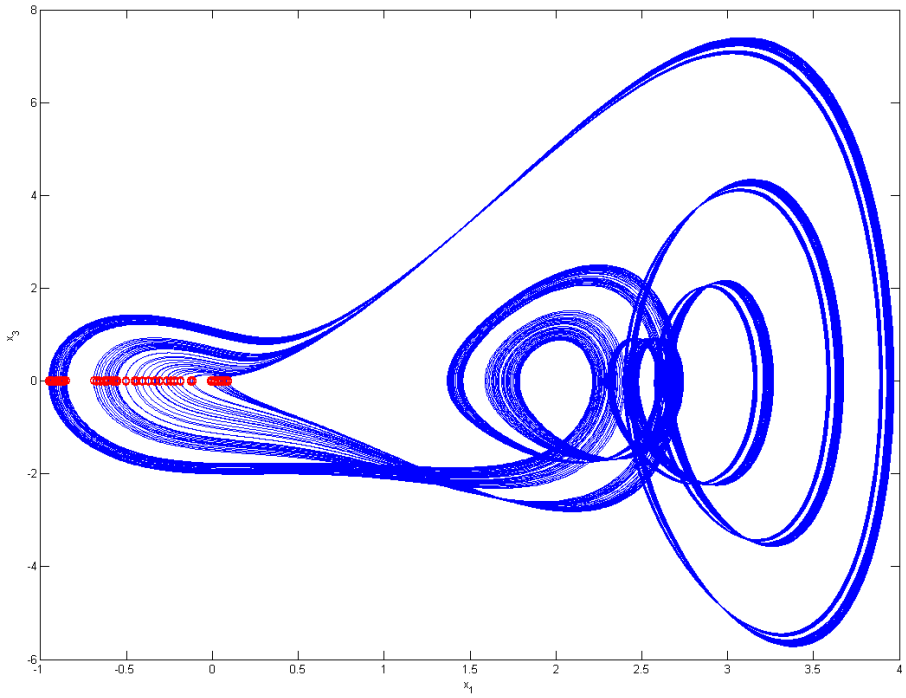

Fig. 4.1 The chaotic attractor of complex state Ge-Ku system Case 1.

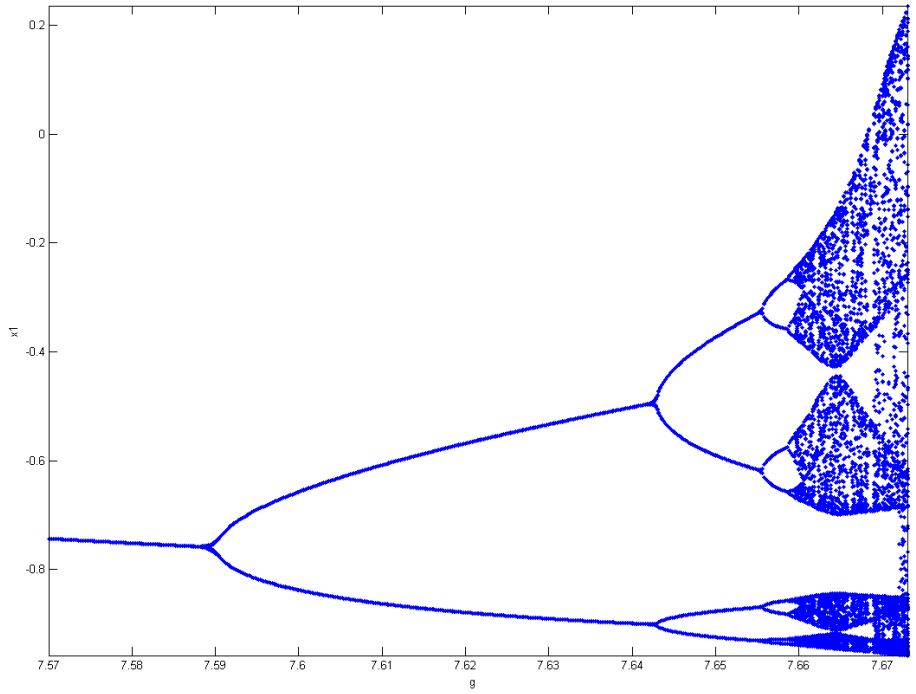

Fig. 4.2 The bifurcation diagram of complex state Ge-Ku system Case 1.

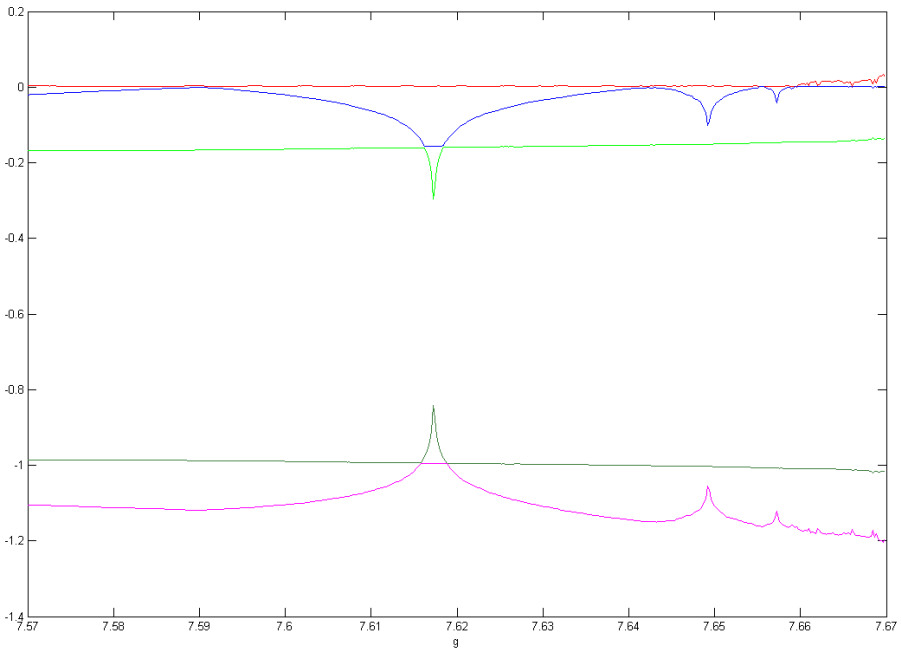

Fig. 4.3 The Lyapunov exponents of complex state Ge-Ku system Case 1.

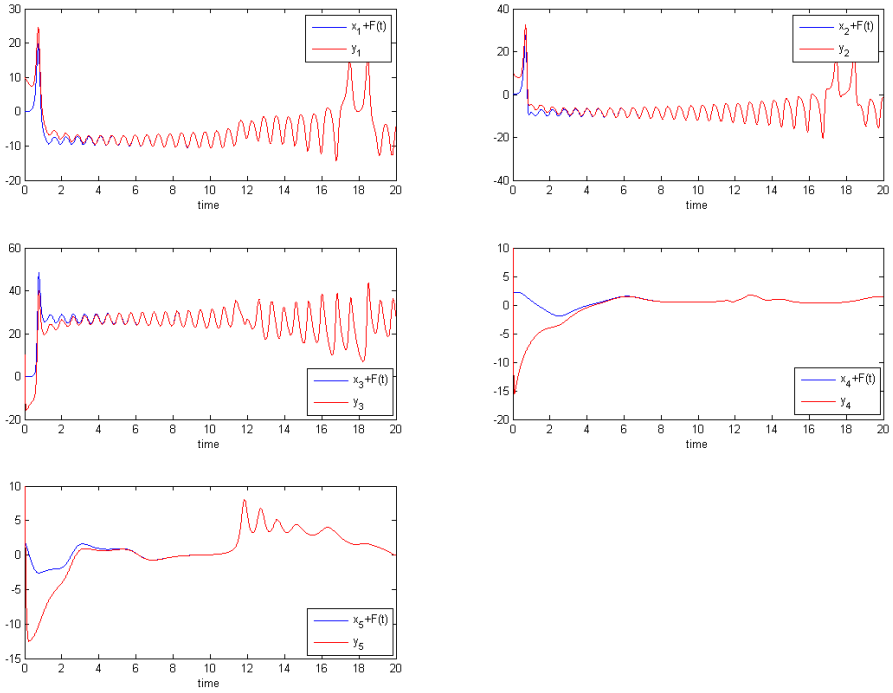

Fig. 4.4 Time histories of $x_i + F(t)$, y_i for Case 1.

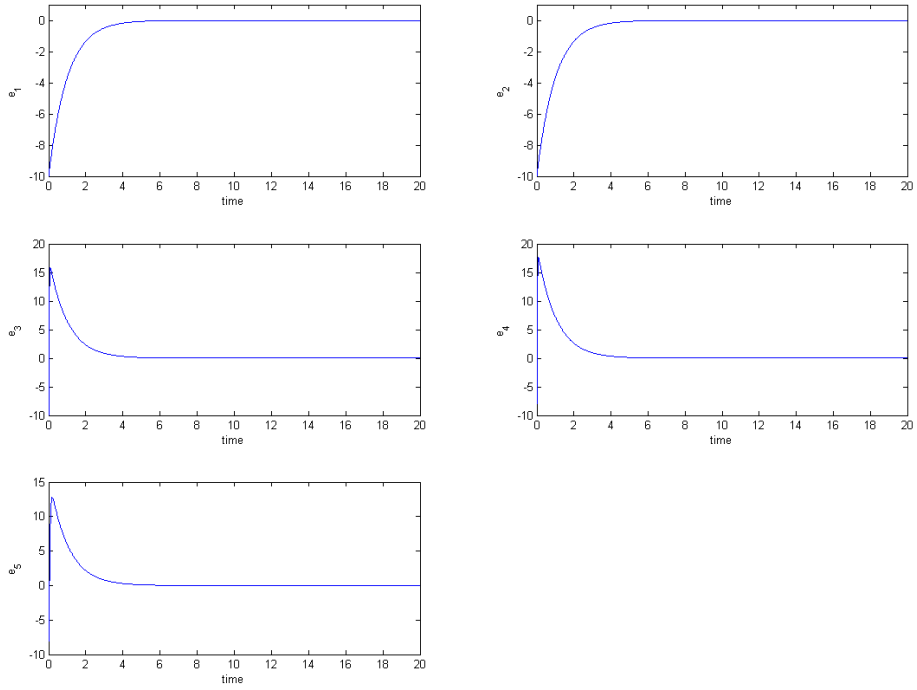

Fig. 4.5 Time histories of errors for Case 1.

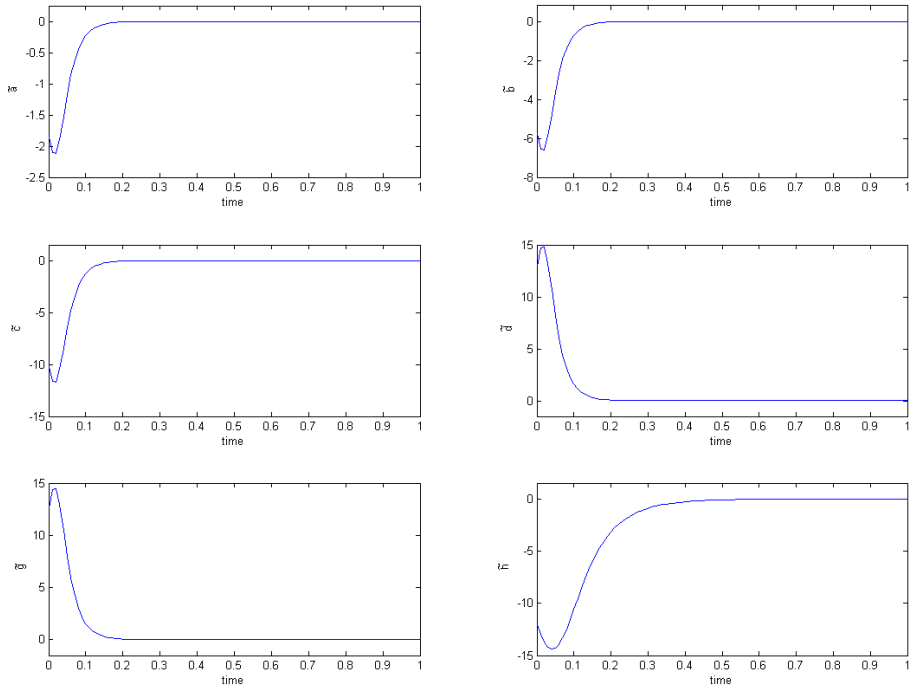

Fig. 4.6 Time histories of parameter errors for Case 1.

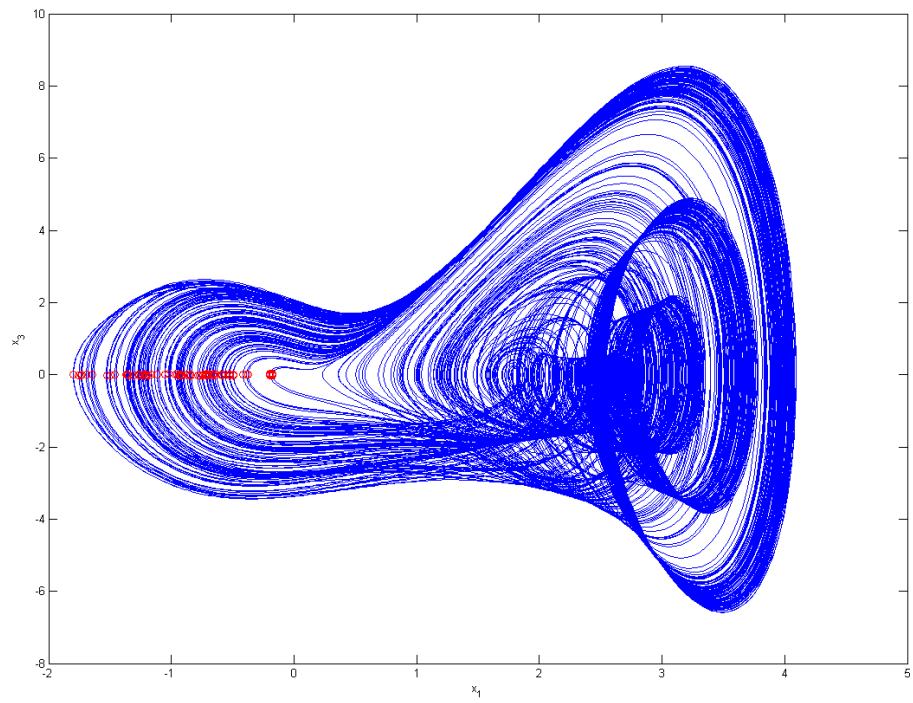

Fig. 4.7 The chaotic attractor of complex state Ge-Ku system Case 2.

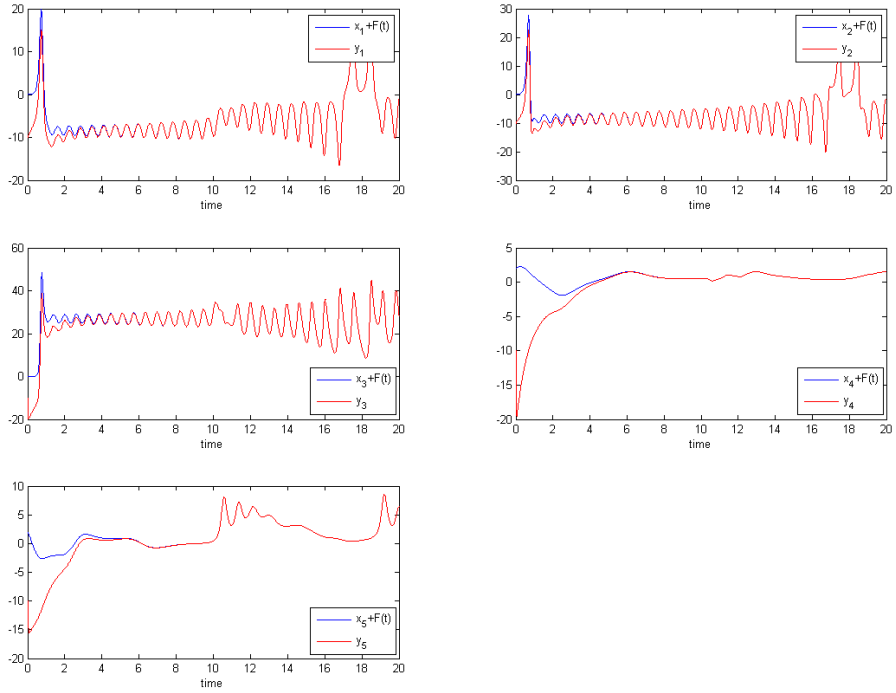

Fig. 4.7 Time histories of $x_i + F(t)$, y_i for Case 2.

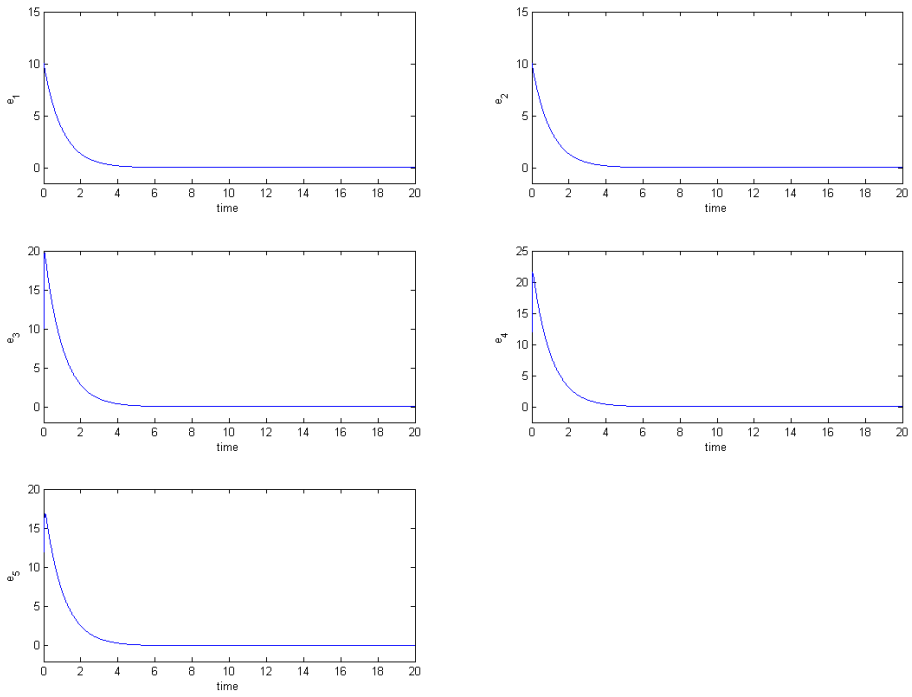

Fig. 4.9 Time histories of errors for Case 2.

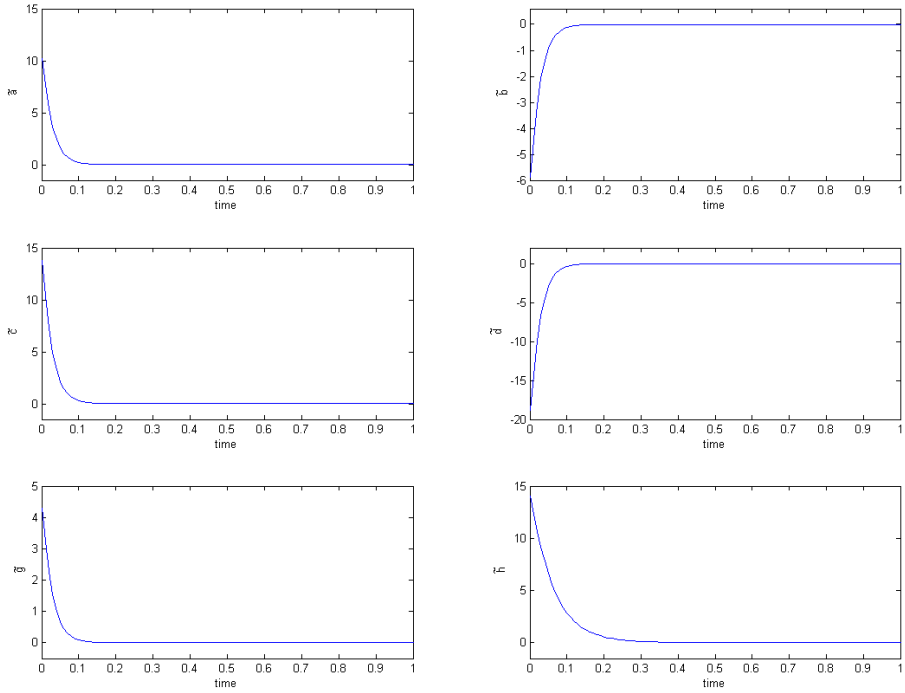

Fig. 4.10 Time histories of parameter errors for Case 2.

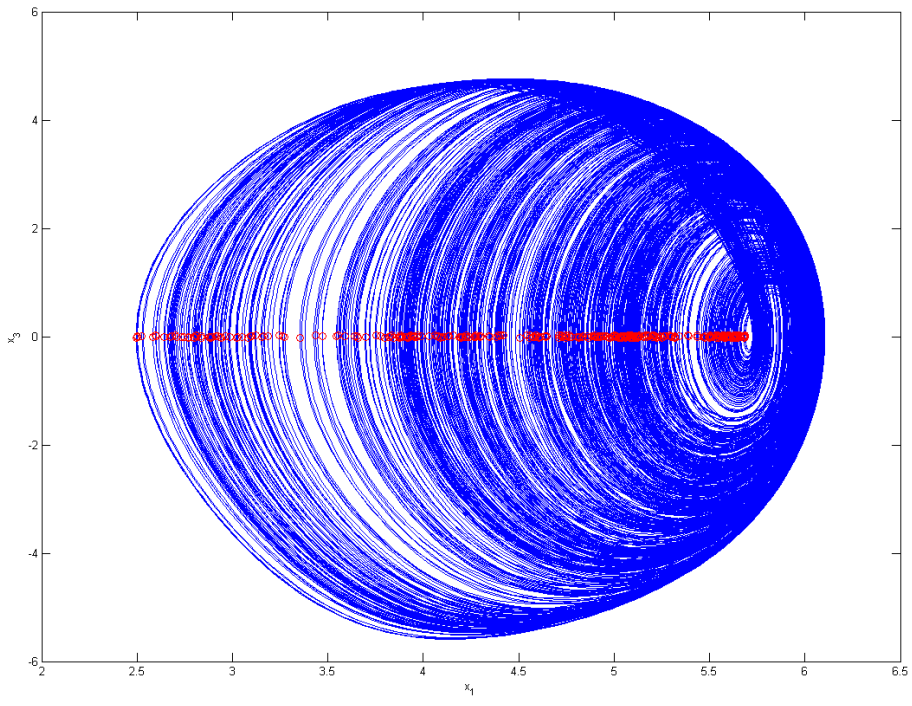

Fig. 4.11 The chaotic attractor of complex state Ge-Ku system Case 3.

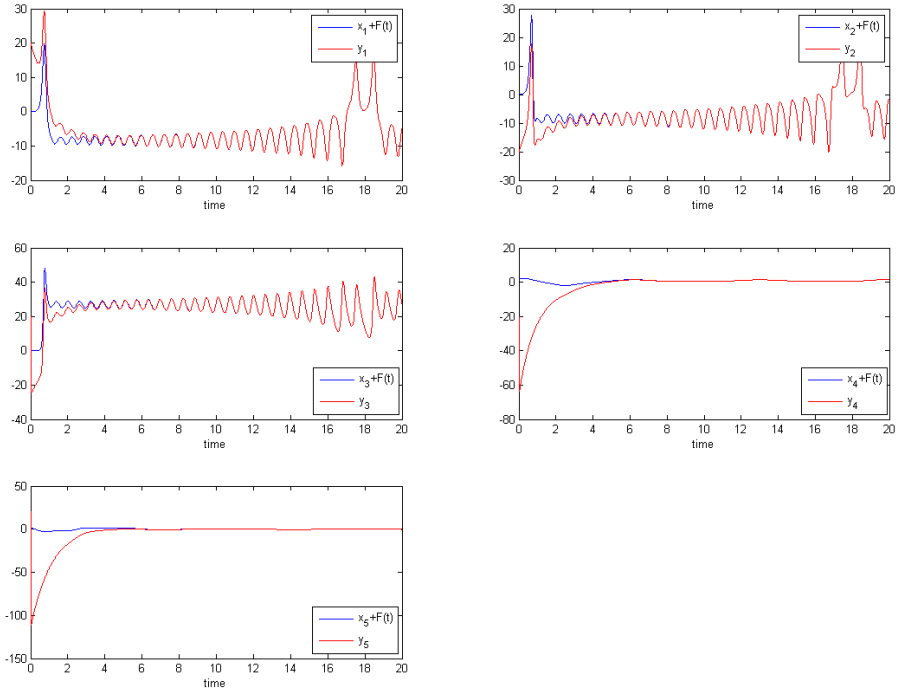

Fig. 4.14 Time histories of $x_i + F(t)$, y_i for Case 3.

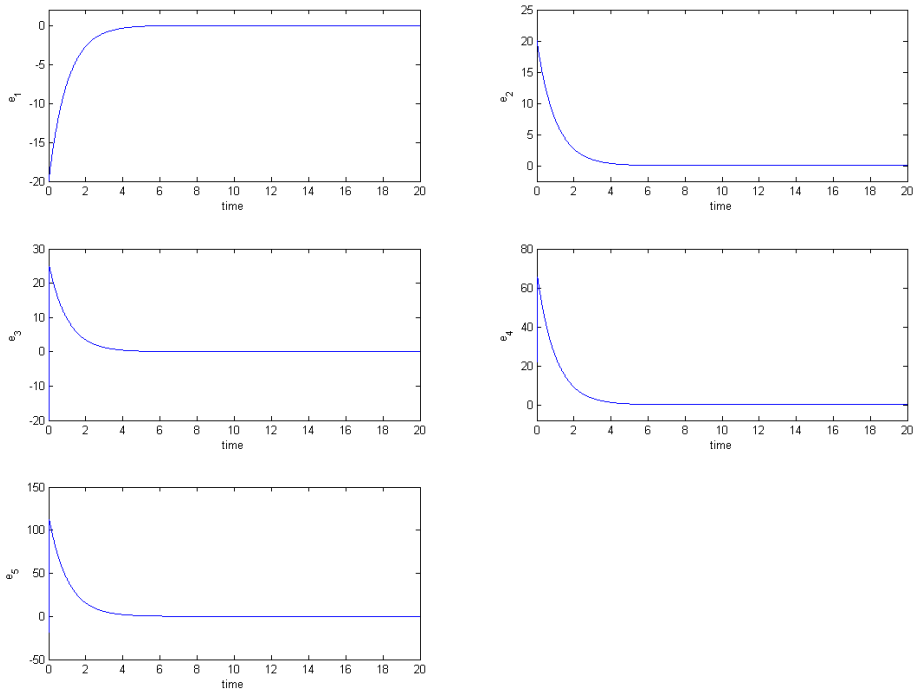

Fig. 4.13 Time histories of errors for Case 3.

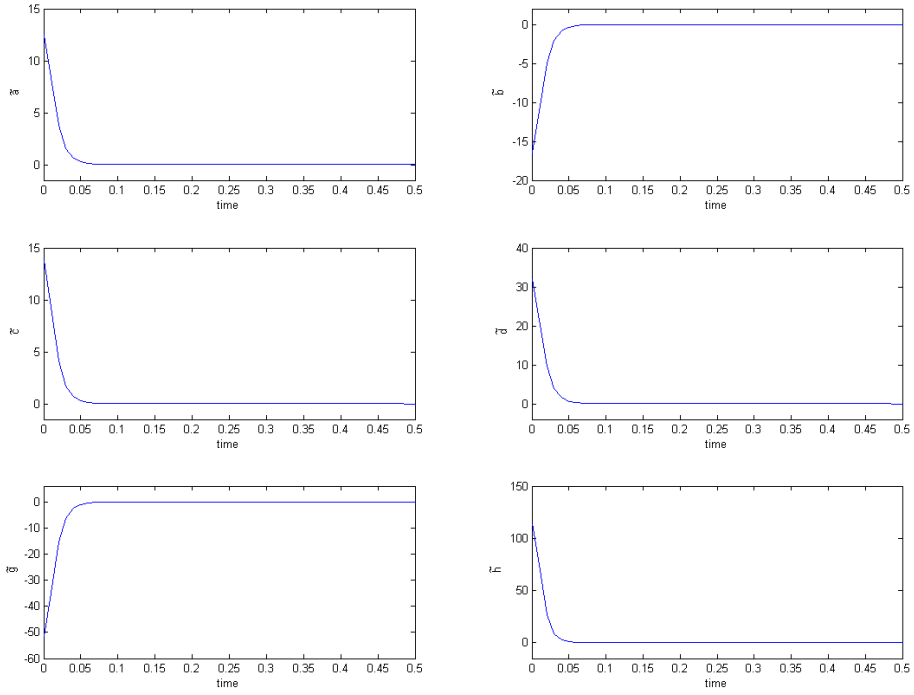

Fig. 4.14 Time histories of parameter errors for Case 3.

Chapter 5

Use Partial Region Stability Theory for Different Translation Synchronization

5.1 Preliminary

In this Chapter, a new strategy by using pragmatical synchronization theorem and GYC partial region stability theory are proposed to achieve chaos generalized synchronization. Using the pragmatical theorem of asymptotical stability and an adaptive control law, it can be proved strictly that the common zero solution of error dynamics and of parameter dynamics is asymptotically stable. In addition, using the GYC partial region stability theorem, the new Lyapunov function used is a simple linear homogeneous function of error states and the lower order controllers are much more simple. Numerical simulations of a new GKv system is given to show the effectiveness of the proposed scheme.

5.2 The Scheme of Using Partial Region Pragmatic Stability Theory for Different Translation Synchronization Scheme

There are two identical nonlinear dynamical systems, and the master system synchronizes the slave system. The master system is given by

$$\dot{\mathbf{x}} = \mathbf{A}\mathbf{x} + \mathbf{f}(\mathbf{x}, \mathbf{B}) \tag{5.1}$$

The master system after the origin of x-coordinate system is translated to $[k_1, k_1, \cdots, k_1]$ is

$$\dot{\mathbf{x}}' = \mathbf{A}\mathbf{x}' + \mathbf{f}(\mathbf{x}', \mathbf{B}) \tag{5.1'}$$

where $\mathbf{x}' = [x_1', x_2', \cdots, x_n']^T = \mathbf{x} - \mathbf{K_1} = [x_1 - k_1, x_2 - k_1, \cdots, x_n - k_1] \in R^n$ denotes a state vector, where $\mathbf{K}_1$ is a constant vector with positive component k_1 as shown in Fig. 5.1. $\mathbf{A}$ is an $n \times n$ uncertain constant coefficients matrix, $\mathbf{f}$ is a nonlinear vector

function, and $\mathbf{B}$ is a vector of uncertain constant coefficients in $\mathbf{f}$.

The slave system is given by

$$\dot{\mathbf{y}} = \mathbf{A}\mathbf{y} + \mathbf{f}(\mathbf{y}, \mathbf{B}) + \mathbf{u}(t) \tag{5.2}$$

The slave system after the origin of y-coordinate system is translated to $[k_2, k_2, \cdots, k_2]$ is

$$\dot{\mathbf{y}}' = \mathbf{A}\mathbf{y}' + \mathbf{f}(\mathbf{y}', \mathbf{B}) + \mathbf{u}(t) \tag{5.2'}$$

where $\mathbf{y}' = [y_1', y_2', \cdots, y_n']^T = \mathbf{y} - \mathbf{K}_2 = [y_1 - k_2, y_2 - k_2, \cdots, y_n - k_2] \in R^n$ denotes a state vector, where $\mathbf{K}_2$ is a constant vector with positive component k_2 as shown in Fig. 5.2. $\mathbf{A}$ is an $n \times n$ estimated coefficient matrix, $\mathbf{B}$ is a vector of estimated coefficients in $\mathbf{f}$, and $\mathbf{u}(t) = [u_1(t), u_2(t), \cdots, u_n(t)]^T \in R^n$ is a control input vector.

Our goal is to design a controller $u(t)$ so that the state vector of the translated slave system Eq. (5.2′) asymptotically approaches the state vector of the translated master system Eq. (5.1′) plus a given chaotic vector function $\mathbf{F}(t) = [F_1(t), F_2(t), \cdots, F_n(t)]^T$. This is a special kind of generalized synchronization, $\mathbf{y}$ is a given function of $\mathbf{x}$

$$\mathbf{y}' = \mathbf{G}(\mathbf{x}', \mathbf{y}', t) = \mathbf{x}' + \mathbf{F}(\mathbf{x}', \mathbf{y}', t) \tag{5.3}$$

The synchronization can be accomplished when $t \to \infty$, the limit of the error vector $\mathbf{e}(t) = [e_1, e_2, \cdots, e_n]^T$ approaches zero:

$$\lim_{t \to \infty} \mathbf{e} = 0 \tag{5.4}$$

where

$$\mathbf{e} = \mathbf{x}' - \mathbf{y}' + \mathbf{F}(t) \tag{5.5}$$

from Eq. (5.5), we have

$$\dot{\mathbf{e}} = \dot{\mathbf{x}}' - \dot{\mathbf{y}}' + \dot{\mathbf{F}}(t) \tag{5.6}$$

$$\dot{\mathbf{e}} = \mathbf{A}\mathbf{x}' - \mathbf{A}\mathbf{y}' + \mathbf{f}(\mathbf{x}', \mathbf{B}) - \mathbf{f}(\mathbf{y}', \mathbf{B}) + \dot{\mathbf{F}}(t) - \mathbf{u}(t) \tag{5.7}$$

where k_1 and k_2 are chosen to guarantee that the error dynamics always occurs in the first guardant of $\mathbf{e}$ coordinate system.

A Lyapunov function $V(\mathbf{e}, \mathbf{A}, \mathbf{B})$ is chosen as a positive definite function in first guardant of $\mathbf{e}$ coordinate system by stability theory in partial region as shown in Appendix A:

$$V(\mathbf{e}, \mathbf{A}, \mathbf{B}) = \mathbf{e} + \mathbf{A} + \mathbf{B} \tag{5.8}$$

where $\mathbf{A} = \mathbf{A} - \mathbf{A}$, $\mathbf{B} = \mathbf{B} - \mathbf{B}$, $\mathbf{A}$ and $\mathbf{B}$ are two column matrices whose elements are all the elements of matrix $\mathbf{A}$ and of matrix $\mathbf{B}$, respectively.

Its derivative along any solution of the differential equation system consisting of Eq. (5.7) and update parameter differential equations for $\mathbf{A}$ and $\mathbf{B}$ is

$$\dot{V}(\mathbf{e}, \mathbf{A}, \mathbf{B}) = \mathbf{A}\mathbf{x} - \mathbf{A}\mathbf{y} + \mathbf{f}(\mathbf{x}', \mathbf{B}) - \mathbf{f}(\mathbf{y}', \mathbf{B}) + \dot{\mathbf{F}}(t) - \mathbf{u}(t) + \dot{\tilde{\mathbf{A}}} + \dot{\tilde{\mathbf{B}}} \tag{5.9}$$

where $\mathbf{u}(t)$, $\dot{\tilde{\mathbf{A}}}$ and $\dot{\tilde{\mathbf{B}}}$ are chosen so that $\dot{V} = \mathbf{C}\mathbf{e}$, $\mathbf{C}$ is a diagonal negative definite matrix, and $\dot{V}$ is a negative semi-definite function of $\mathbf{e}$ and parameter differences $\tilde{\mathbf{A}}$ and $\tilde{\mathbf{B}}$. By pragmatical asymptotically stability theorem in Appendix B.

In this Chapter, a new GKv system is used as an example. The Lyapunov function used is a simple linear homogeneous function of states and the controllers are simpler than tradition. Because they in lower order than the that of traditional controllers. In many paper [32-35], traditional Lyapunov stability theorem and Babalat's lemma [26] are used to prove the error vector approaches zero, as time approaches infinity. But the question, why the estimated parameters also approach to the uncertain parameters, remains no answer. By pragmatical asymptotical stability theorem, the question can be answered strictly.

5.3 Different Translation Pragmatical Generalized Synchronization of New Ge-Ku-van der Pol Chaotic System

Case 1.

The following chaotic systems are two translated GKv of which the old origin is translated to $(x_1, x_2, x_3) = (k_1, k_1, k_1)$, $(y_1, y_2, y_3) = (k_2, k_2, k_2)$ to guarantee the uncontrolled error dynamics always happen in the first quadrant of e coordinate system when $k_1 = 150, k_2 = 30$.

$$\begin{cases} \dot{x}_1 = (x_2 - k_1) \\ \dot{x}_2 = -a(x_2 - k_1) - (x_3 - k_1)(b(c - (x_1 - k_1)^2) + d(x_3 - k_1)) \\ \dot{x}_3 = -g(x_3 - k_1) + h(1 - (x_3 - k_1)^2)(x_2 - k_1) + l(x_1 - k_1) \end{cases} \tag{5.10}$$

$$\begin{cases} \dot{y}_1 = (y_2 - k_2) + u_1 \\ \dot{y}_2 = -a(y_2 - k_2) - (y_3 - k_2)(\hat{b}(\hat{c} - (y_1 - k_2)^2) + d(y_3 - k_2)) + u_2 \\ \dot{y}_3 = -g(y_3 - k_2) + h(1 - (y_3 - k_2)^2)(y_2 - k_2) + \hat{l}(y_1 - k_2) + u_3 \end{cases} \tag{5.11}$$

Let initial states be $(x_1, x_2, x_3) = (k_1 + 0.01, k_1 + 0.01, k_1 + 0.01)$, $(y_1, y_2, y_3) = (k_2 + 0.01, k_2 + 0.01, k_2 + 0.01)$ and system parameters $a = 0.08, b = -0.35, c = 100.56, d = -1000.02, g = 0.61, h = 0.08, l = 0.01$.

The state error is $e = x' - y' + F(t) = x' - y' + e^{-\sin t}$ where $F(t) = e^{-\sin t}$ is a non-chaotic given function of time. We find that the uncontrolled error dynamics always exist in first quadrant as shown in Fig. 5.3.

$$\lim_{t \to \infty} e_i = \lim_{t \to \infty} (x_i - y_i + e^{-\sin t}) = 0, \quad i = 1, 2, 3 \tag{5.12}$$

Our aim is $\lim_{t \to \infty} e = 0$. We obtain the error dynamics:

$$\begin{cases} \dot{e}_1 = \dot{x}_1 - \dot{y}_1 - \cos t \cdot e^{-\sin t} \\ \dot{e}_2 = \dot{x}_2 - \dot{y}_2 - \cos t \cdot e^{-\sin t} \\ \dot{e}_3 = \dot{x}_3 - \dot{y}_3 - \cos t \cdot e^{-\sin t} \end{cases} \tag{5.13}$$

where $\tilde{a} = a - \hat{a}$, $\tilde{b} = b - \hat{b}$, $\tilde{c} = c - \hat{c}$, $\tilde{d} = d - \hat{d}$, $\tilde{g} = g - \hat{g}$, $\tilde{h} = h - \hat{h}$, $\tilde{l} = l - \hat{l}$,

and a, $\hat{b}$, $\hat{c}$, d, g, h, $\hat{l}$ are estimates of uncertain parameters a, b, c, d, g, h and l respectively.

Using different translation pragmatical synchronization by stability theory of partial region, we can choose a Lyapunov function in the form of a positive definite function in first quadrant:

$$V = e_1 + e_2 + e_3 + a + \tilde{b} + \tilde{c} + d + g + h + \tilde{l} \tag{5.14}$$

Its time derivative is

$$\begin{aligned}
\dot{V} &= \dot{e}_1 + \dot{e}_2 + \dot{e}_3 + \dot{\tilde{a}} + \dot{\tilde{b}} + \dot{\tilde{c}} + \dot{\tilde{d}} + \dot{\tilde{g}} + \dot{\tilde{h}} + \dot{\tilde{l}} \\
&= ((x_2 - k_1) - (y_2 + k_2) - u_1 - \cos t \cdot e^{-\sin t}) \\
&\quad + (-a(x_2 - k_1) - (x_3 - k_1)(b(c - (x_1 - k_1)^2) + d(x_3 - k_1)) \\
&\quad + a(y_2 - k_2) + (y_3 - k_2)(\hat{b}(\hat{c} - (y_1 - k_2)^2) + d(y_3 - k_2)) - u_2 - \cos t \cdot e^{-\sin t}) \\
&\quad + (-g(x_3 - k_1) + h(1 - (x_3 - k_1)^2)(x_2 - k_1) + l(x_1 - k_1) \\
&\quad + \widehat{g(y_3 - k_2)} - \widehat{h(1 - (y_3 - k_2)^2)(y_2 - k_2)} - \hat{l}(y_1 - k_2) - u_3 - \cos t \cdot e^{-\sin t}) \\
&\quad + \dot{\tilde{a}} + \dot{\tilde{b}} + \dot{\tilde{c}} + \dot{\tilde{d}} + \dot{\tilde{g}} + \dot{\tilde{h}} + \dot{\tilde{l}}
\end{aligned} \tag{5.15}$$

Choose

$$\begin{cases}
\dot{\tilde{a}} = -\dot{\hat{a}} = -\tilde{a}e_2 \\
\dot{\tilde{b}} = -\dot{\hat{b}} = -\tilde{b}e_2 \\
\dot{\tilde{c}} = -\dot{\hat{c}} = -\tilde{c}e_2 \\
\dot{\tilde{d}} = -\dot{\hat{d}} = -\tilde{d}e_2 \\
\dot{\tilde{g}} = -\dot{\hat{g}} = -\tilde{g}e_3 \\
\dot{\tilde{h}} = -\dot{\hat{h}} = -\tilde{h}e_3 \\
\dot{\tilde{l}} = -\dot{\hat{l}} = -\tilde{l}e_3
\end{cases} \tag{5.16}$$

$$
\begin{cases}
u_1 = (x_2 - k_1) - (y_2 - k_2) - \cos t \cdot e^{-\sin t} + e_1 \\
u_2 = -a(x_2 - k_1) - (x_3 - k_1)(b(c - (x_1 - k_1)^2) + d(x_3 - k_1)) \\
\quad + a(y_2 - k_2) + (y_3 - k_2)(\hat{b}(\hat{c} - (y_1 - k_2)^2) + d(y_3 - k_2)) \\
\quad - \cos t \cdot e^{-\sin t} + (1 - a - \tilde{b} - \tilde{c} - d)e_2 \\
u_3 = -g(x_3 - k_1) + h(1 - (x_3 - k_1)^2)(x_2 - k_1) + l(x_1 - k_1) \\
\quad + \widehat{g(y_3 - k_2)} - \widehat{h(1 - (y_3 - k_2)^2)}(y_2 - k_2) - \hat{l}(y_1 - k_2) \\
\quad - \cos t \cdot e^{-\sin t} + (1 - \widetilde{g - h - l})e_3
\end{cases}
\tag{5.17}
$$

We obtain

$$\dot{V} = -e_1 - e_2 - e_3 < 0 \tag{5.18}$$

which is a negative semi-definite function of e_1, e_2, e_3, $\tilde{a}$, $\tilde{b}$, $\tilde{c}$, $\tilde{d}$, $\tilde{g}$, $\tilde{h}$, $\tilde{l}$ in the first quadrant. The Lyapunov asymptotical stability theorem is not satisfied. We can't obtain that common origin of error dynamics Eq. (5.13) and parameter dynamics Eq. (5.16) are asymptotically stable. However, by pragmatical asymptotically stability theorem, D is a 10-manifold, n=10 and the number of error state variables p=3.

When $e_1 = e_2 = e_3 = 0$ and $\tilde{a}$, $\tilde{b}$, $\tilde{c}$, $\tilde{d}$, $\tilde{g}$, $\tilde{h}$, $\tilde{l}$ take arbitrary values, $\dot{V} = 0$, so X is of 3 dimensions, m=n-p=10-3=7, m+1<n is satisfied. According to the pragmatical asymptotically stability theorem, error vector e approaches zero and the estimated parameters also approach the uncertain parameters. The equilibrium point is pragmatically asymptotically stable. Under the assumption of equal probability, it is actually asymptotically stable. The simulation results are shown in Figs. 5.4-5.7.

Case 2.

The following chaotic systems are two translated GKv of which the old origin is translated to $(x_1, x_2, x_3) = (k_1, k_1, k_1)$, $(y_1, y_2, y_3) = (k_2, k_2, k_2)$ to guarantee the uncontrolled error dynamics always happen in the first quadrant of e coordinate system when $k_1 = 200, k_2 = 30$.

$$\begin{cases} \dot{x}_1 = (x_2 - k_1) \\ \dot{x}_2 = -a(x_2 - k_1) - (x_3 - k_1)(b(c - (x_1 - k_1)^2) + d(x_3 - k_1)) \\ \dot{x}_3 = -g(x_3 - k_1) + h(1 - (x_3 - k_1)^2)(x_2 - k_1) + l(x_1 - k_1) \end{cases} \tag{5.19}$$

$$\begin{cases} \dot{y}_1 = (y_2 - k_2) + u_1 \\ \dot{y}_2 = -a(y_2 - k_2) - (y_3 - k_2)(\hat{b}(\hat{c} - (y_1 - k_2)^2) + d(y_3 - k_2)) + u_2 \\ \dot{y}_3 = -g(y_3 - k_2) + h(1 - (y_3 - k_2)^2)(y_2 - k_2) + \hat{l}(y_1 - k_2) + u_3 \end{cases} \tag{5.20}$$

Let initial states be $(x_1, x_2, x_3) = (k_1 + 0.01, k_1 + 0.01, k_1 + 0.01)$, $(y_1, y_2, y_3) = (k_2 + 0.01, k_2 + 0.01, k_2 + 0.01)$ and system parameters $a = 0.08, b = -0.35, c = 100.56, d = -1000.02, g = 0.61, h = 0.08, l = 0.01$.

The state error is $e = x - y + F(t)$ where $F(t) = \mathbf{z} = (z_1, z_2, z_3)$ is the state vector of Chen-Lee (CL) chaotic system:

$$\begin{cases} \dot{z}_1 = -z_2 z_3 + \delta_1 z_1 \\ \dot{z}_2 = z_1 z_3 + \delta_2 z_2 \\ \dot{z}_3 = (1/3) z_1 z_2 + \delta_3 z_3 \end{cases} \tag{5.21}$$

where $\delta_1 = 5, \delta_2 = -10, \delta_3 = -3.8$ and initial states are $z_1 = 0.01, z_2 = 0.01, z_3 = 0.01$. And we find that the uncontrolled error dynamics always exist in first quadrant as shown in Fig. 5.8.

Our aim is $\lim_{t \to \infty} e = 0$. We obtain the error dynamics.

$$\lim_{t \to \infty} e_i = \lim_{t \to \infty} (x_i - y_i + z_i) = 0, \quad i = 1, 2, 3 \tag{5.22}$$

$$\begin{cases} \dot{e}_1 = \dot{x}_1 - \dot{y}_1 + \dot{z}_1 \\ \dot{e}_2 = \dot{x}_2 - \dot{y}_2 + \dot{z}_2 \\ \dot{e}_3 = \dot{x}_3 - \dot{y}_3 + \dot{z}_3 \end{cases} \tag{5.23}$$

where $\tilde{a} = a - \hat{a}$, $\tilde{b} = b - \hat{b}$, $\tilde{c} = c - \hat{c}$, $\tilde{d} = d - \hat{d}$, $\tilde{g} = g - \hat{g}$, $\tilde{h} = h - \hat{h}$, $\tilde{l} = l - \hat{l}$, and a, $\hat{b}$, $\hat{c}$, d, g, h, $\hat{l}$ are estimates of uncertain parameters a, b, c, d, g, h and l respectively.

Using different translation pragmatic synchronization by stability theory of

partial region, we can choose a Lyapunov function in the form of a positive definite function in first quadrant:

$$V = e_1 + e_2 + e_3 + a + \tilde{b} + \tilde{c} + d + g + h + \tilde{l} \tag{5.24}$$

Its time derivative is

$$\begin{aligned}
\dot{V} &= \dot{e}_1 + \dot{e}_2 + \dot{e}_3 + \dot{\tilde{a}} + \dot{\tilde{b}} + \dot{\tilde{c}} + \dot{\tilde{d}} + \dot{\tilde{g}} + \dot{\tilde{h}} + \dot{\tilde{l}} \\
&= ((x_2 - k_1) - (y_2 + k_2) - u_1 - z_2 z_3 + \delta_1 z_1) + (-a(x_2 - k_1) \\
&\quad - (x_3 - k_1)(b(c - (x_1 - k_1)^2) + d(x_3 - k_1)) + a(y_2 - k_2) \\
&\quad + (y_3 - k_2)(\hat{b}(\hat{c} - (y_1 - k_2)^2) + d(y_3 - k_2)) - u_2 + z_1 z_3 + \delta_2 z_2) \\
&\quad + (-g(x_3 - k_1) + h(1 - (x_3 - k_1)^2)(x_2 - k_1) + l(x_1 - k_1) \\
&\quad + \widehat{g(y_3 - k_2)} - \widehat{h(1 - (y_3 - k_2)^2)}(y_2 - k_2) - \hat{l}(y_1 - k_2) - u_3 \\
&\quad + (1/3) z_1 z_2 + \delta_3 z_3) + \dot{\tilde{a}} + \dot{\tilde{b}} + \dot{\tilde{c}} + \dot{\tilde{d}} + \dot{\tilde{g}} + \dot{\tilde{h}} + \dot{\tilde{l}}
\end{aligned} \tag{5.25}$$

Choose

$$\begin{cases}
\dot{\tilde{a}} = -\dot{\hat{a}} = -\tilde{a} e_2 \\
\dot{\tilde{b}} = -\dot{\hat{b}} = -\tilde{b} e_2 \\
\dot{\tilde{c}} = -\dot{\hat{c}} = -\tilde{c} e_2 \\
\dot{\tilde{d}} = -\dot{\hat{d}} = -\tilde{d} e_2 \\
\dot{\tilde{g}} = -\dot{\hat{g}} = -\tilde{g} e_3 \\
\dot{\tilde{h}} = -\dot{\hat{h}} = -\tilde{h} e_3 \\
\dot{\tilde{l}} = -\dot{\hat{l}} = -\tilde{l} e_3
\end{cases} \tag{5.26}$$

$$\begin{cases}
u_1 = (x_2 - k_1) - (y_2 - k_2) - z_2 z_3 + \delta_1 z_1 + e_1 \\
u_2 = -a(x_2 - k_1) - (x_3 - k_1)(b(c - (x_1 - k_1)^2) + d(x_3 - k_1)) \\
\qquad + a(y_2 - k_2) + (y_3 - k_2)(\hat{b}(\hat{c} - (y_1 - k_2)^2) + d(y_3 - k_2)) \\
\qquad + z_1 z_3 + \delta_2 z_2 + (1 - a - \tilde{b} - \tilde{c} - d) e_2 \\
u_3 = -g(x_3 - k_1) + h(1 - (x_3 - k_1)^2)(x_2 - k_1) + l(x_1 - k_1) \\
\qquad + \widehat{g(y_3 - k_2)} - \widehat{h(1 - (y_3 - k_2)^2)}(y_2 - k_2) - \hat{l}(y_1 - k_2) \\
\qquad + (1/3) z_1 z_2 + \delta_3 z_3 + (1 - \widetilde{g - h - l}) e_3
\end{cases} \tag{5.27}$$

We obtain

$$\dot{V} = -e_1 - e_2 - e_3 < 0 \tag{5.28}$$

which is a negative semi-definite function of e_1, e_2, e_3, $\tilde{a}$, $\tilde{b}$, $\tilde{c}$, $\tilde{d}$, $\tilde{g}$, $\tilde{h}$, $\tilde{l}$ in the first quadrant. The Lyapunov asymptotical stability theorem is not satisfied. We can't obtain that common origin of error dynamics Eq. (5.23) and parameter dynamics Eq. (5.26) are asymptotically stable. However, by pragmatical asymptotically stability theorem, D is a 10-manifold, n=10 and the number of error state variables p=3.

When $e_1 = e_2 = e_3 = 0$ and $\tilde{a}$, $\tilde{b}$, $\tilde{c}$, $\tilde{d}$, $\tilde{g}$, $\tilde{h}$, $\tilde{l}$ take arbitrary values, $\dot{V} = 0$, so X is of 3 dimensions, m=n-p=10-3=7, m+1<n is satisfied. According to the pragmatical asymptotically stability theorem, error vector e approaches zero and the estimated parameters also approach the uncertain parameters. The equilibrium point is pragmatically asymptotically stable. Under the assumption of equal probability, it is actually asymptotically stable. The simulation results are shown in Figs. 5.9-5.12.

Case 3.

The following chaotic systems are two translated GKv of which the old origin is translated to $(x_1, x_2, x_3) = (k_1, k_1, k_1)$, $(y_1, y_2, y_3) = (k_2, k_2, k_2)$ to guarantee the uncontrolled error dynamics always happen in the first quadrant of e coordinate system when $k_1 = 300, k_2 = 30$.

$$\begin{cases} \dot{x}_1 = (x_2 - k_1) \\ \dot{x}_2 = -a(x_2 - k_1) - (x_3 - k_1)(b(c - (x_1 - k_1)^2) + d(x_3 - k_1)) \\ \dot{x}_3 = -g(x_3 - k_1) + h(1 - (x_3 - k_1)^2)(x_2 - k_1) + l(x_1 - k_1) \end{cases} \tag{5.29}$$

$$\begin{cases} \dot{y}_1 = (y_2 - k_2) + u_1 \\ \dot{y}_2 = -a(y_2 - k_2) - (y_3 - k_2)(\hat{b}(\hat{c} - (y_1 - k_2)^2) + d(y_3 - k_2)) + u_2 \\ \dot{y}_3 = -g(y_3 - k_2) + h(1 - (y_3 - k_2)^2)(y_2 - k_2) + \hat{l}(y_1 - k_2) + u_3 \end{cases} \tag{5.30}$$

Let initial states be $(x_1, x_2, x_3) = (k_1 + 0.01, k_1 + 0.01, k_1 + 0.01)$, $(y_1, y_2, y_3) = (k_2 + 0.01, k_2 + 0.01, k_2 + 0.01)$ and system parameters $a = 0.08, b = -0.35, c = 100.56, d = -1000.02, g = 0.61, h = 0.08, l = 0.01$.

The state error is $e = x' - y' + F(t)$ where $F(t) = \mathbf{z} = (z_1, z_2, z_3)$ is the state

vector of Ge-Ku-Duffing (GKD) chaotic system:

$$\begin{cases} \dot{z}_1 = z_2 \\ \dot{z}_2 = -\delta_1 z_2 - z_1(\delta_2(\delta_3 - z_1^{\,2}) + \delta_4 z_3) \\ \dot{z}_3 = -z_3 - z_3^{\,3} - \delta_5 z_2 + \delta_6 z_1 \end{cases} \tag{5.31}$$

where $\delta_1 = 0.1, \delta_2 = 11, \delta_3 = 40, \delta_4 = 54, \delta_5 = 6, \delta_6 = 30$ and initial states are $z_1 = 0.01$, $z_2 = 0.01, z_3 = 0.01$, the GKD is chaotic Fig. 5.14. And we find that the uncontrolled error dynamics always exist in first quadrant as shown in Fig. 5.13.

Our aim is $\lim_{t\to\infty} e = 0$. We obtain the error dynamics.

$$\lim_{t\to\infty} e_i = \lim_{t\to\infty}(x_i - y_i + z_i) = 0, \quad i = 1,2,3 \tag{5.32}$$

$$\begin{cases} \dot{e}_1 = \dot{x}_1 - \dot{y}_1 + \dot{z}_1 \\ \dot{e}_2 = \dot{x}_2 - \dot{y}_2 + \dot{z}_2 \\ \dot{e}_3 = \dot{x}_3 - \dot{y}_3 + \dot{z}_3 \end{cases} \tag{5.33}$$

where $\tilde{a} = a - \hat{a}$, $\tilde{b} = b - \hat{b}$, $\tilde{c} = c - \hat{c}$, $\tilde{d} = d - \hat{d}$, $\tilde{g} = g - \hat{g}$, $\tilde{h} = h - \hat{h}$, $\tilde{l} = l - \hat{l}$, and a, $\hat{b}$, $\hat{c}$, d, g, h, $\hat{l}$ are estimates of uncertain parameters a, b, c, d, g, h and l respectively.

Using different translation pragmatic synchronization by stability theory of partial region, we can choose a Lyapunov function in the form of a positive definite function in first quadrant:

$$V = e_1 + e_2 + e_3 + a + \tilde{b} + \tilde{c} + d + g + h + \tilde{l} \tag{5.34}$$

Its time derivative is

$$
\begin{aligned}
\dot{V} &= \dot{e}_1 + \dot{e}_2 + \dot{e}_3 + \dot{\tilde{a}} + \dot{\tilde{b}} + \dot{\tilde{c}} + \dot{\tilde{d}} + \dot{\tilde{g}} + \dot{\tilde{h}} + \dot{\tilde{l}} \\
&= ((x_2 - k_1) - (y_2 + k_2) - u_1 + z_2) \\
&\quad + (-a(x_2 - k_1) - (x_3 - k_1)(b(c - (x_1 - k_1)^2) + d(x_3 - k_1)) \\
&\quad + a(y_2 - k_2) + (y_3 - k_2)(\hat{b}(\hat{c} - (y_1 - k_2)^2) + d(y_3 - k_2)) \\
&\quad - u_2 - \delta_1 z_2 - z_1(\delta_2(\delta_3 - z_1^{\,2}) + \delta_4 z_3)) \\
&\quad + (-g(x_3 - k_1) + h(1 - (x_3 - k_1)^2)(x_2 - k_1) + l(x_1 - k_1) \\
&\quad + \widehat{g(y_3 - k_2)} - \widehat{h(1 - (y_3 - k_2)^2)}(y_2 - k_2) - \hat{l}(y_1 - k_2) \\
&\quad - u_3 - z_3 - z_3^{\,3} - \delta_5 z_2 + \delta_6 z_1) + \dot{\tilde{a}} + \dot{\tilde{b}} + \dot{\tilde{c}} + \dot{\tilde{d}} + \dot{\tilde{g}} + \dot{\tilde{h}} + \dot{\tilde{l}}
\end{aligned}
\tag{5.35}
$$

Choose

$$
\begin{cases}
\dot{\tilde{a}} = -\dot{\hat{a}} = -\tilde{a}e_2 \\
\dot{\tilde{b}} = -\dot{\hat{b}} = -\tilde{b}e_2 \\
\dot{\tilde{c}} = -\dot{\hat{c}} = -\tilde{c}e_2 \\
\dot{\tilde{d}} = -\dot{\hat{d}} = -\tilde{d}e_2 \\
\dot{\tilde{g}} = -\dot{\hat{g}} = -\tilde{g}e_3 \\
\dot{\tilde{h}} = -\dot{\hat{h}} = -\tilde{h}e_3 \\
\dot{\tilde{l}} = -\dot{\hat{l}} = -\tilde{l}e_3
\end{cases}
\tag{5.36}
$$

$$
\begin{cases}
u_1 = (x_2 - k_1) - (y_2 - k_2) + z_2 + e_1 \\
u_2 = -a(x_2 - k_1) - (x_3 - k_1)(b(c - (x_1 - k_1)^2) + d(x_3 - k_1)) \\
\qquad + a(y_2 - k_2) + (y_3 - k_2)(\hat{b}(\hat{c} - (y_1 - k_2)^2) + d(y_3 - k_2)) \\
\qquad - \delta_1 z_2 - z_1(\delta_2(\delta_3 - z_1^{\,2}) + \delta_4 z_3) + (1 - a - \tilde{b} - \tilde{c} - d)e_2 \\
u_3 = -g(x_3 - k_1) + h(1 - (x_3 - k_1)^2)(x_2 - k_1) + l(x_1 - k_1) \\
\qquad + \widehat{g(y_3 - k_2)} - \widehat{h(1 - (y_3 - k_2)^2)}(y_2 - k_2) - \hat{l}(y_1 - k_2) \\
\qquad - z_3 - z_3^{\,3} - \delta_5 z_2 + \delta_6 z_1 + (1 - \widetilde{g - h - l})e_3
\end{cases}
\tag{5.37}
$$

We obtain

$$
\dot{V} = -e_1 - e_2 - e_3 < 0 \tag{5.38}
$$

which is a negative semi-definite function of e_1, e_2, e_3, $\tilde{a}$, $\tilde{b}$, $\tilde{c}$, $\tilde{d}$, $\tilde{g}$, $\tilde{h}$, $\tilde{l}$ in the first quadrant. The Lyapunov asymptotical stability theorem is not satisfied. We can't obtain that common origin of error dynamics Eq. (5.33) and parameter dynamics Eq. (5.36) are asymptotically stable. However, By pragmatical asymptotically stability

theorem, D is a 10-manifold, n=10 and the number of error state variables p=3.

When $e_1 = e_2 = e_3 = 0$ and $\tilde{a}$, $\tilde{b}$, $\tilde{c}$, $\tilde{d}$, $\tilde{g}$, $\tilde{h}$, $\tilde{l}$ take arbitrary values, $\dot{V} = 0$, so X is of 3 dimensions, m=n-p=10-3=7, m+1<n is satisfied. According to the pragmatical asymptotically stability theorem, error vector e approaches zero and the estimated parameters also approach the uncertain parameters. The equilibrium point is pragmatically asymptotically stable. Under the assumption of equal probability, it is actually asymptotically stable. The simulation results are shown in Figs. 5.15-5.18.

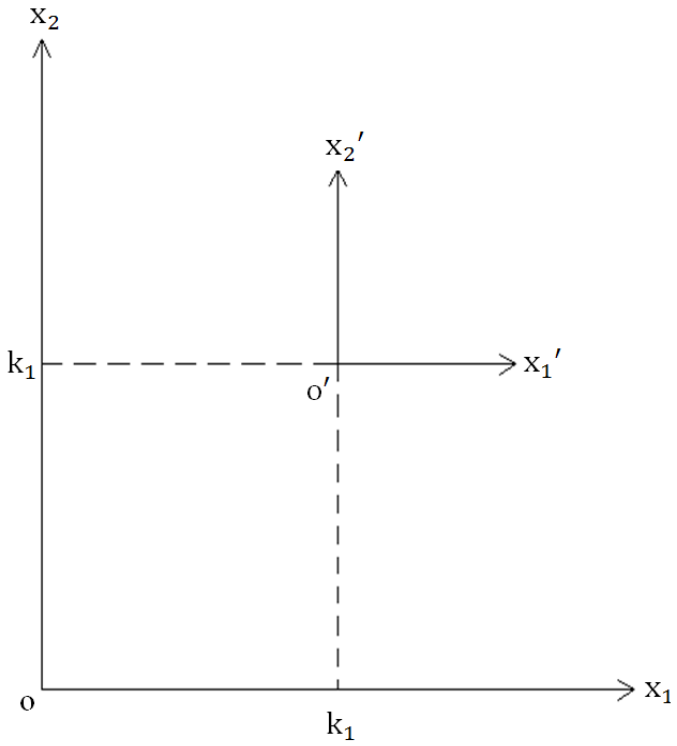

Fig. 5.1 Coordinate translation of x-states.

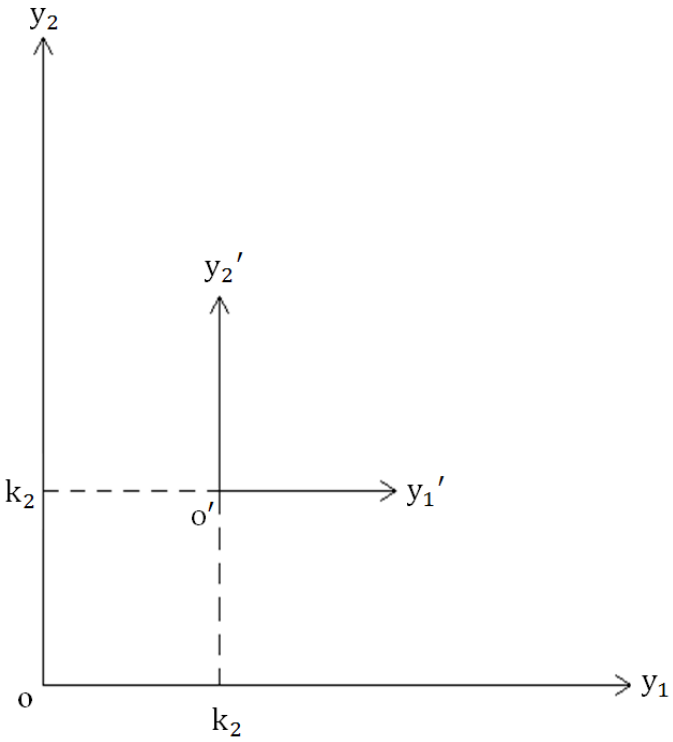

Fig. 5.2 Coordinate translation of y-states.

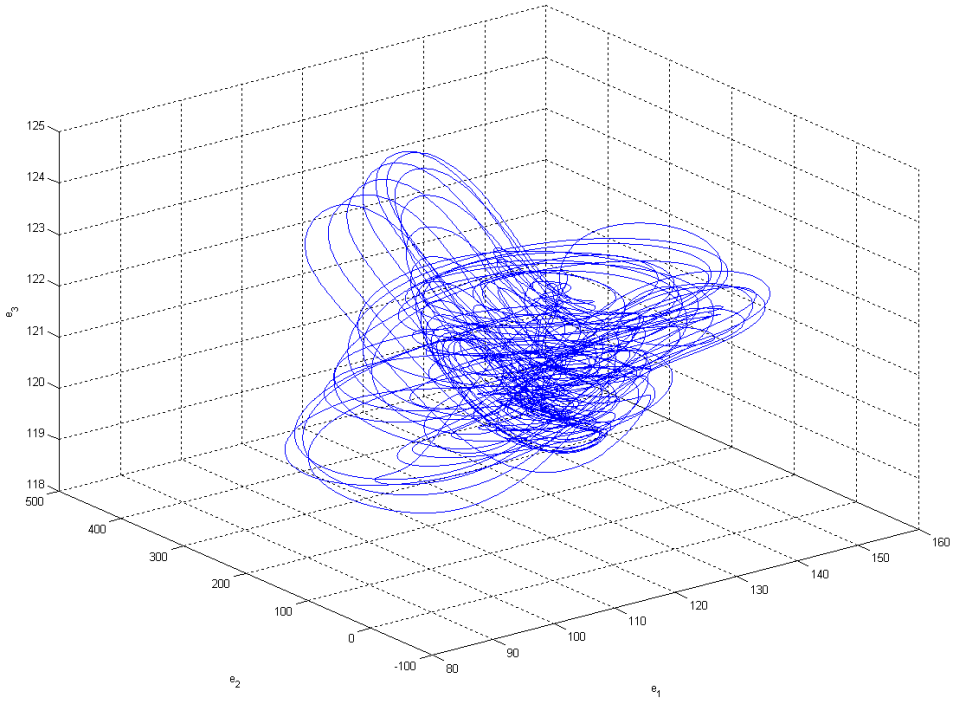

Fig. 5.3 Phase portrait of the error dynamic for Case 1.

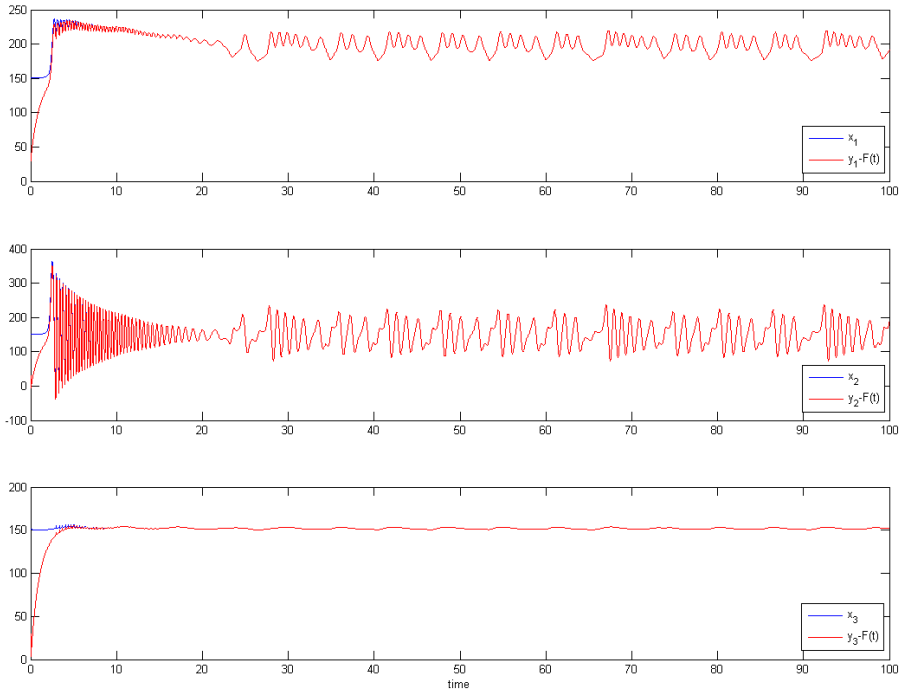

Fig. 5.4 Time histories of x_i, y_i for Case 1.

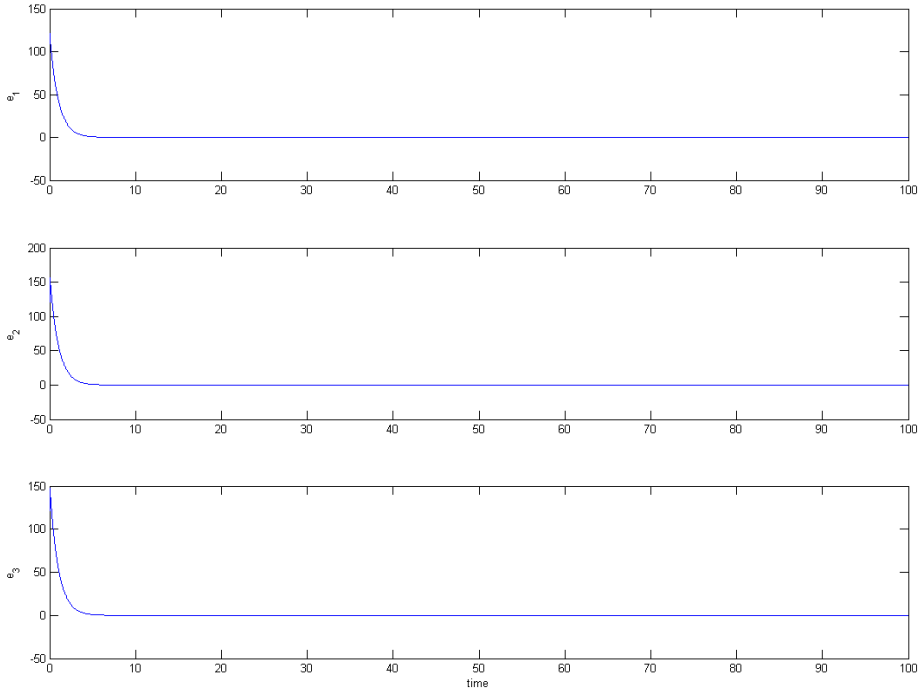

Fig. 5.5 Time histories of errors for Case 1.

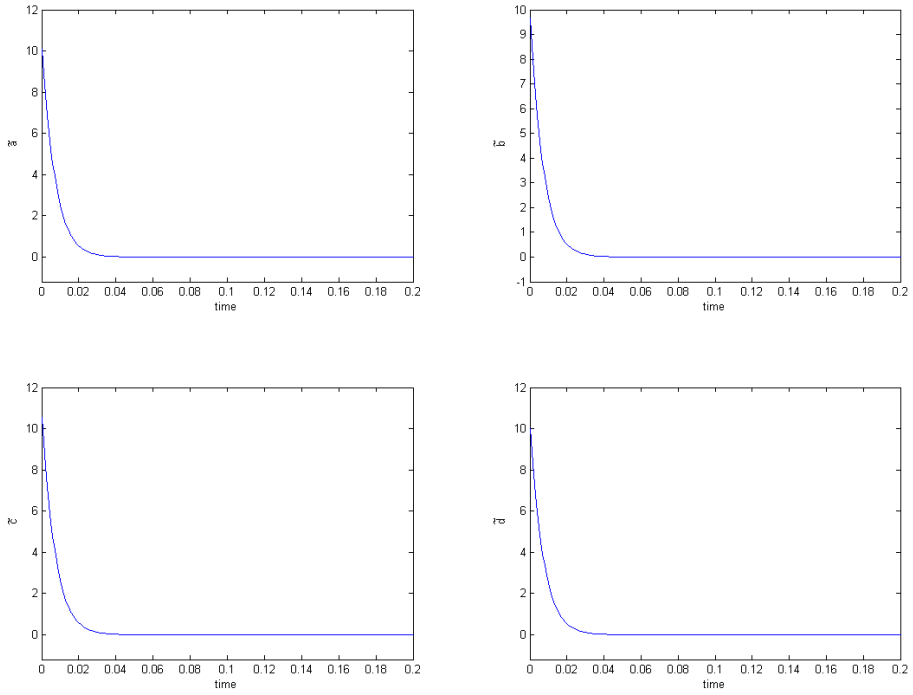

Fig. 5.6 Time histories of parameter errors for Case 1.

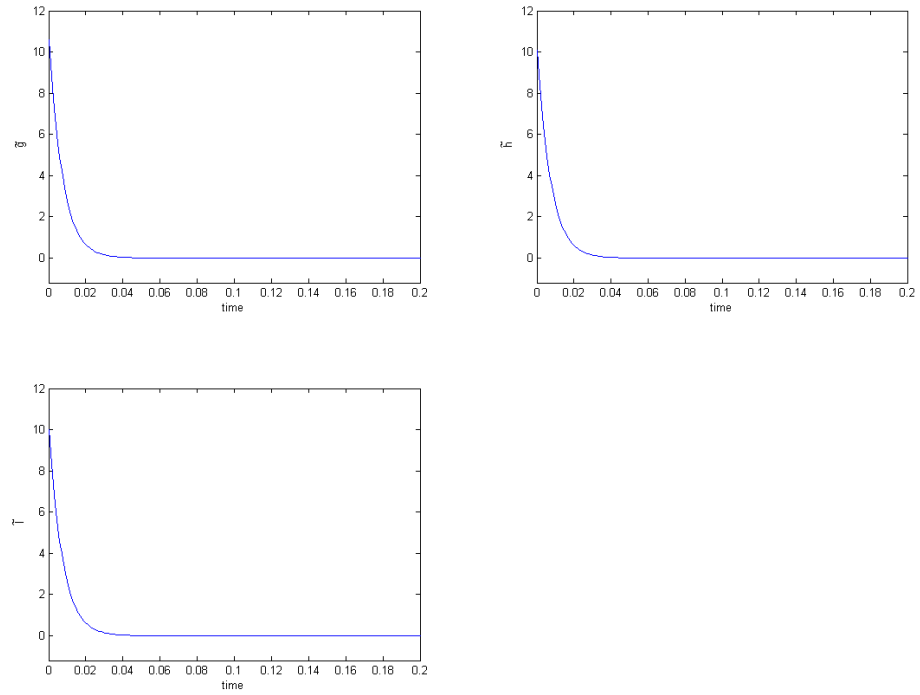

Fig. 5.7 Time histories of parameter errors for Case 1.

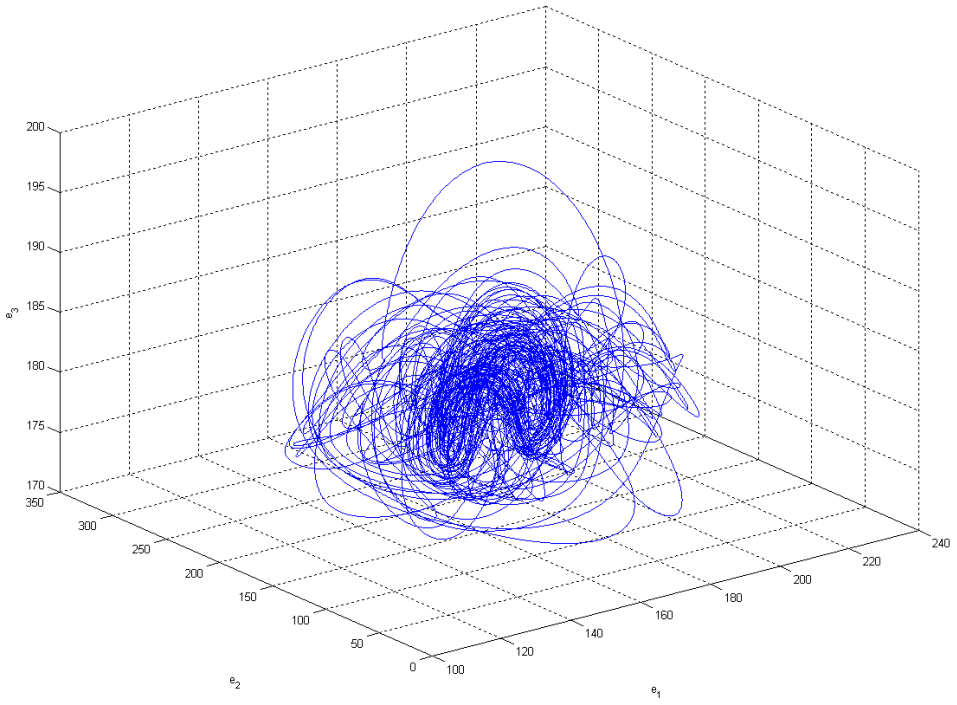

Fig. 5.8 Phase portrait of the error dynamic for Case 2.

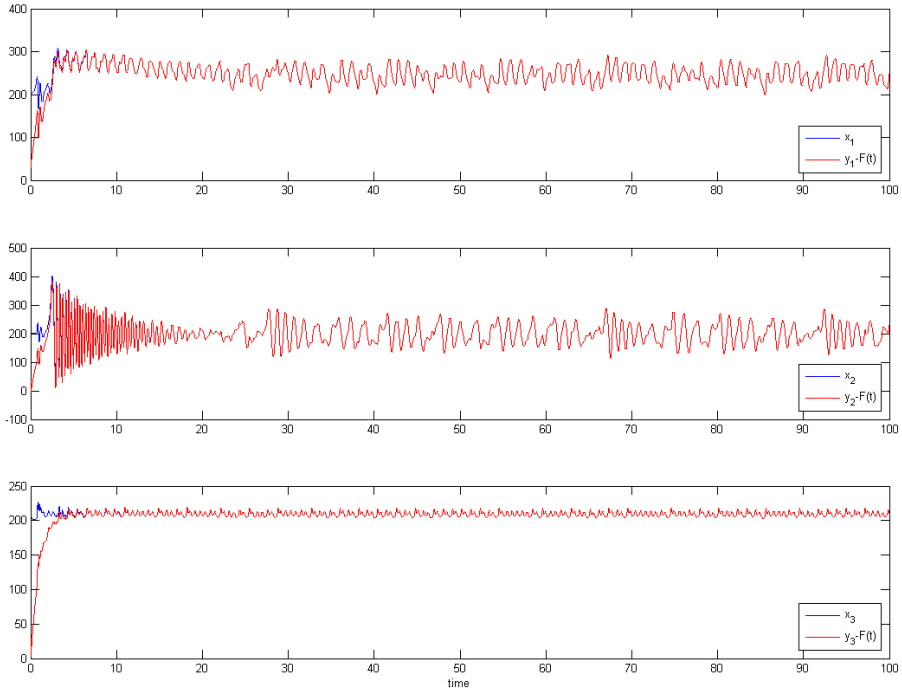

Fig. 5.9 Time histories of x_i, y_i for Case 2.

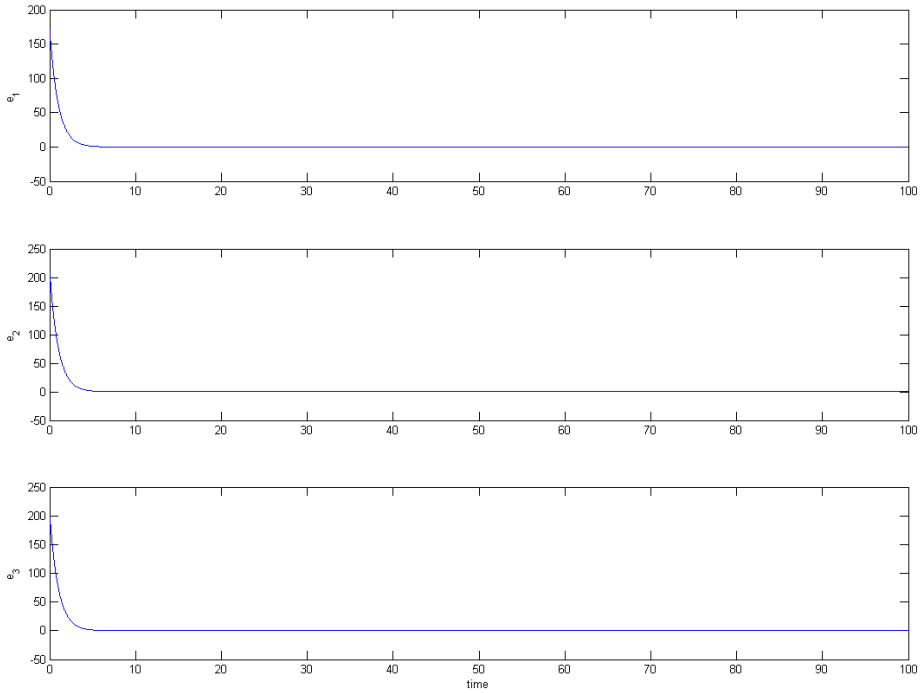

Fig. 5.10 Time histories of errors for Case 2.

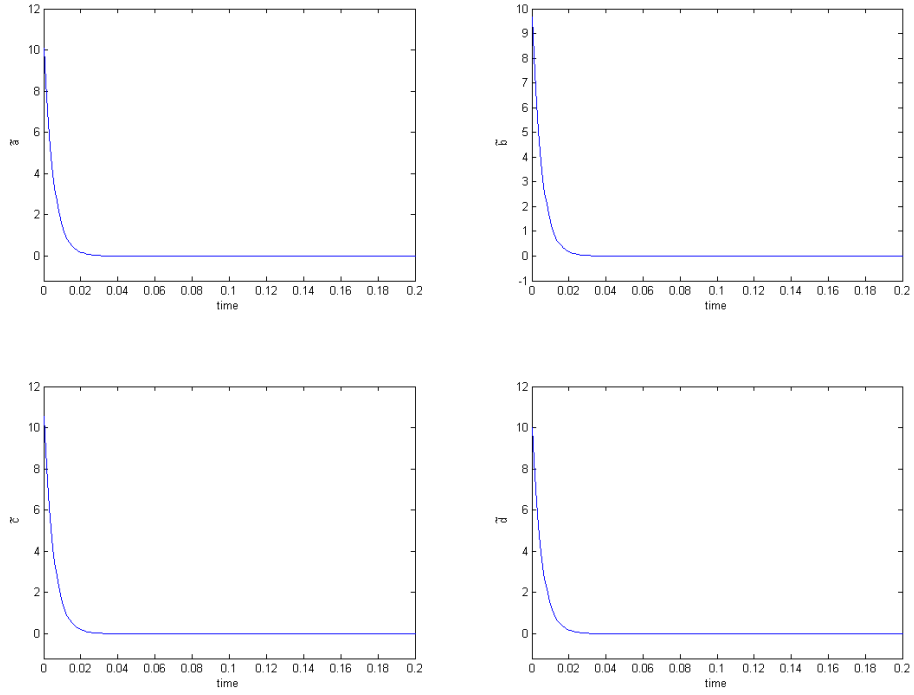

Fig. 5.11 Time histories of parameter errors for Case 2.

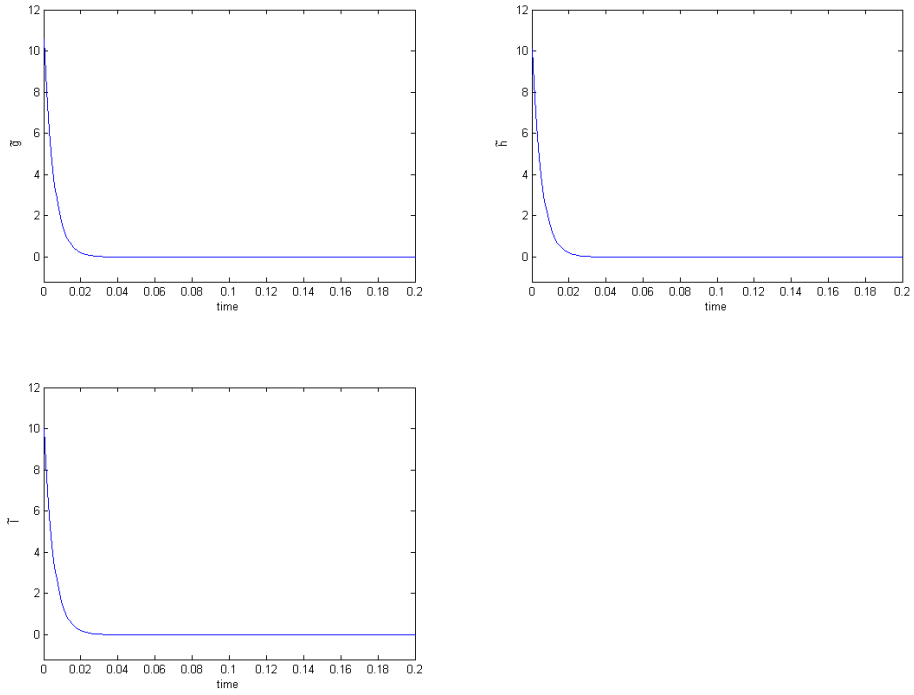

Fig. 5.12 Time histories of parameter errors for Case 2.

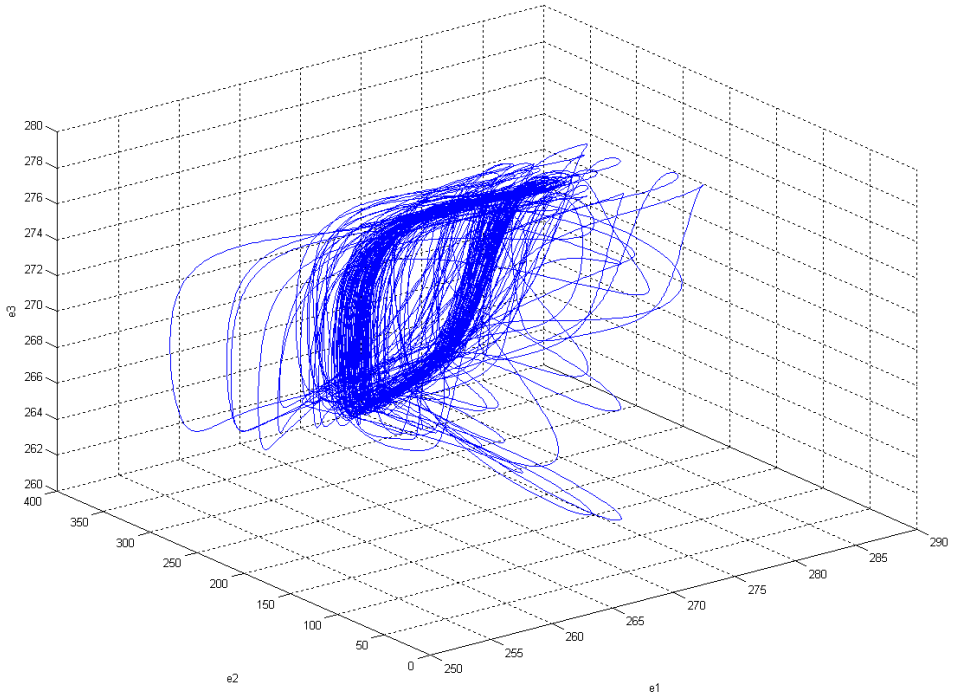

Fig. 5.13 Phase portrait of the error dynamic for Case 3.

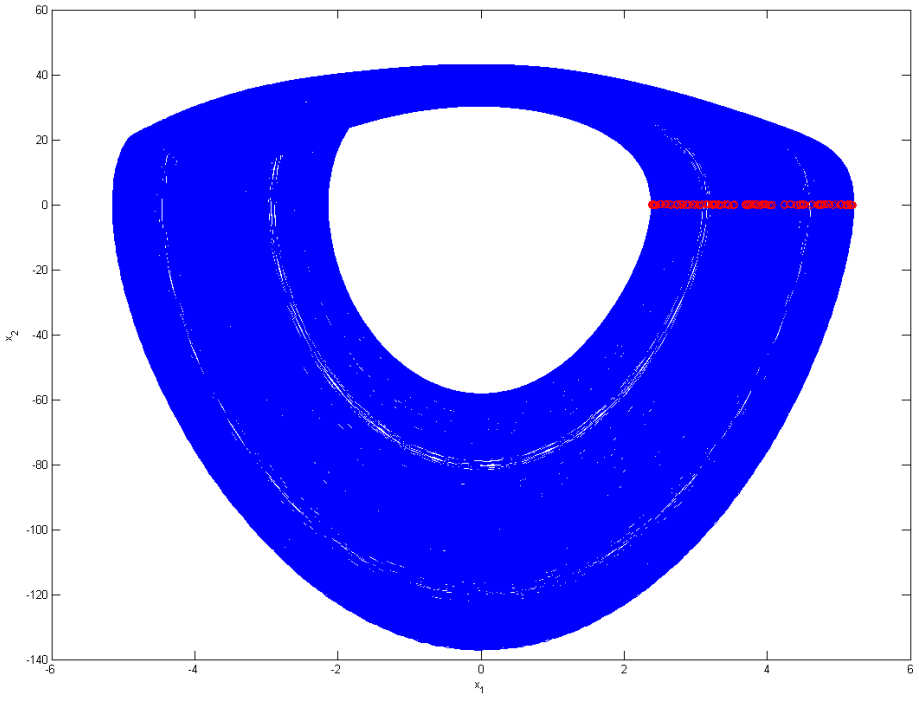

Fig. 5.14 The chaotic attractor of the GKD system.

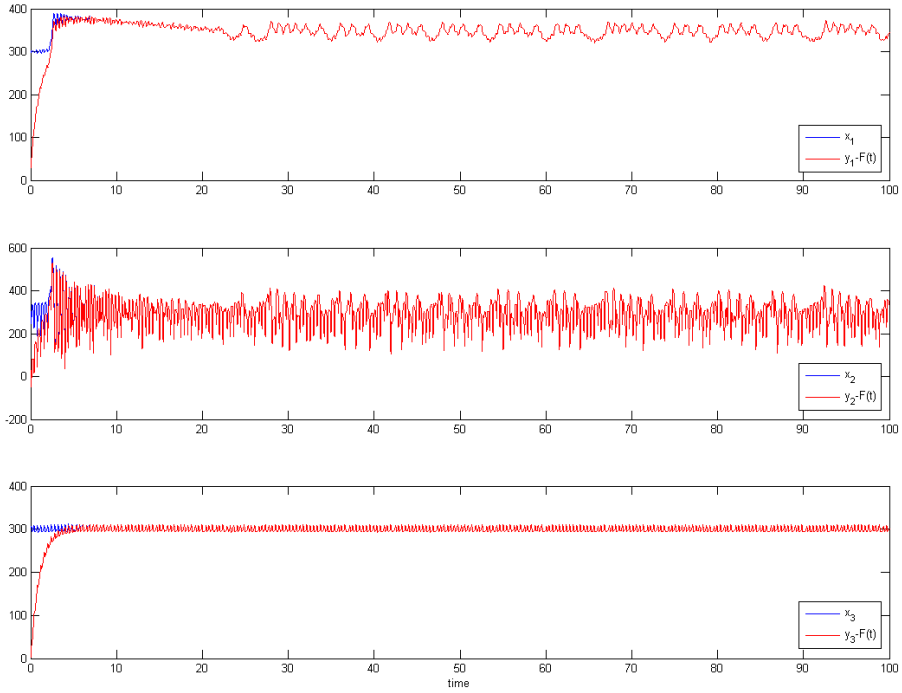

Fig. 5.15 Time histories of x_i, y_i for Case 3.

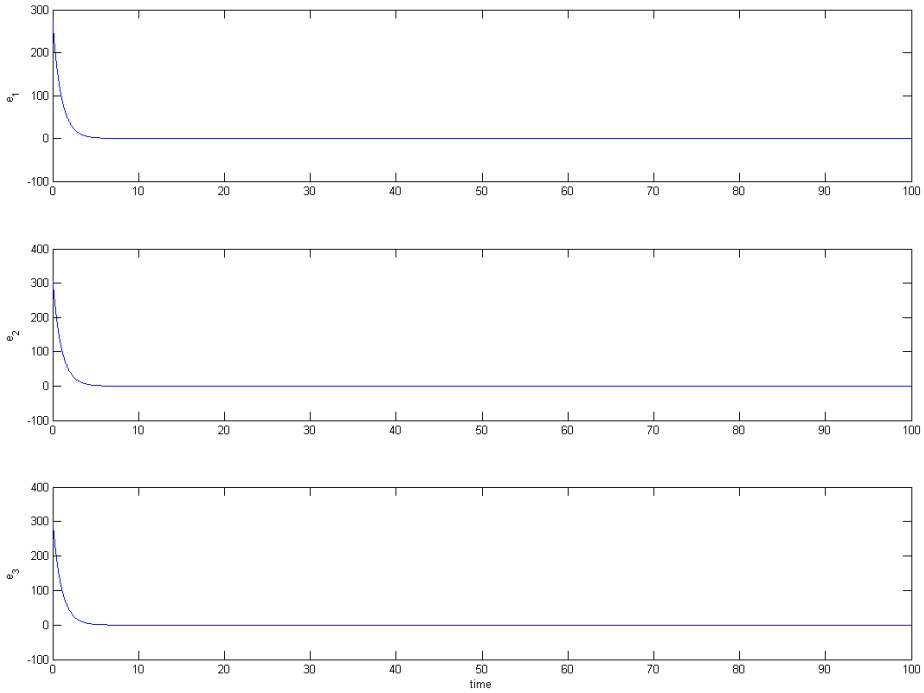

Fig. 5.16 Time histories of errors for Case 3.

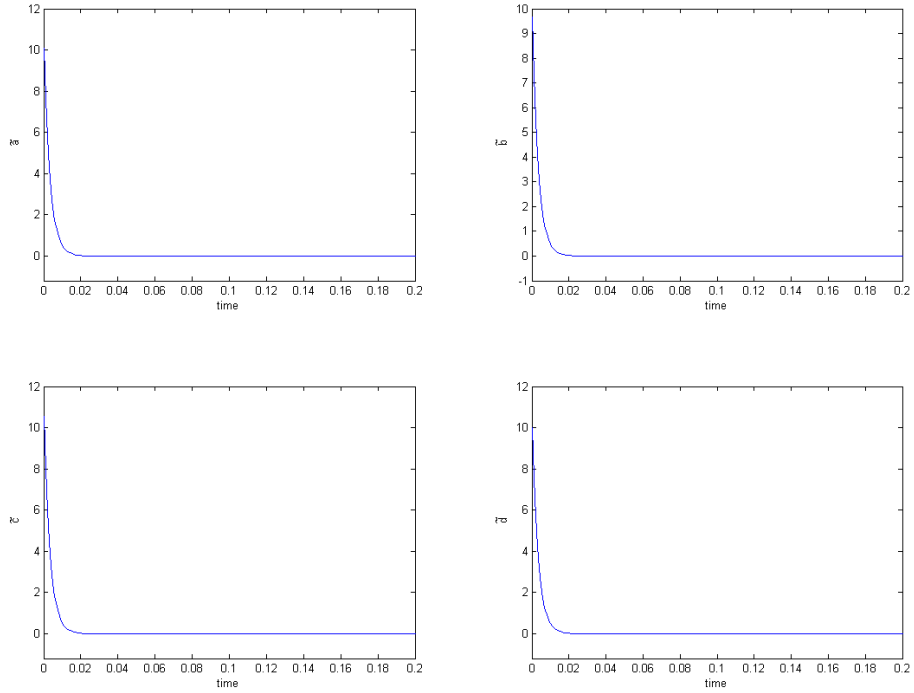

Fig. 5.17 Time histories of parameter errors for Case 3.

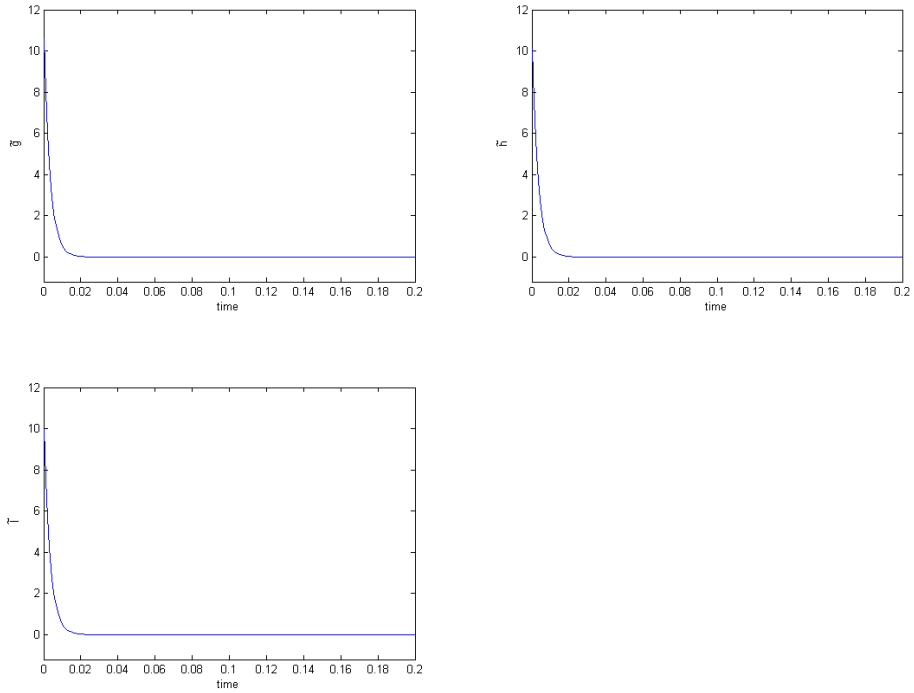

Fig. 5.18 Time histories of parameter errors for Case 3.

Chapter 6

Robust Projective Synchronization of Uncertain Stochastic Chaotic Systems by Fuzzy Logic Constant Controller

6.1 Preliminary

In this Chapter, a simplest fuzzy logic constant controller (FLCC) which is derived via fuzzy logic design and Lyapunov direct method is presented for projective synchronization of non-autonomous chaotic systems with uncertain and stochastic disturbances. Controllers in traditional Lyapunov direct method are always nonlinear and complicated. However, FLCC proposed are such simple controllers which are constant numbers, decided via the values of the upper and lower bounds of the error derivatives. This new method is used in projective synchronization of non-autonomous chaotic systems with stochastic disturbance to show the robustness and effectiveness of FLCC. There are two cases illustrated in simulation results to show the feasibility of the FLCC, two cases are Sprott system and Ge-Ku-van der Pol system. Comparison at the efficiency, accuracy and complexity of the FLCC with that of traditional nonlinear controllers is also given in tables and figures.

6.2 Projective Chaos Synchronization by FLCC Scheme

Consider the following master chaotic system

$$\dot{\mathbf{x}} = (\mathbf{A} + \mathbf{\Delta})\mathbf{x} + \mathbf{f}(\mathbf{x}) + \zeta \tag{6.1}$$

where $\mathbf{x} = [x_1, x_2, \cdots x_n]^T \in R^n$ denotes a state vector, $\mathbf{A}$ is an $n \times n$ constant coefficient matrix , $\mathbf{f}$ is a nonlinear vector function, $\mathbf{\Delta}$ is non-autonomous term and ζ is stochastic disturbance.

The slave system which can be either identical or different from the master is

$$\dot{\mathbf{y}} = \mathbf{B}\mathbf{y} + \mathbf{g}(\mathbf{y}) + \mathbf{u} \tag{6.2}$$

where $\mathbf{y} = [y_1, y_2, \cdots y_n]^T \in R^n$ denotes a state vector, $\mathbf{B}$ is an $n \times n$ constant coefficient matrix, $\mathbf{g}$ is a nonlinear vector function and $\mathbf{u} = [u_1, u_2, \cdots u_n]^T \in R^n$ is the fuzzy logic controller needed to be designed.

For projective synchronization, in order to make the state $\mathbf{y}$ and projective number λ approaching the goal state $\lambda\mathbf{x}$, projective number λ is a constant, define $\mathbf{e} = \lambda\mathbf{x} - \mathbf{y}$ as the state error. The chaos projective synchronization is accomplished in the sense that [20-23]:

$$\lim_{t\to\infty} \mathbf{e} = \lim_{t\to\infty} (\lambda\mathbf{x} - \mathbf{y}) = 0 \tag{6.3}$$

where

$$\mathbf{e} = [e_1, \cdots, e_n]^T = \lambda\mathbf{x} - \mathbf{y} \tag{6.4}$$

From Eq. (6-4) we have the following error dynamics:

$$\dot{\mathbf{e}} = \lambda\dot{\mathbf{x}} + \dot{\mathbf{y}} = \lambda[(\mathbf{A} + \Delta\mathbf{A})\mathbf{x} + \mathbf{f}(\mathbf{x}) + \zeta] + [\mathbf{B}\mathbf{y} + \mathbf{g}(\mathbf{y}) + \mathbf{u}] \tag{6.5}$$

According to Lyapunov direct method, we have the following Lyapunov function to derive the fuzzy logic controller for projective synchronization:

$$V = f(e_1, \cdots, e_m, \cdots, e_n) = \frac{1}{2}(e_1^2 + \ldots + e_m^2 + \ldots e_n^2) > 0 \tag{6.6}$$

The derivative of the Lyapunov function in Eq. (6.6) is:

$$\dot{V} = e_1\dot{e}_1 + \ldots + e_m\dot{e}_m + \ldots + e_n\dot{e}_n \tag{6.7}$$

If the vector controller in Eq. (6.5) can be suitably designed to achieve $\dot{V} < 0$, then the zero solution $\mathbf{e} = \mathbf{0}$ of Eq. (6.5) are asymptotically stable i.e. the projective synchronization is accomplished. Next, the design process of FLCC is introduced. The design process of FLCC is introduced in the following section.

We use the error derivatives $\dot{\mathbf{e}}(t) = [\dot{e}_1, \dot{e}_2, \cdots, \dot{e}_m, \cdots, \dot{e}_n]^T$, as the antecedent part of the proposed FLCC to design the control input $\mathbf{u}$ which is used in the consequent part of the proposed FLCC:

$$\mathbf{u} = [u_1, u_2, \cdots, u_m, \cdots, u_n]^T \tag{6.8}$$

where $\mathbf{u}$ is a constant column vector and accomplishes the objective to stabilize the error dynamics in Eq. (6.5).

The strategy of the FLCC designed is proposed as follow and the configuration of the strategy is shown in Fig. 6.1.

Assume the upper bound and lower bound of $\dot{e}_m$ are Z_m and $-Z_m$, then the FLCC can be design step by step:

(1) If e_m is detected as positive ($e_m > 0$), we have to design a controller for $\dot{e}_m < 0$ for the purpose $\dot{V} = e_m \dot{e}_m < 0$. Therefore we have the following i-th (i=1,2,3) if–then fuzzy rule as:

$$\textit{Rule 1 : IF } \dot{e}_m \textit{ is } M_1 \textit{ THEN } u_{m1} = Z_m \tag{6.9}$$

$$\textit{Rule 2 : IF } \dot{e}_m \textit{ is } M_2 \textit{ THEN } u_{m2} = Z_m \tag{6.10}$$

$$\textit{Rule 3 : IF } \dot{e}_m \textit{ is } M_3 \textit{ THEN } u_{m3} = e_m \tag{6.11}$$

(2) If e_m is detected as negative ($e_m < 0$), we have to design a controller for $\dot{e}_m > 0$, for the purpose $\dot{V} = e_m \dot{e}_m < 0$. Therefore we have the following m-th if–then fuzzy rule as:

$$\textit{Rule 1 : IF } \dot{e}_m \textit{ is } M_1 \textit{ THEN } u_{m1} = -Z_m \tag{6.12}$$

$$\textit{Rule 2 : IF } \dot{e}_m \textit{ is } M_2 \textit{ THEN } u_{m2} = -Z_m \tag{6.13}$$

$$\textit{Rule 3 : IF } \dot{e}_m \textit{ is } M_3 \textit{ THEN } u_{m3} = e_m \tag{6.14}$$

(3) If e_m approaches to zero, then the synchronization is nearly achieved. Therefore we have the following m-th if–then fuzzy rule as:

$$Rule\ 1: IF\ \ \dot{e}_m\ is\ \ M_1\ \ \ THEN\ u_{m1} = e_m \approx 0 \tag{6.15}$$

$$Rule\ 2: IF\ \ \dot{e}_m\ is\ \ M_2\ \ \ THEN\ u_{m2} = e_m \approx 0 \tag{6.16}$$

$$Rule\ 3: IF\ \ \dot{e}_m\ is\ \ M_3\ \ \ THEN\ u_{m3} = e_m \approx 0 \tag{6.17}$$

where $M_1 = \frac{|\dot{e}_m|}{Z_m}$, $M_2 = \frac{|\dot{e}_m|}{Z_m}$ and $M_3 = \text{sgn}(\frac{Z_m - \dot{e}_m}{Z_m}) + \text{sgn}(\frac{\dot{e}_m - Z_m}{Z_m})$, M_1, M_2 and M_3 refer to the membership functions of positive (P), negative (N) and zero (Z) separately which are presented in Fig. 6.2. For each case, u_{mi}, i= 1~3 is the i-th output of $\dot{e}_m$, which is a constant controller. The centriod defuzzifier evaluates the output of all rules as follows:

$$u_m = \frac{\sum_{i=1}^{3} M_i \times u_{mi}}{\sum_{i=1}^{3} M_i} \tag{6.18}$$

The fuzzy rule base is listed in Table 1, in which the input variables in the antecedent part of the rules are $\dot{e}_m$ and the output variable in the consequent part is u_{mi}.

Table 1 Rule-table of FLCC

Rule	Antecedent	Consequent Part
	$\dot{e}_m$	u_{mi}
1	Negative (N)	u_{m1}
2	Positive (P)	u_{m2}
3	Zero (Z)	u_{m3}

With appropriate fuzzy logic constant controllers in Eq. (6.7), a negative definite of derivatives Lyapunov function $\dot{V}$ can be obtained and the asymptotically stability

of Lyapunov theorem can be achieved.

Consequently, the processes of FLCC designed to control a system following the trajectory of a goal system are getting the upper bound and lower bound of the error derivatives of the master and control systems without any controller, i.e. $-Z_m \le \dot{e}_m \le Z_m$. Through the fuzzy logic system which follows the rules of Eq. (6.9-6.17), a negative definite derivatives of Lyapunov function $\dot{V}$ can be obtained and the asymptotically stability of Lyapunov theorem can be achieved.

6.3. Simulation Results

There are two examples in this Section. Each example is divided into two parts, projective synchronization by FLCC and that by traditional method. In the end of each example, we give the simulation results of two controllers and list the tables and figures to show the effectiveness and robustness of our method.

6.3.1 Case 1 Projective synchronization of identical master and slave Sprott 22 systems [60] by new FLCC

The Sprott 22 system is:

$$\begin{cases} \dot{x} = y \\ \dot{y} = z \\ \dot{z} = -\alpha z - y - \sin x \end{cases} \tag{6.19}$$

The initial condition $(x_0, y_0, z_0) = (0.01, 1, 0.01)$. The parameter $\alpha = 0.25$, chaos of the Sprott 22 system appears. The chaotic behavior of Eq. (6.19) is shown in Fig 6.3.

6.3.1.1 Robust projective synchronization of non-autonomous Sprott 22 system by FLCC

The master non-autonomous Sprott 22 system is:

$$\begin{cases} \dot{x}_1 = x_2 \\ \dot{x}_2 = x_3 \\ \dot{x}_3 = -(\alpha + \Delta)x_3 - x_2 - \sin x_1 \end{cases} \tag{6.20}$$

When initial condition $(x_{10}, x_{20}, x_{30}) = (0.01, 1, 0.01)$, $\Delta = \gamma \sin(\omega t)$ is a non-autonomous term with $\gamma = 0.07$, $\omega = 10$. The parameter is the same as that of Eq. (6.19). Chaos of the non-autonomous Sprott 22 system appears. The chaotic behavior of Eq. (6.20) is shown in Fig. 6.4.

The slave system is:

$$\begin{cases} \dot{y}_1 = y_2 + u_1 \\ \dot{y}_2 = y_3 + u_2 \\ \dot{y}_3 = -\alpha y_3 - y_2 - \sin y_1 + u_3 \end{cases} \tag{6.21}$$

The initial condition $(y_{10}, y_{20}, y_{30}) = (10, 10, 10)$. The parameter is the same as that of Eq. (6.19), chaos of the slave system appears as well. u_1, u_2 and u_3 are FLCC to synchronize projectively the slave system to master one, i.e.,

$$\lim_{\mathbf{t}\to\infty} \mathbf{e} = 0 \tag{6.22}$$

where the error vector

$$\mathbf{e} = \begin{bmatrix} e_1 \\ e_2 \\ e_3 \end{bmatrix} = \lambda \begin{bmatrix} x_1 \\ x_2 \\ x_3 \end{bmatrix} - \begin{bmatrix} y_1 \\ y_2 \\ y_3 \end{bmatrix} \tag{6.23}$$

where $\lambda = 4$. We have the following error dynamics:

$$\begin{cases} \dot{e}_1 = \lambda \dot{x}_1 - y_1 = \lambda x_2 - (y_2 + u_1) \\ \dot{e}_2 = \lambda \dot{x}_2 - y_2 = \lambda x_3 - (y_3 + u_2) \\ \dot{e}_3 = \lambda \dot{x}_3 - y_3 = \lambda(-(\alpha + \Delta_1) x_3 - x_2 - \sin x_1) - (-\alpha y_3 - y_2 - \sin y_1 + u_3) \end{cases} \tag{6.24}$$

Choosing Lyapunov function as:

$$V = \frac{1}{2}(e_1^2 + e_2^2 + e_3^2) > 0 \tag{6.25}$$

Its time derivative is:

$$\begin{aligned}\dot{V} &= e_1\dot{e}_1 + e_2\dot{e}_2 + e_3\dot{e}_3 \\ &= e_1(\lambda x_2 - (y_2 + u_1)) \\ &\quad + e_2(\lambda x_3 - (y_3 + u_2)) \\ &\quad + e_3(\lambda(-(\alpha+\Delta)x_3 - x_2 - \sin x_1) - (-\alpha y_3 - y_2 - \sin y_1 + u_3))\end{aligned} \tag{6.26}$$

In order to design FLCC, we divide Eq. (6.26) into three parts as follows:

Assume $V = \frac{1}{2}(e_1^2 + e_2^2 + e_3^2) = V_1 + V_2 + V_3$, then $\dot{V} = e_1\dot{e}_1 + e_2\dot{e}_2 + e_3\dot{e}_3 = \dot{V}_1 + \dot{V}_2 + \dot{V}_3$, where $V_1 = \frac{1}{2}e_1^2$, $V_2 = \frac{1}{2}e_2^2$ and $V_3 = \frac{1}{2}e_3^2$.

Part 1: $\dot{V}_1 = e_1\dot{e}_1 = e_1(\lambda x_2 - (y_2 + u_1))$

Part 2: $\dot{V}_2 = e_2\dot{e}_2 = e_2(\lambda x_3 - (y_3 + u_2))$

Part 3: $\dot{V}_3 = e_3\dot{e}_3 = e_3(\lambda(-(\alpha+\Delta)x_3 - x_2 - \sin x_1) - (-\alpha y_3 - y_2 - \sin y_1 + u_3))$

FLCC in *Part 1, 2* and *3* can be obtained via the fuzzy rules in Table 1. The maximum value and minimum value without any controller can be observed in time histories of error derivatives shown in Fig 6.5: $Z_1 = 20$, $Z_2 = 20$, $Z_3 = 20$.

The synchronization scheme is proposed in *Part 1, 2* and *3* and makes $\dot{V}_1 = e_1\dot{e}_1 < 0$, $\dot{V}_2 = e_2\dot{e}_2 < 0$ and $\dot{V}_3 = e_3\dot{e}_3 < 0$. Hence we have $\dot{V} = \dot{V}_1 + \dot{V}_2 + \dot{V}_3 < 0$. It is clear that all of the rules in FLCC can lead that the Lyapunov function satisfies the asymptotical stability theorem. The simulation results are shown in Fig. 6.6 and Fig. 6.7.

6.3.1.2 Robust projective synchronization of stochastic Sprott 22 system by FLCC

The master non-autonomous Sprott 22 system with robust of stochastic disturbances is:

$$\begin{cases}\dot{x}_1 = x_2 + \zeta \\ \dot{x}_2 = x_3 + \zeta \\ \dot{x}_3 = -(\alpha+\Delta)x_3 - x_2 - \sin x_1\end{cases} \tag{6.27}$$

When initial condition $(x_{10}, x_{20}, x_{30}) = (0.01, 1, 0.01)$, $\zeta =$ band-limited white noise (PSD=0.01) and parameter is the same as that of Eq. (6.19). The stochastic disturbance ζ is shown in Fig 6.8. Chaos of the non-autonomous stochastic Sprott 22 system appears. The chaotic behavior of Eq. (6.27) is shown in Fig 6.9.

The slave system is the same as Eq. (6.21) and Lyapunov function derived through the Eq. (6.22-6.26).

Let $\lambda = 4$, we have the following error dynamics:

$$\begin{cases} \dot{e}_1 = \lambda \dot{x}_1 - y_1 = \lambda(x_2 + \zeta) - (y_2 + u_1) \\ \dot{e}_2 = \lambda \dot{x}_2 - y_2 = \lambda(x_3 + \zeta) - (y_3 + u_2) \\ \dot{e}_3 = \lambda \dot{x}_3 - y_3 = \lambda(-(\alpha + \Delta)x_3 - x_2 - \sin x_1) - (-\alpha y_3 - y_2 - \sin y_1 + u_3) \end{cases} \tag{6.28}$$

And time derivative of Lyapunov function is:

$$\begin{aligned} \dot{V} &= e_1\dot{e}_1 + e_2\dot{e}_2 + e_3\dot{e}_3 \\ &= e_1(\lambda(x_2 + \zeta) - (y_2 + u_1)) \\ &\quad + e_2(\lambda(x_3 + \zeta) - (y_3 + u_2)) \\ &\quad + e_3(\lambda(-(\alpha + \Delta)x_3 - x_2 - \sin x_1) - (-\alpha y_3 - y_2 - \sin y_1 + u_3)) \end{aligned} \tag{6.29}$$

The maximum values and minimum values without any controller can be observed in time histories of error derivatives shown in Fig. 6.10: $Z_1 = 25$, $Z_2 = 30$, $Z_3 = 15$. The synchronization scheme makes $\dot{V} = e_1\dot{e}_1 + e_2\dot{e}_2 + e_3\dot{e}_3 < 0$. It is clear that all of the rules in FLCC can lead that the Lyapunov function satisfies the asymptotical stability theorem. The simulation results are shown in Fig. 6.11-13.

6.3.1.3 Robust projective synchronization of stochastic Sprott 22 system by traditional method

According to Eq. (6.29), we design complicated controllers to synchronize chaotic system with uncertainty by traditional method.

We choose controllers are

$$\begin{cases} u_1 = \lambda(x_2 + \zeta) - y_2 + e_1 \\ u_2 = \lambda(x_3 + \zeta) - y_3 + e_2 \\ u_3 = \lambda[-(\alpha + \Delta)x_3 - x_2 - \sin x_1] + \alpha y_3 + y_2 + \sin y_1 + e_3 \end{cases} \tag{6.30}$$

and obtain

$$\dot{V} = -e_1 e_1 - e_2 e_2 - e_3 e_3 < 0 \tag{6.31}$$

The derivative of Lyapunov function is negative definite and the error dynamics in Eq. (6.28) are going to achieve asymptotically stable. The simulation results are shown in Fig. 6.14 and Fig. 6.15.

6.3.1.4 Robust projective synchronization of stochastic Sprott 22 system by new FLCC compared to using traditional method

In this subsection, the controllers and numerical simulation results in subsection 6.3.1.2 and subsection 6.3.1.3 are listed in Tables 2 and 3 for comparison. Comparing two kinds of controller in Table 2 and two kinds of errors in Table 3, it is clear to find out that (1) The controllers in FLCC designing are much simpler than traditional ones; (2) The performance of the error convergence of states by FLCC is much better than that by traditional method.

Consequently, even the system contains noise and parameter uncertainty, the FLCC can still remain the high performance to synchronize the two chaotic systems with uncertainty and stochastic disturbances exactly and efficiently.

Table 2 The controllers of FLCC and of traditional method.

Controller	FLCC	Traditional method

u_1	$Z_1 = 25$	$\lambda(x_2 + \zeta) - y_2 + e_1$
u_2	$Z_2 = 30$	$\lambda(x_3 + \zeta) - y_3 + e_2$
u_3	$Z_3 = 15$	$\lambda[-(\alpha - \Delta)x_3 - x_2 - \sin x_1] + \alpha y_3 + y_2 + \sin y_1 + e_3$

Table 3 Errors data after the action of controllers.

Time after the action of controllers	FLCC	Traditional
	e_1	e_1
32.00 s	0.0000000000048992	-3.5187301833233740
32.01 s	0.0000000000048512	-3.4837182330074956
32.02 s	-0.0000000000032614	-3.4490546574179977
32.03 s	-0.0000000000032419	-3.4147359901684879
32.04 s	0.0000000000006413	-3.3807587993636190
	e_2	e_2
31.46 s	0.000000000001907	1.8995112214353798
31.47 s	-0.000000000007070	1.8806107689867746
31.48 s	-0.000000000007022	1.8618983791822554
31.49 s	-0.000000000006962	1.8433721807672345
31.50 s	0.000000000002132	1.8250303211064454
	e_3	e_3
30.44 s	-0.0000000000029234	3.1426420748209738
30.45 s	-0.0000000000029008	3.1113722637096530
30.46 s	-0.0000000000028781	3.0804135924175107
30.47 s	-0.0000000000028564	3.0497629650516407
30.48 s	-0.0000000000028346	3.0194173165237430

6.3.2 Case 2 Projective synchronization of identical master and slave Ge-Ku-van der Pol systems by new FLCC

The GKv system is:

$$\begin{cases} \dot{x} = y \\ \dot{y} = -\beta_1 y - z(\beta_2(\beta_3 - x^2) + \beta_4 z) \\ \dot{z} = -\beta_5 z + \beta_6(1 - z^2)y + \beta_7 x \end{cases} \tag{6.32}$$

The initial condition $(x_0, y_0, z_0) = (0.01, 0.01, 0.01)$. The parameters are $\beta_1 = 0.08$, $\beta_2 = -0.35$, $\beta_3 = 100.56$, $\beta_4 = -1000.02$, $\beta_5 = 0.61$, $\beta_6 = 0.08$, $\beta_7 = 0.01$, chaos of the GKv system appears. The chaotic behavior of Eq. (6.32) is shown in Fig 6.16.

6.3.2.1 Robust projective synchronization of non-autonomous GKv system by FLCC

The master non-autonomous GKv system is:

$$\begin{cases} \dot{x}_1 = x_2 \\ \dot{x}_2 = -\beta_1 x_2 - x_3(\beta_2(\beta_3 - x_1^2) + \beta_4 x_3) \\ \dot{x}_3 = -(\beta_5 + \Delta)x_3 + \beta_6(1 - x_3^2)x_2 + \beta_7 x_1 \end{cases} \tag{6.33}$$

When initial condition $(x_{10}, x_{20}, x_{30}) = (0.01, 0.01, 0.01)$, $\Delta = \gamma \sin(\omega t)$ is a non-autonomous term with $\gamma = 0.5$, $\omega = 10$. The parameters are the same as that of Eq. (6.32). Chaos of the non-autonomous GKv system appears. The chaotic behavior of Eq. (6.33) is shown in Fig 6.17.

The slave system is:

$$\begin{cases} \dot{y}_1 = y_2 + u_1 \\ \dot{y}_2 = -\beta_1 y_2 - y_3(\beta_2(\beta_3 - y_1^2) + \beta_4 y_3) + u_2 \\ \dot{y}_3 = -\beta_5 y_3 + \beta_6(1 - y_3^2)y_2 + \beta_7 y_1 + u_3 \end{cases} \tag{6.34}$$

The initial condition $(y_{10}, y_{20}, y_{30}) = (10, 10, 10)$. The parameters are the same as that of Eq. (6.32), chaos of the slave system appears as well. u_1, u_2 and u_3 are FLCC to synchronize projectively the slave system to master one, i.e.,

$$\lim_{\mathbf{t}\to\infty} \mathbf{e} = 0 \tag{6.35}$$

where the error vector

$$\mathbf{e} = \begin{bmatrix} e_1 \\ e_2 \\ e_3 \end{bmatrix} = \lambda \begin{bmatrix} x_1 \\ x_2 \\ x_3 \end{bmatrix} - \begin{bmatrix} y_1 \\ y_2 \\ y_3 \end{bmatrix} \tag{6.36}$$

where $\lambda = 2$. We have the following error dynamics:

$$\begin{cases} \dot{e}_1 = \lambda \dot{x}_1 - y_1 = \lambda x_2 - (y_2 + u_1) \\ \dot{e}_2 = \lambda \dot{x}_2 - y_2 = \lambda(-\beta_1 x_2 - x_3(\beta_2(\beta_3 - x_1^{\,2}) + \beta_4 x_3)) \\ \qquad\qquad -(-\beta_1 y_2 - y_3(\beta_2(\beta_3 - y_1^{\,2}) + \beta_4 y_3) + u_2) \\ \dot{e}_3 = \lambda \dot{x}_3 - y_3 = \lambda(-(\beta_5 + \Delta)x_3 + \beta_6(1 - x_3^{\,2})x_2 + \beta_7 x_1) \\ \qquad\qquad -(-\beta_5 y_3 + \beta_6(1 - y_3^{\,2})y_2 + \beta_7 y_1 + u_3) \end{cases} \tag{6.37}$$

Choosing Lyapunov function as:

$$V = \frac{1}{2}(e_1^2 + e_2^2 + e_3^2) \tag{6.38}$$

Its time derivative is:

$$\begin{aligned} \dot{V} &= e_1\dot{e}_1 + e_2\dot{e}_2 + e_3\dot{e}_3 \\ &= e_1(\lambda x_2 - (y_2 + u_1)) + \\ &\quad e_2(\lambda(-\beta_1 x_2 - x_3(\beta_2(\beta_3 - x_1^{\,2}) + \beta_4 x_3)) \\ &\quad -(-\beta_1 y_2 - y_3(\beta_2(\beta_3 - y_1^{\,2}) + \beta_4 y_3) + u_2)) + \\ &\quad e_3(\lambda(-(\beta_5 + \Delta)x_3 + \beta_6(1 - x_3^{\,2})x_2 + \beta_7 x_1) \\ &\quad -(-\beta_5 y_3 + \beta_6(1 - y_3^{\,2})y_2 + \beta_7 y_1 + u_3)) \end{aligned} \tag{6.39}$$

In order to design FLCC, we divide Eq. (6.39) into three parts as follows:

Assume $V = \frac{1}{2}(e_1^2 + e_2^2 + e_3^2) = V_1 + V_2 + V_3$, then $\dot{V} = e_1\dot{e}_1 + e_2\dot{e}_2 + e_3\dot{e}_3 = \dot{V}_1 + \dot{V}_2 + \dot{V}_3$,

where $V_1 = \frac{1}{2}e_1^2$, $V_2 = \frac{1}{2}e_2^2$ and $V_3 = \frac{1}{2}e_3^2$.

Part 1: $\dot{V}_1 = e_1\dot{e}_1 = e_1(\lambda x_2 - (y_2 + u_1))$

Part 2: $\dot{V}_2 = e_2\dot{e}_2 = e_2(\lambda(-\beta_1 x_2 - x_3(\beta_2(\beta_3 - x_1^{\,2}) + \beta_4 x_3)) - (-\beta_1 y_2 - y_3(\beta_2(\beta_3 - y_1^{\,2}) + \beta_4 y_3) + u_2))$

Part 3: $\dot{V}_3 = e_3\dot{e}_3 = e_3(\lambda(-(\beta_5+\Delta_1)x_3 + \beta_6(1-x_3^{\,2})x_2 + \beta_7 x_1)$
$-(-\beta_5 y_3 + \beta_6(1-y_3^{\,2})y_2 + \beta_7 y_1 + u_3))$

FLCC in *Part 1, 2* and *3* can be obtained via the fuzzy rules in Table 1. The maximum value and minimum value without any controller can be observed in time histories of error derivatives shown in Fig 6.18. $Z_1 = 250$, $Z_2 = 1600$, $Z_3 = 15$.

The synchronization scheme is proposed in *Part 1, 2* and *3* and makes $\dot{V}_1 = e_1\dot{e}_1 < 0$, $\dot{V}_2 = e_2\dot{e}_2 < 0$ and $\dot{V}_3 = e_3\dot{e}_3 < 0$. Hence we have $\dot{V} = \dot{V}_1 + \dot{V}_2 + \dot{V}_3 < 0$. It is clear that all of the rules in FLCC can lead that the Lyapunov function satisfies the asymptotical stability theorem. The simulation results are shown in Fig. 6.19 and Fig. 6.20.

6.3.2.2 Robust projective synchronization of stochastic GKv system by FLCC

The master non-autonomous GKv system with robust of stochastic disturbances is:

$$\begin{cases} \dot{x}_1 = x_2 + \zeta_1 \\ \dot{x}_2 = -\beta_1 x_2 - x_3(\beta_2(\beta_3 - x_1^{\,2}) + \beta_4 x_3) + \zeta_2 \\ \dot{x}_3 = -(\beta_5 + \Delta)x_3 + \beta_6(1-x_3^{\,2})x_2 + \beta_7 x_1 \end{cases} \tag{6.40}$$

When initial condition $(x_{10}, x_{20}, x_{30}) = (0.01, 0.01, 0.01)$, ζ_1 = band-limited white noise (PSD=1). The parameters are the same as that of Eq. (6.32). Here $\zeta_2 = [(\omega_1 + \omega_2 e^{-\omega_3 t}) \cdot$ (band-limited white noise)] (PSD=0.5) with $\omega_1 = 1$, $\omega_2 = 5$, $\omega_3 = 0.01$. The stochastic disturbances ζ_1 and ζ_2 signal are shown in Fig. 6.21 and Fig. 6.22. Chaos of the non-autonomous stochastic GKv system appears. The chaotic behavior of Eq. (6.40) is shown in Fig 6.23.

The slave system is the same as Eq. (6.34) and Lyapunov function derived through the Eq. (6.35-6.39).

where $\lambda = 2$. We have the following error dynamics:

$$\begin{cases} \dot{e}_1 = \lambda \dot{x}_1 - y_1 = \lambda(x_2 + \zeta_1) - (y_2 + u_1) \\ \dot{e}_2 = \lambda \dot{x}_2 - y_2 = \lambda(-\beta_1 x_2 - x_3(\beta_2(\beta_3 - x_1^{\,2}) + \beta_4 x_3) + \zeta_2) \\ \qquad\qquad - (-\beta_1 y_2 - y_3(\beta_2(\beta_3 - y_1^{\,2}) + \beta_4 y_3) + u_2) \\ \dot{e}_3 = \lambda \dot{x}_3 - y_3 = \lambda(-(\beta_5 + \Delta)x_3 + \beta_6(1 - x_3^{\,2})x_2 + \beta_7 x_1) \\ \qquad\qquad - (-\beta_5 y_3 + \beta_6(1 - y_3^{\,2})y_2 + \beta_7 y_1 + u_3) \end{cases} \tag{6.41}$$

And time derivative of Lyapunov function is:

$$\begin{aligned} \dot{V} &= e_1\dot{e}_1 + e_2\dot{e}_2 + e_3\dot{e}_3 \\ &= e_1(\lambda(x_2 + \zeta_1) - (y_2 + u_1)) + \\ &\quad e_2(\lambda(-\beta_1 x_2 - x_3(\beta_2(\beta_3 - x_1^{\,2}) + \beta_4 x_3) + \zeta_2) \\ &\quad - (-\beta_1 y_2 - y_3(\beta_2(\beta_3 - y_1^{\,2}) + \beta_4 y_3) + u_2)) + \\ &\quad e_3(\lambda(-(\beta_5 + \Delta)x_3 + \beta_6(1 - x_3^{\,2})x_2 + \beta_7 x_1) \\ &\quad - (-\beta_5 y_3 + \beta_6(1 - y_3^{\,2})y_2 + \beta_7 y_1 + u_3)) \end{aligned} \tag{6.42}$$

The maximum values and minimum values without any controller can be observed in time histories of error derivatives shown in Fig. 6.24: $Z_1 = 300$, $Z_2 = 3500$, $Z_3 = 40$. The projective synchronization scheme makes $\dot{V} = e_1\dot{e}_1 + e_2\dot{e}_2 + e_3\dot{e}_3 < 0$. It is clear that all of the rules in FLCC can lead that the Lyapunov function satisfies the asymptotical stability theorem. The simulation results are shown in Fig. 6.25 and Fig. 6.26.

6.3.2.3 Robust projective synchronization of stochastic GKv system by traditional method

According to Eq. (6.42), we design complicated controllers to synchronize chaotic system with stochastic disturbance by traditional method.

We choose controllers are

$$\begin{cases} u_1 = \lambda(x_2 + \zeta_1) - y_2 + e_1 \\ u_2 = \lambda[-\beta_1 x_2 - x_3(\beta_2(\beta_3 - x_1^{\,2}) + \beta_4 x_3) + \zeta_2] \\ \qquad + \beta_1 y_2 + y_3(\beta_2(\beta_3 - y_1^{\,2}) + \beta_4 y_3) + e_2 \\ u_3 = \lambda[-(\beta_5 + \Delta)x_3 + \beta_6(1 - x_3^{\,2})x_2 + \beta_7 x_1] \\ \qquad + \beta_5 y_3 - \beta_6(1 - y_3^{\,2})y_2 - \beta_7 y_1 + e_3 \end{cases} \tag{6.43}$$

and obtain

$$\dot{V} = -e_1 \dot{e}_1 - \dot{e}_2 e_2 - \dot{e}_3 e_3 < 0 \tag{6.44}$$

The derivative of Lyapunov function is negative definite and the error dynamics in Eq. (6.41) achieve asymptotical stability. The simulation results are shown in Fig. 6.27 and Fig. 6.28.

6.3.2.4 Robust projective synchronization of stochastic GKv system by new FLCC compared to using traditional method

In this case, the controllers and numerical simulation results of subsection 6.3.2.2 and subsection 6.3.2.3 are listed in Table 4 and Table 5 for comparison. The mater and slave systems are more complex than Case 1, but the good-robustness and high performance can be still achieved through FLCC. The two main superiorities are still existed: (1) The controllers in FLCC designing are much simpler than traditional ones; (2) The performance of the convergence of error states by FLCC is much better than by traditional method.

Table 4 The controller of FLCC and of traditional method.

Controller	FLCC	Traditional
u_1	$Z_1 = 300$	$\lambda(x_2 + \zeta_1) - y_2 + e_1$
u_2	$Z_2 = 3500$	$\lambda[-\beta_1 x_2 - x_3(\beta_2(\beta_3 - x_1^2) + \beta_4 x_3) + \zeta_2]$ $+\beta_1 y_2 + y_3(\beta_2(\beta_3 - y_1^2) + \beta_4 y_3) + e_2$
u_3	$Z_3 = 40$	$\lambda[-(\beta_5 + \Delta)x_3 + \beta_6(1 - x_3^2)x_2 + \beta_7 x_1]$ $+\beta_5 y_3 - \beta_6(1 - y_3^2)y_2 - \beta_7 y_1 + e_3$

Table 5 Errors data after the action of controllers.

Time after	FLCC	Traditional

the action of controllers	e_1	e_1
30.50 s	0.0000000000000853	18.895920723453898
30.51 s	0.0000000000000853	18.707903170792974
30.52 s	0.0000000000000853	18.521756424039154
30.53 s	0.0000000000000711	18.337461868362539
30.54 s	0.0000000000000711	18.155001074154072
	e_2	e_2
31.64 s	0.0000000000039790	10.117976168390220
31.65 s	0.0000000000039506	10.017300623392766
31.66 s	0.0000000000038938	9.9176268168054662
31.67 s	0.0000000000038654	9.8189447811645270
31.68 s	0.0000000000038369	9.7212446481842232
	e_3	e_3
30.06 s	0.0000000000000066	-1.1818139746755154
30.07 s	0.0000000000000066	-1.1700547291499359
30.08 s	0.0000000000000064	-1.1584124900723243
30.09 s	0.0000000000000063	-1.1468860932090630
30.10 s	0.0000000000000060	-1.1354743859108640

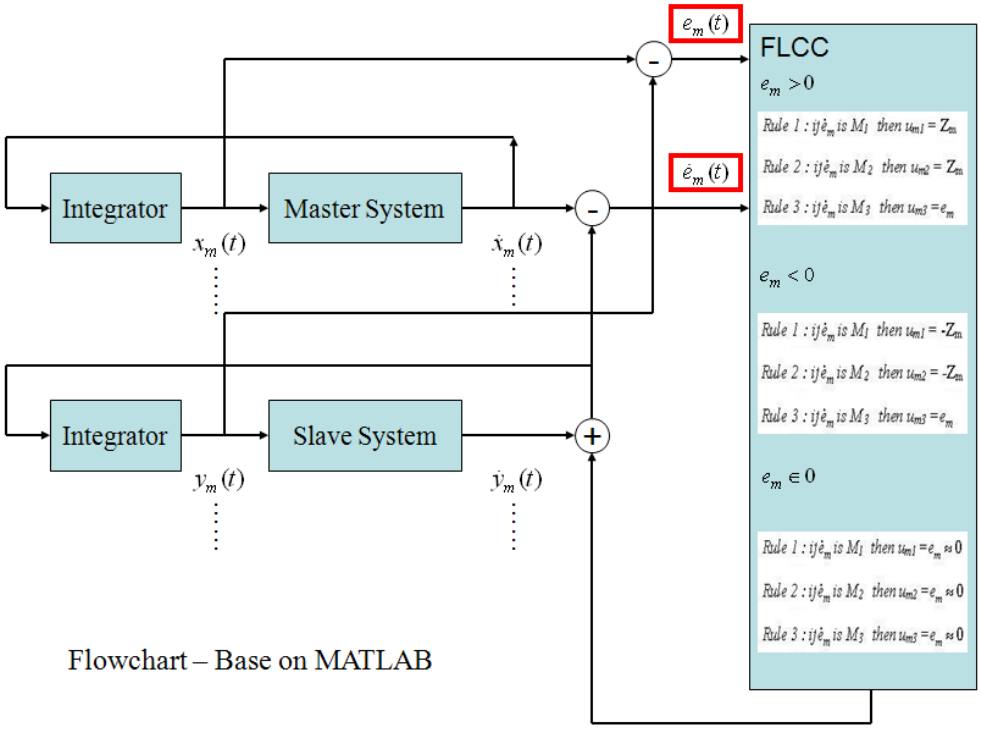

Fig.6.1 The configuration of fuzzy logic controller.

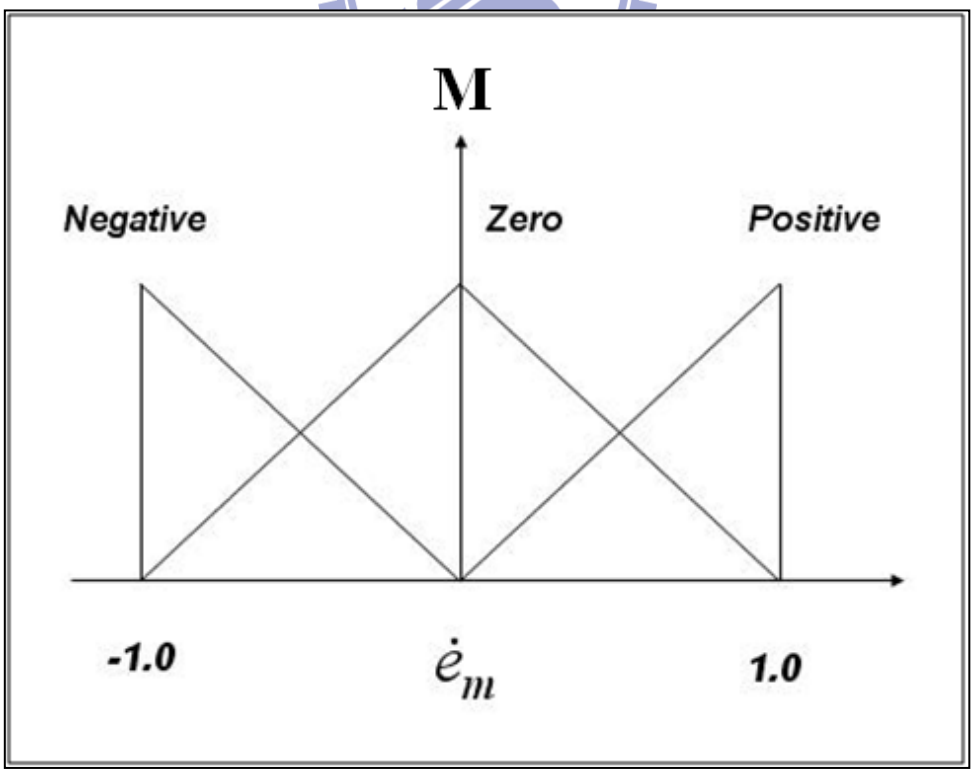

Fig. 6.2 Membership function.

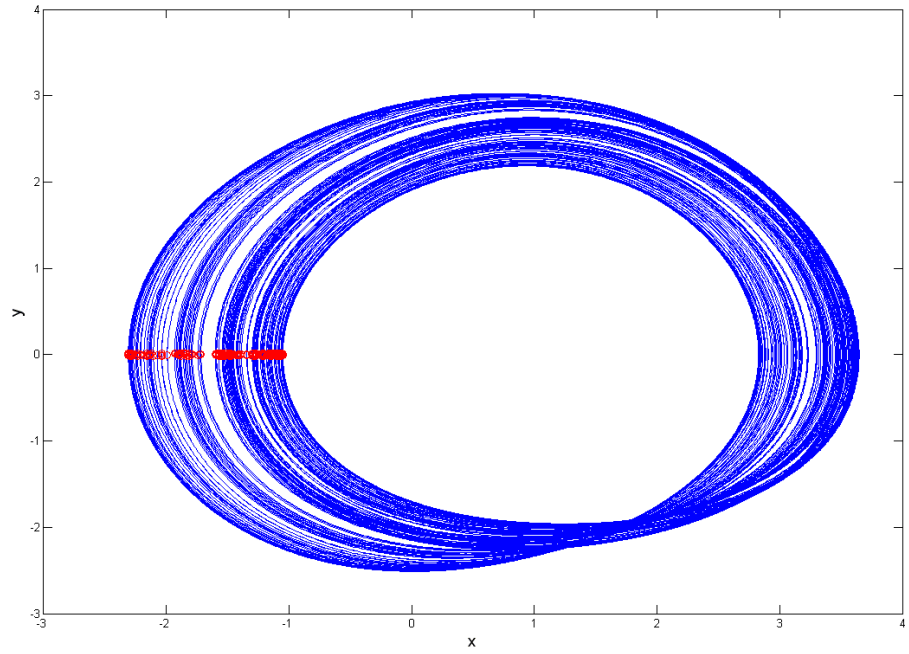

Fig. 6.3 The phase portrait of chaotic Sprott 22 system.

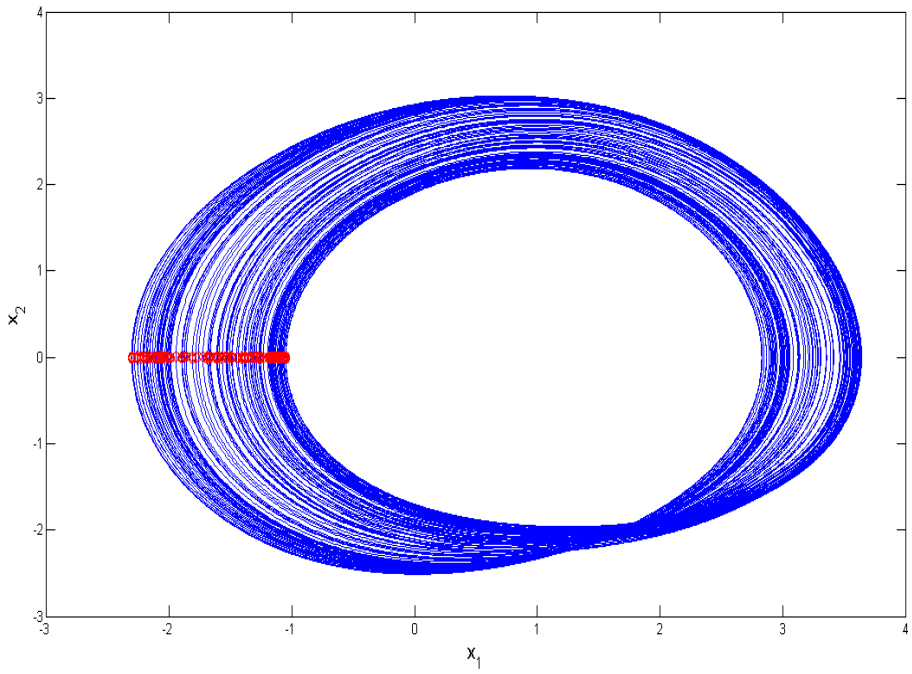

Fig. 6.4 The phase portrait of chaotic non-autonomous Sprott 22 system which has parameters uncertainty.

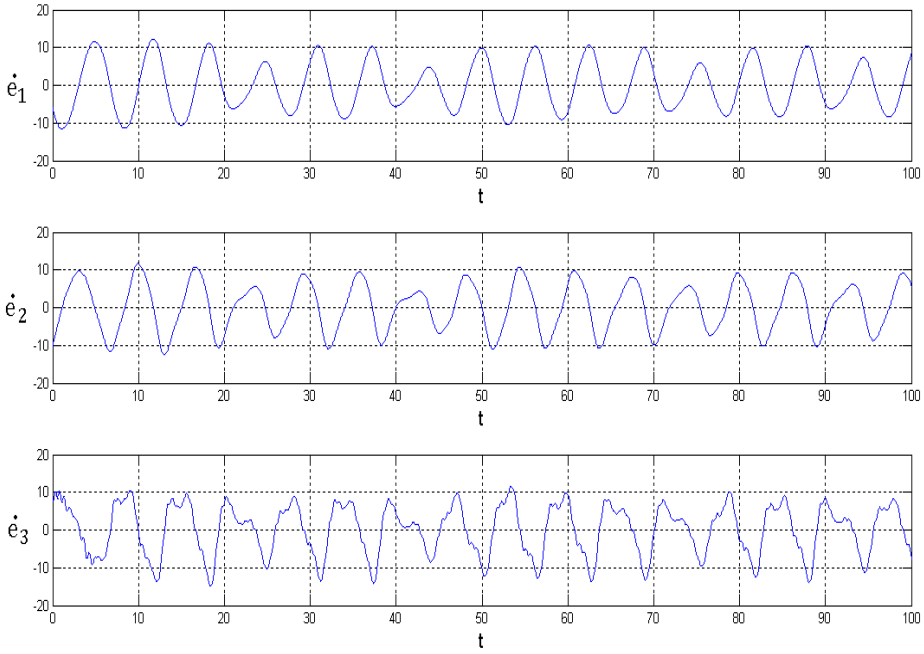

Fig. 6.5 Time histories of error derivatives for identical master and slave chaotic non-autonomous Sprott 22 system without controllers.

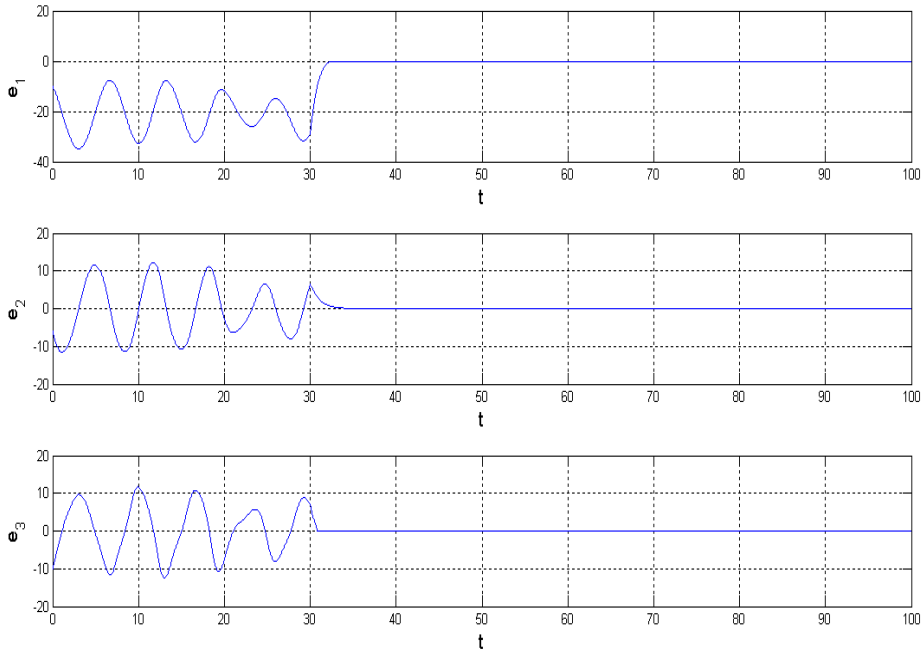

Fig. 6.6 Time histories of errors for projective synchronization of non-autonomous Sprott 22 system by FLCC, the FLCC is coming into after 30s.

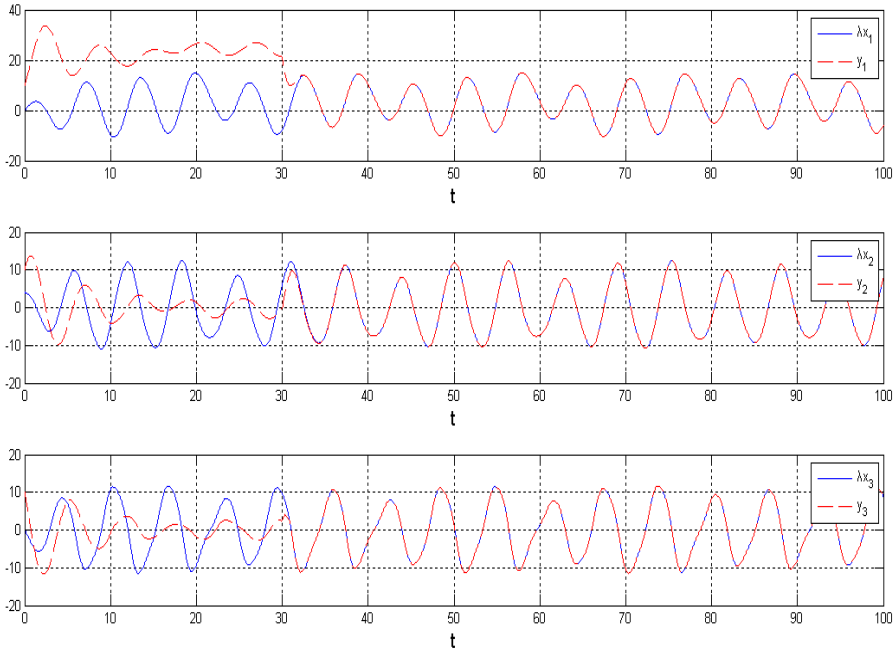

Fig. 6.7 Time histories of states for projective synchronization of non-autonomous Sprott 22 system by FLCC, the FLCC is coming into after 30s.

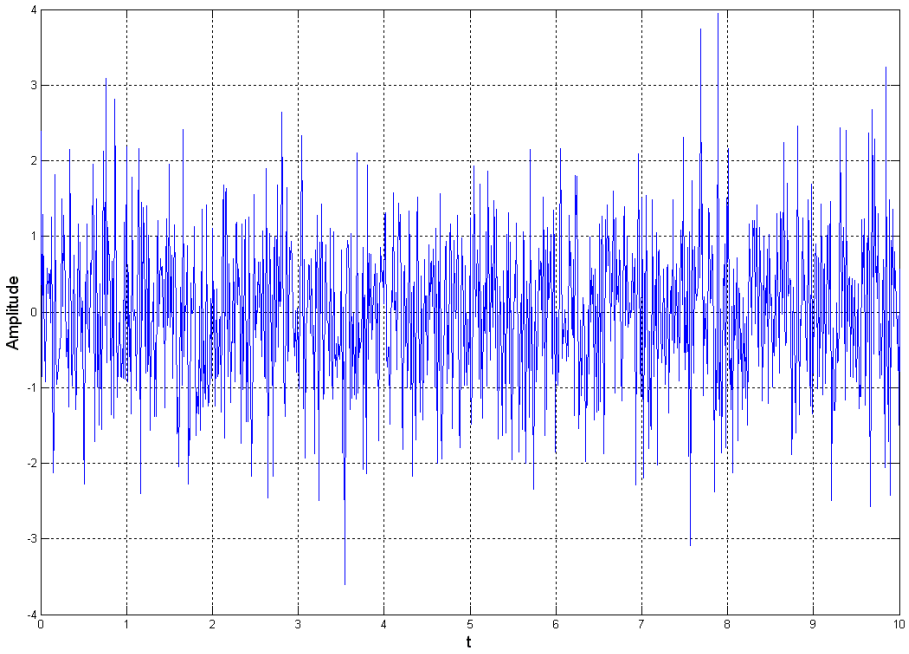

Fig. 6.8 The stochastic disturbance of ζ = band-limited white noise (PSD=0.01).

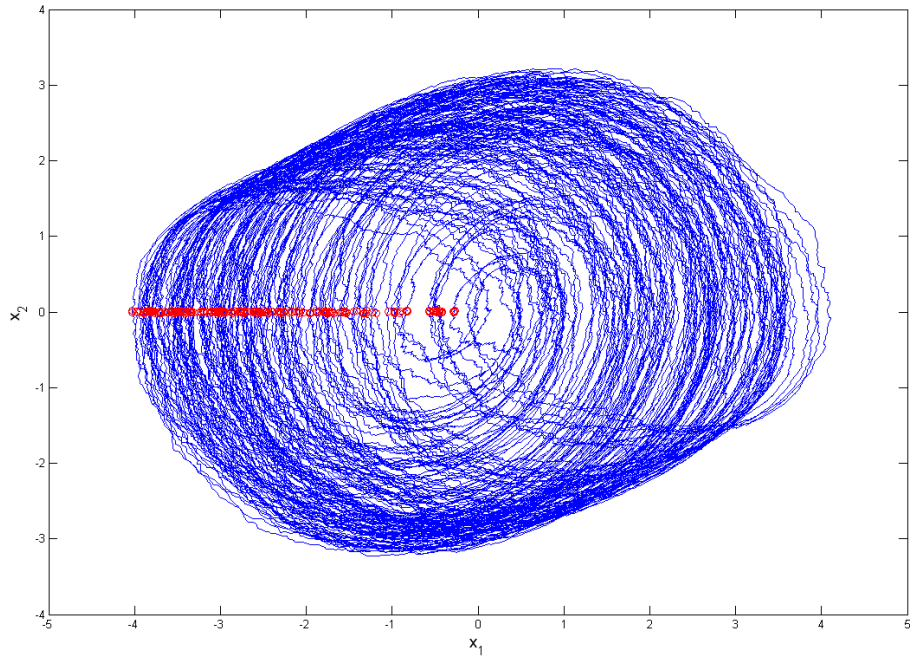

Fig. 6.9 The phase portrait of chaotic Sprott 22 system with stochastic disturbance.

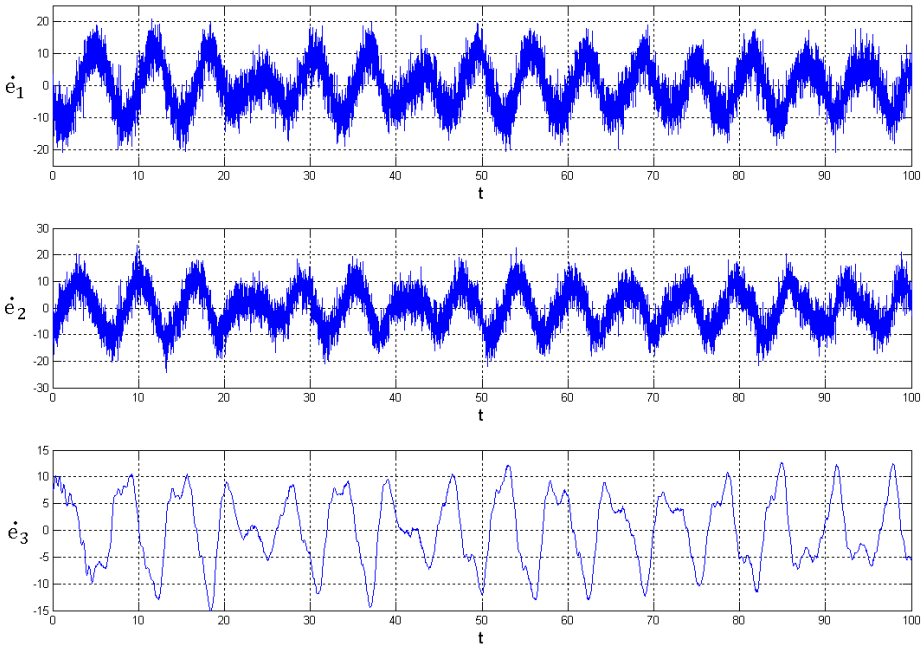

Fig. 6.10 Time histories of error derivatives for identical master and slave chaotic stochastic Sprott 22 system without controllers.

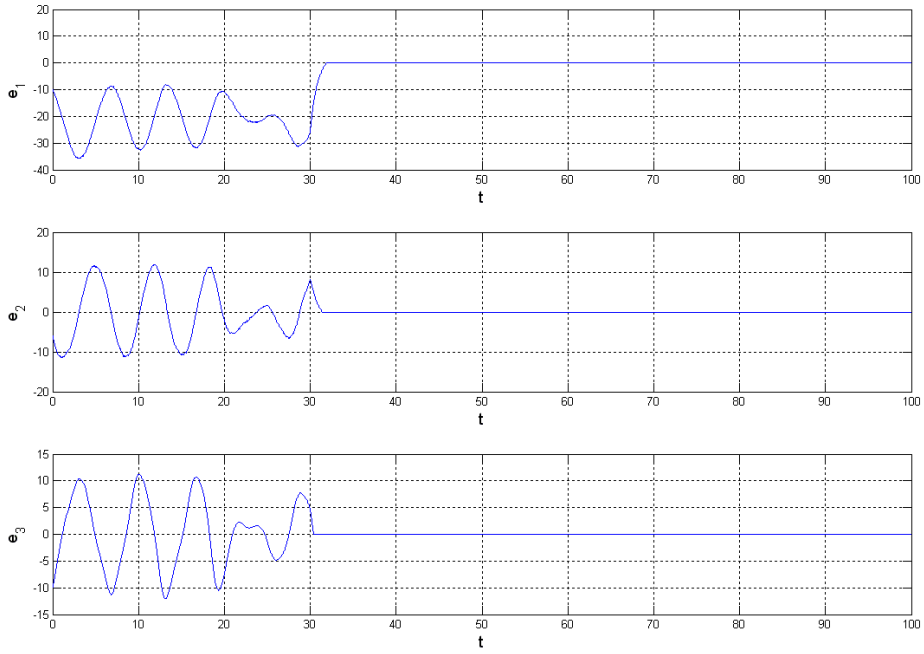

Fig. 6.11 Time histories of errors for projective synchronization of stochastic Sprott 22 system by FLCC, the FLCC is coming into after 30s.

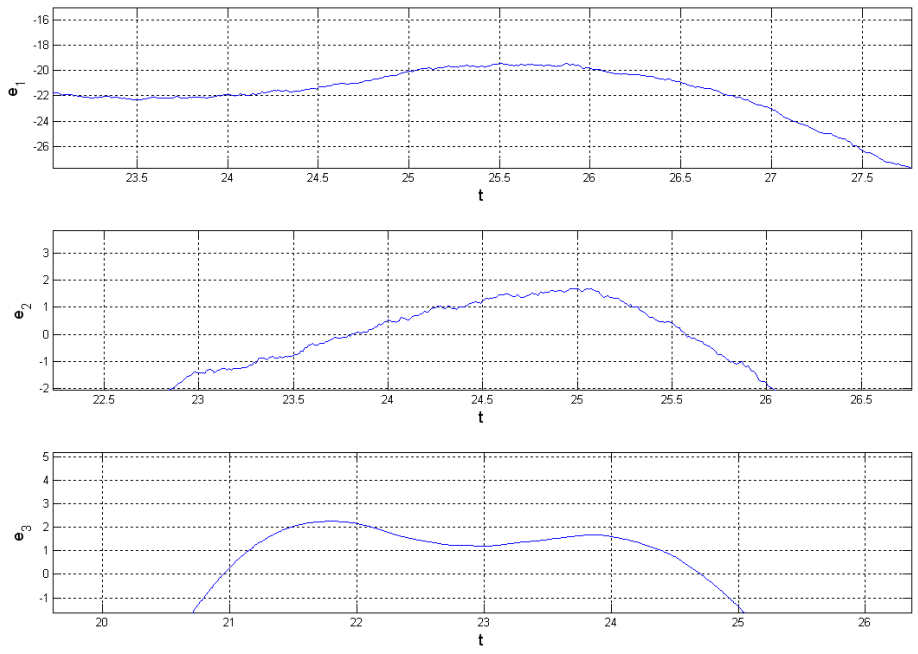

Fig. 6.12 There are irregular ripplies in the detailed time histories of errors which are caused by white noise.

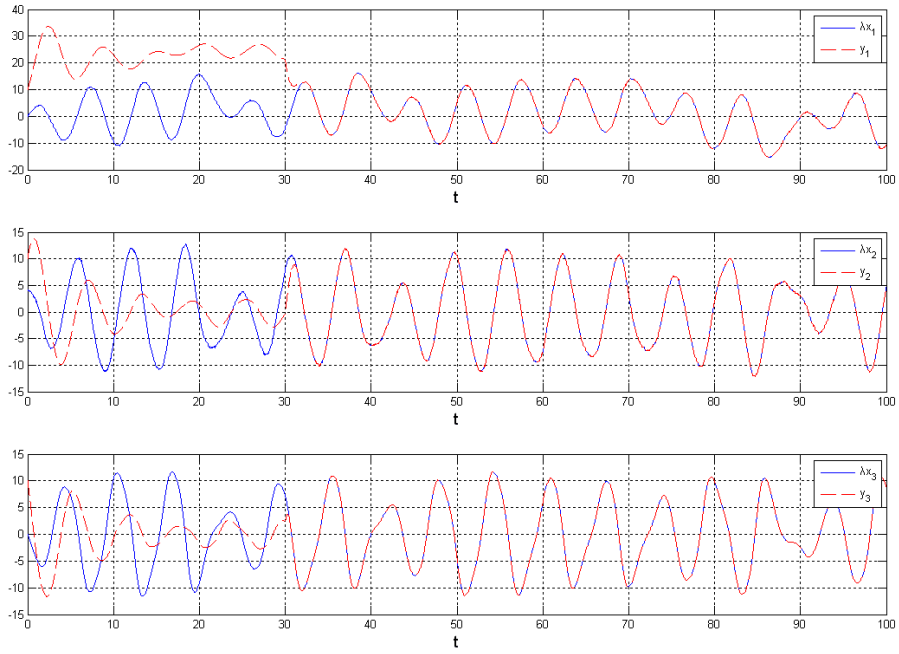

Fig. 6.13 Time histories of states for projective synchronization of stochastic Sprott 22 system by FLCC, the FLCC is coming into after 30s.

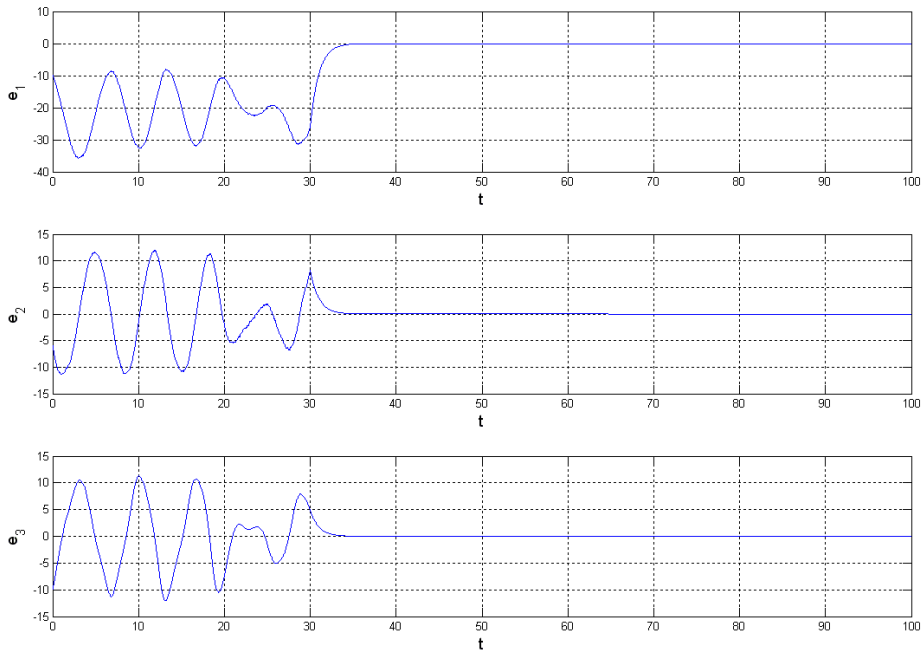

Fig. 6.14 Time histories of states for projective synchronization of stochastic Sprott 22 system by traditional method, the traditional controller is coming into after 30s

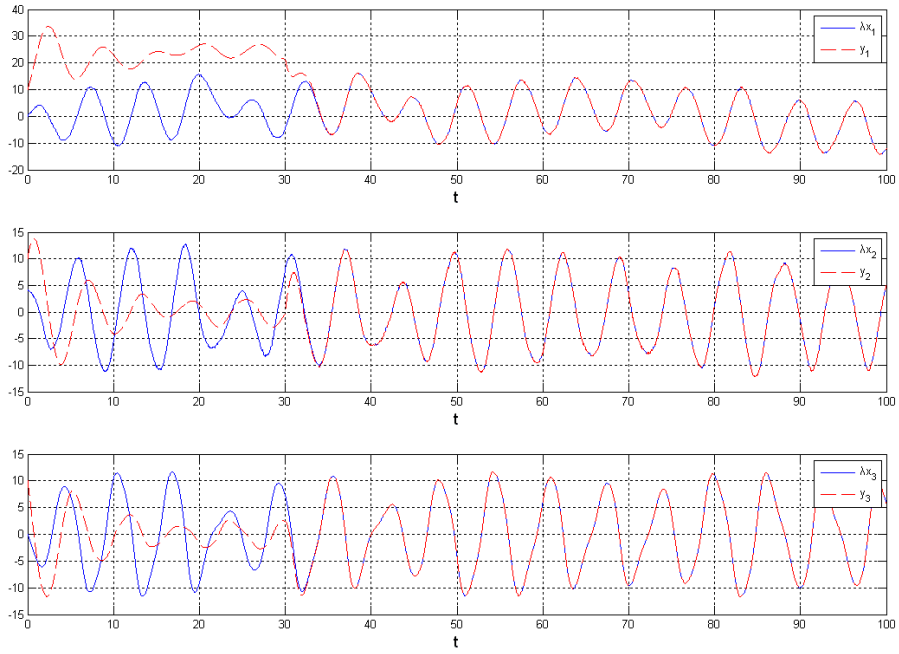

Fig. 6.15 Time histories of states for projective synchronization of stochastic Sprott 22 system by traditional method, the traditional controller is coming into after 30s.

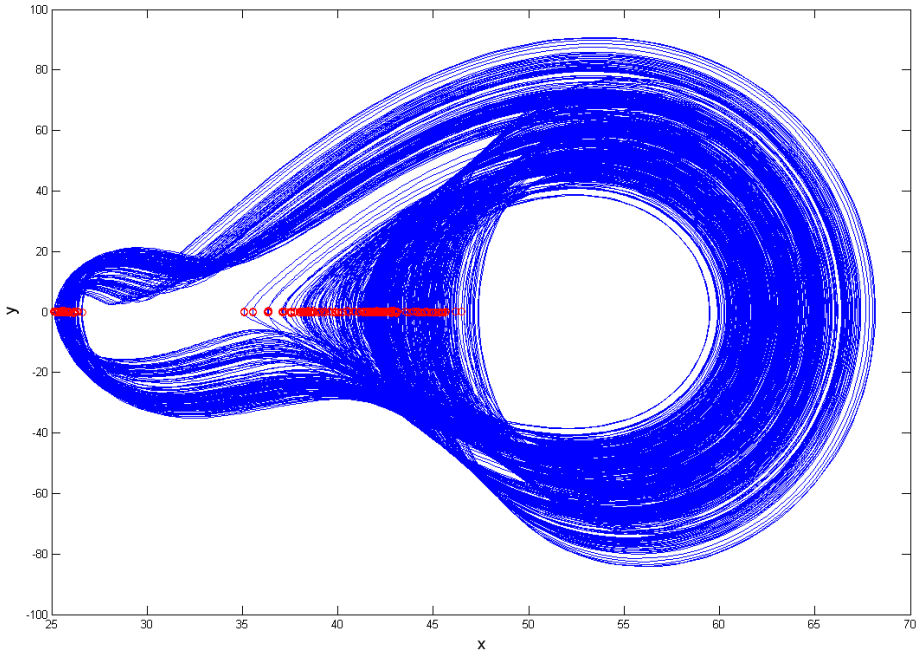

Fig. 6.16 The phase portrait of chaotic GKv system.

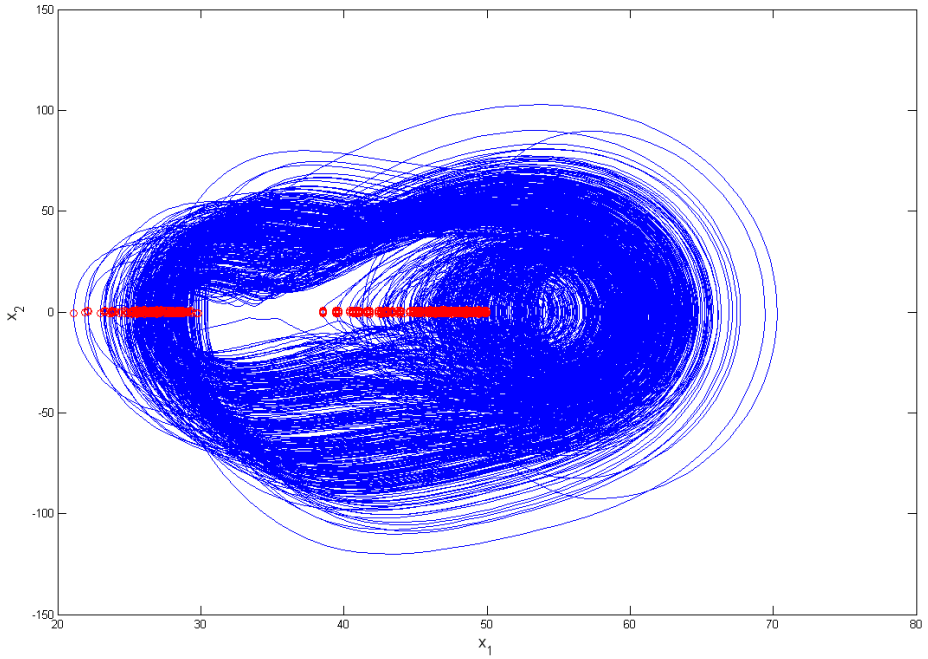

Fig. 6.17 The phase portrait of chaotic non-autonomous GKv system which has parameters uncertainty.

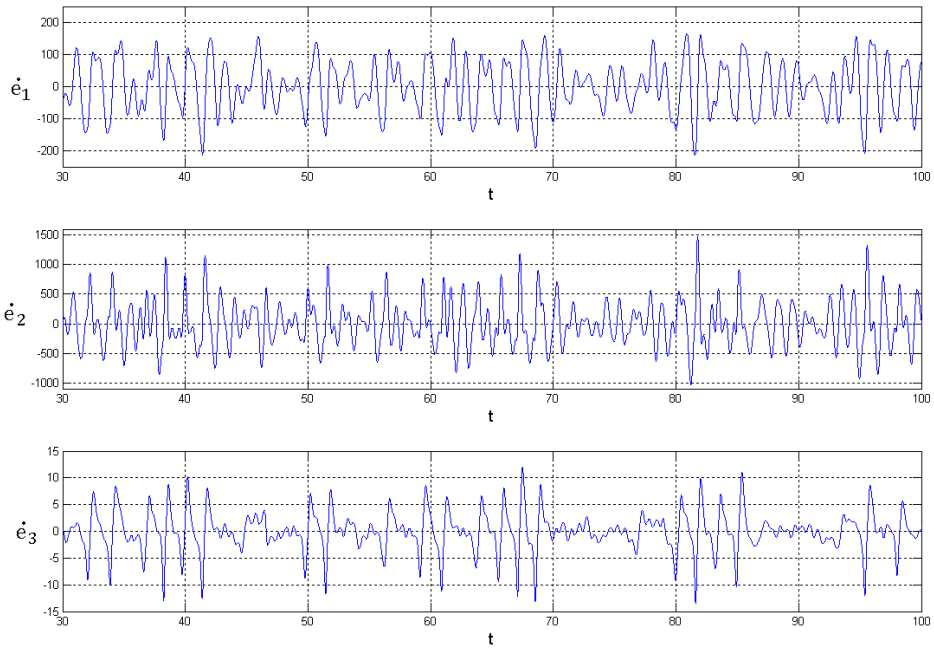

Fig. 6.18 Time histories of error derivatives for identical master and slave chaotic non-autonomous GKv system without controllers.

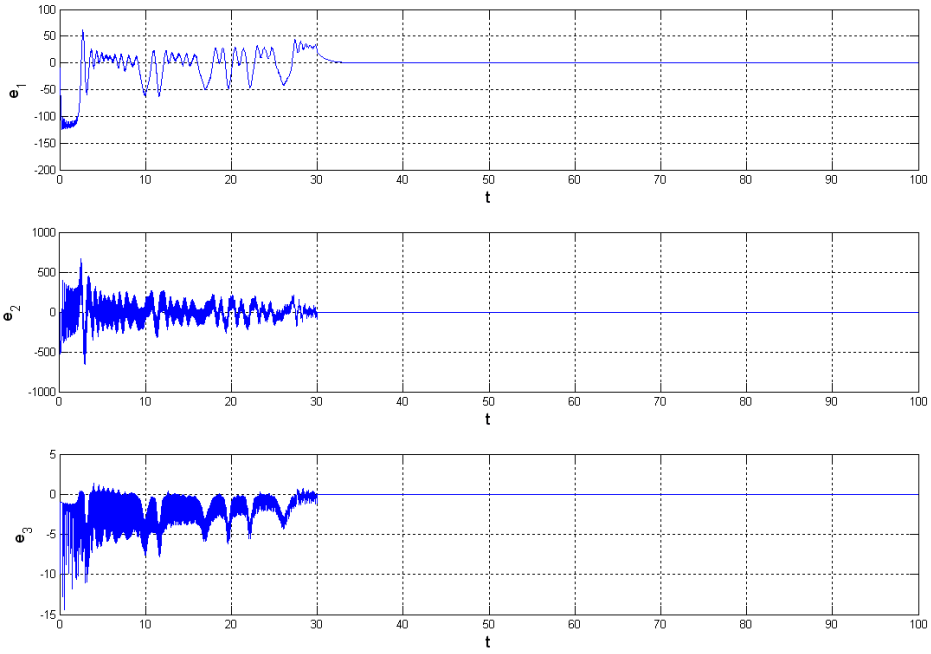

Fig. 6.19 Time histories of errors for projective synchronization of non-autonomous GKv system by FLCC, the FLCC is coming into after 30s.

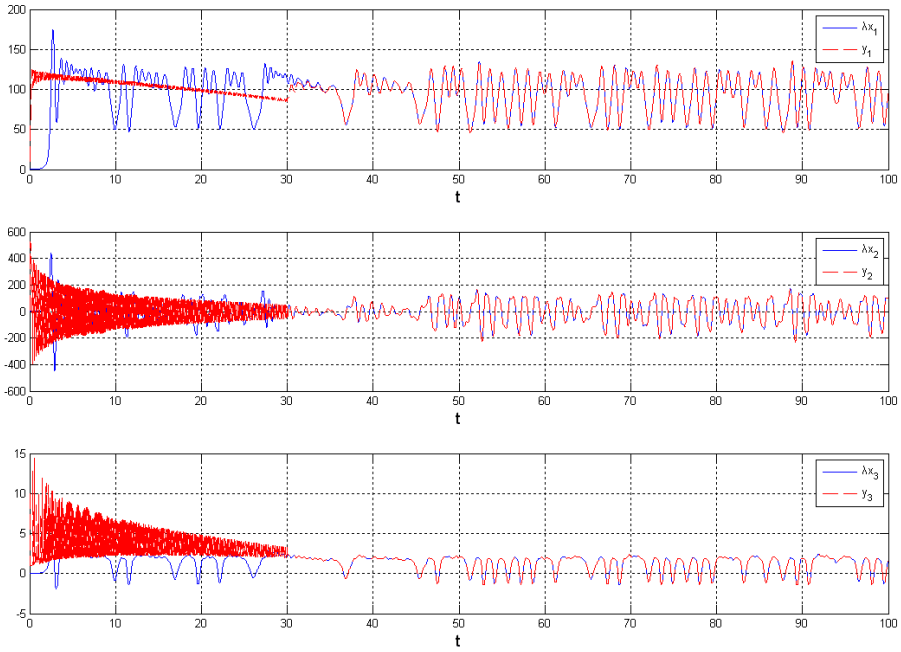

Fig. 6.20 Time histories of states for projective synchronization of non-autonomous GKv system by FLCC, the FLCC is coming into after 30s.

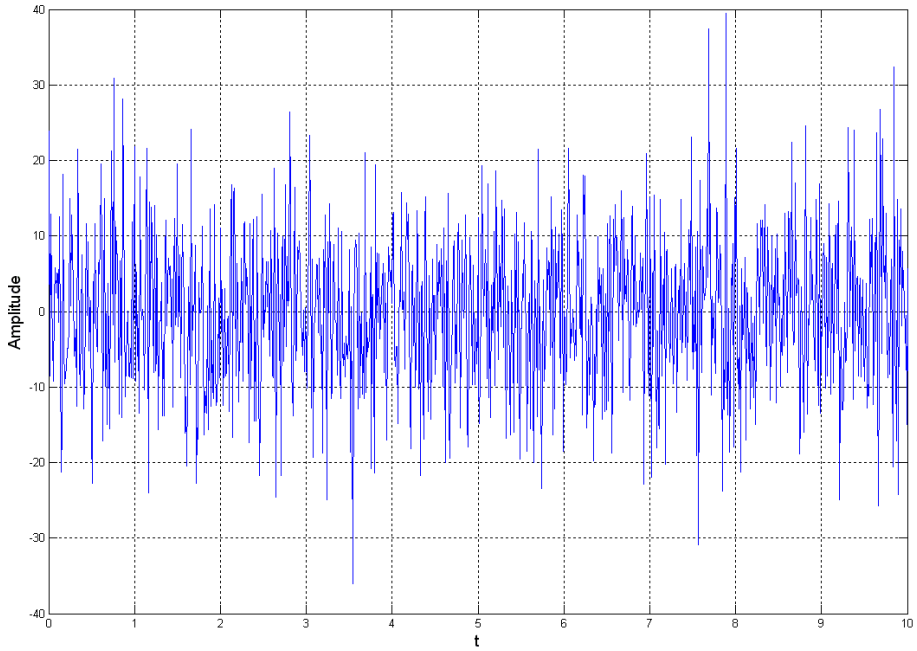

Fig. 6.21 The stochastic disturbance of ζ_1 = band-limited white noise (PSD=1).

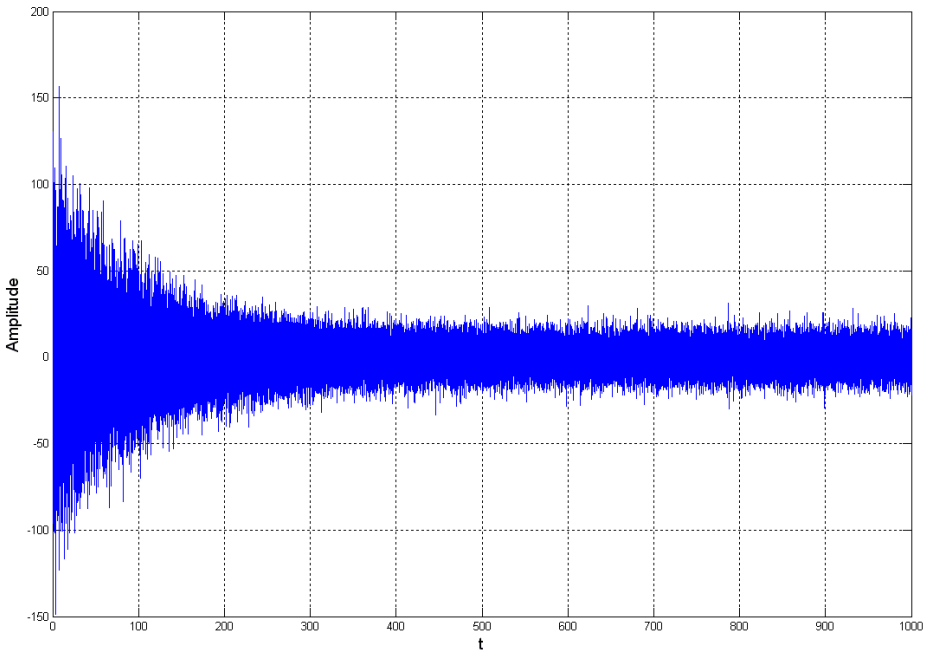

Fig. 6.22 The stochastic disturbance of $\zeta_2 = (\omega_1 + \omega_2 e^{-\omega_3 t}) \cdot$[band-limited white noise] (PSD=0.5).

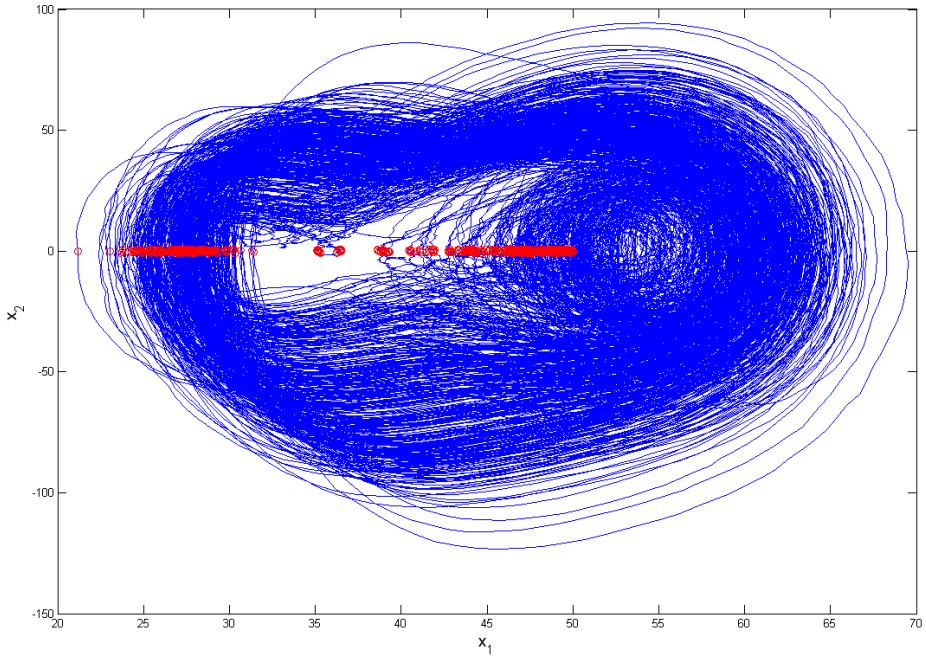

Fig. 6.23 The phase portrait of chaotic GKv system with stochastic disturbances.

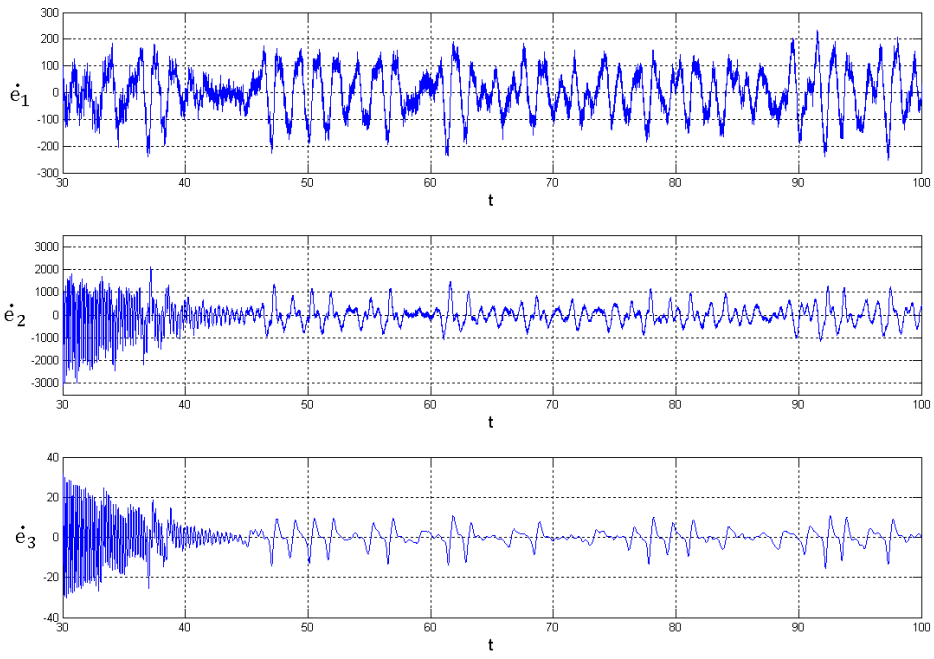

Fig. 6.24 Time histories of error derivatives for identical master and slave chaotic stochastic GKv system without controllers.

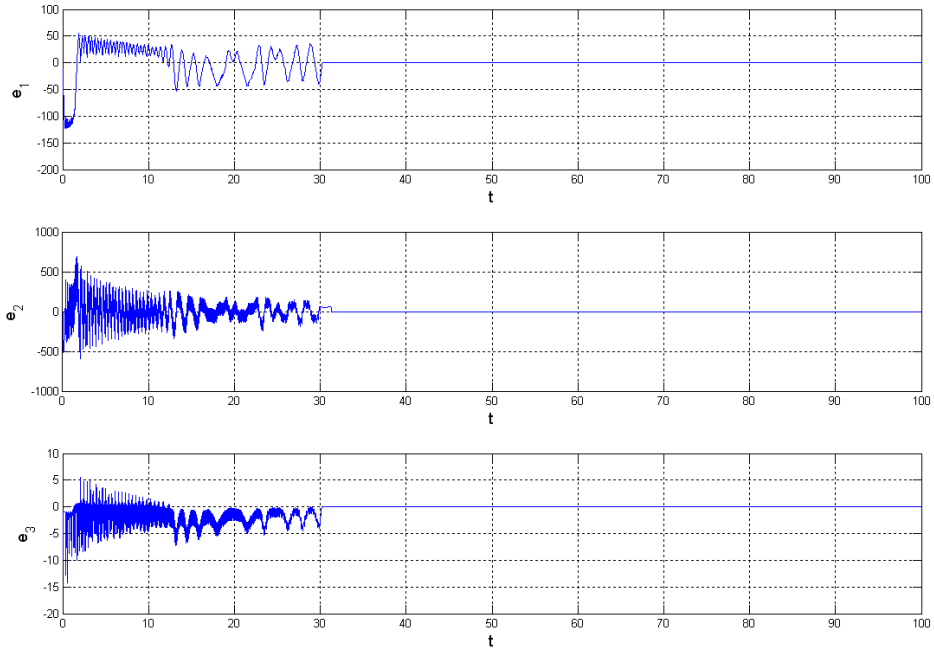

Fig. 6.25 Time histories of errors for projective synchronization of stochastic GKv system by FLCC, the FLCC is coming into after 30s.

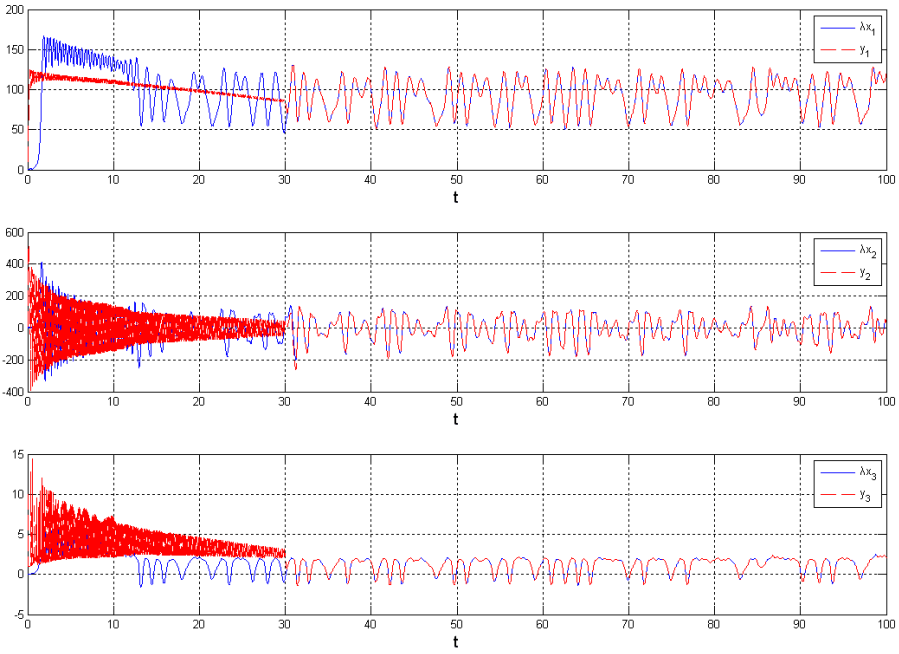

Fig. 6.26 Time histories of states for projective synchronization of stochastic GKv system by FLCC, the FLCC is coming into after 30s.

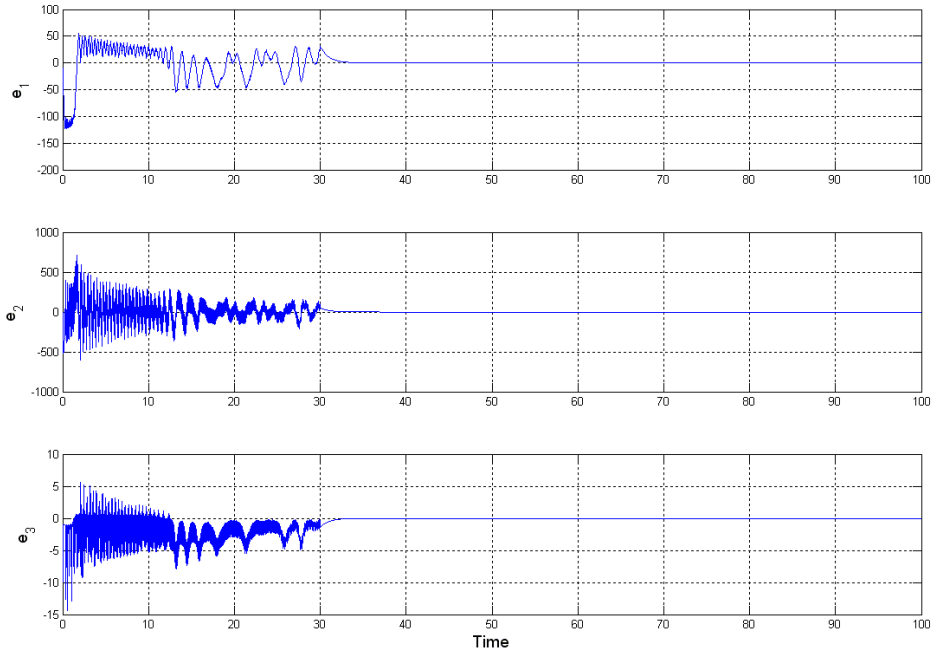

Fig. 6.27 Time histories of states for projective synchronization of stochastic GKv system by traditional method, the traditional controller is coming into after 30s.

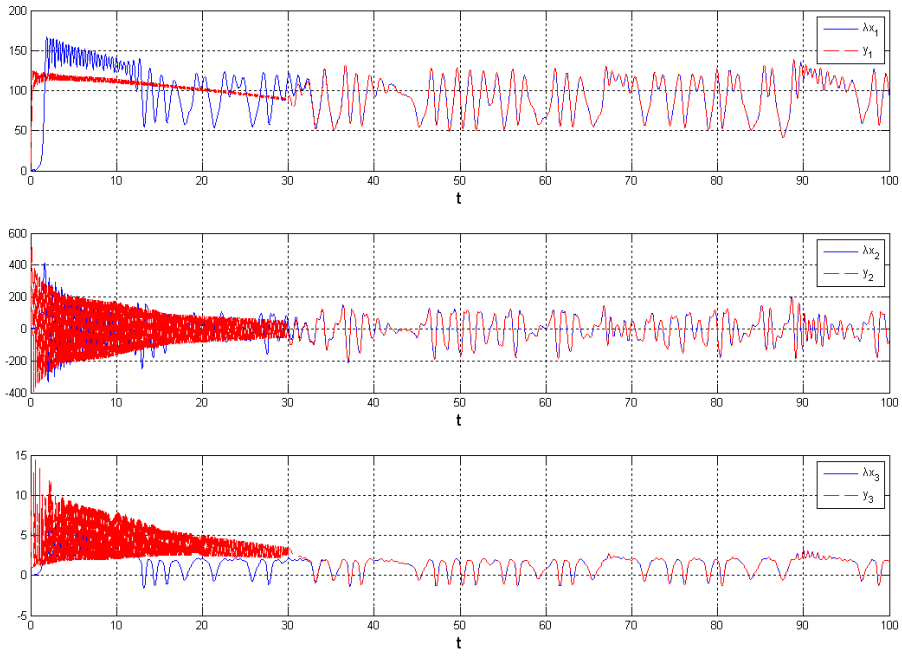

Fig. 6.28 Time histories of states for projective synchronization of stochastic GKv system by traditional method, the traditional controller is coming into after 30s.

Chapter 7

Fuzzy Modeling and Synchronization of Chaotic Systems by a Newfangled Fuzzy Model

7.1 Preliminary

In this Chapter, a newfangled fuzzy model is used to simulate and synchronize two complex nonlinear systems, Ge-Ku-van der Pol system and extended Ge-Ku-van der Pol system. Through the fuzzy model mention above, only two linear subsystems are needed to generate the complicated chaotic behavior of original nonlinear system. In traditional Takagi-Sugeno fuzzy model (T-S fuzzy model) [47], the process of fuzzy modeling focus on the whole system. Therefore, there will be 2^N linear subsystems (according to 2^N fuzzy rules) and $m \times 2^N$ equations in the T-S fuzzy system, where N is the number of nonlinear terms and m is the order of the system. If N is large, the number of linear subsystems in T-S fuzzy system is huge. It becomes more inefficient and complicated.

In Ge-Li fuzzy model (G-L fuzzy model) [59], we focus on each equation of the system. The numbers of fuzzy rules can be reduced from 2^N to $2 \times N$. The fuzzy equations become much simpler. However, the limitation of G-L fuzzy model is that there should be one nonlinear terms in each equation. Consequently, the newfangled fuzzy model is proposed to solve this defect—all nonlinear terms in each equation will be treated as one nonlinear term. It can be used to model various kinds of complex nonlinear systems, even if the nonlinear terms are copious and complicated. Ge-Ku-van der Pol (GKv) systems and Ge-Ku-Mathieu (GKM) system are illustrated in numerical simulations to show the effectiveness and feasibility of new model.

7.2 Newfangled Fuzzy Model Theory

In system analysis and design, it is important to select an appropriate model

representing a real system. As an expression model of a real plant, the fuzzy implications and the fuzzy reasoning method suggested by Takagi and Sugeno are traditionally used. The new fuzzy model is also described by fuzzy IF-THEN rules. The core of the newfangled fuzzy model is that we express each nonlinear equation into two linear sub-equations by fuzzy IF-THEN rules and take all the first linear sub-equations to form one linear subsystem and all the second linear sub-equations to form another linear subsystem. And all nonlinear terms in each state equation will be treated as *one* nonlinear term. The overall fuzzy model of the system is achieved by fuzzy blending of this two linear subsystem models. Consider a continuous-time nonlinear dynamic system as follows:

Equation i:

rule 1:

IF $z_i(t)$ is M_{i1}

THEN $\dot{x}_i(t) = A_{i1}x(t) + B_{i1}u(t)$, (7.1)

rule 2:

IF $z_i(t)$ is M_{i2}

THEN $\dot{x}_i(t) = A_{i2}x(t) + B_{i2}u(t)$, (7.2)

where

$$\mathbf{x}(t) = [x_1(t), x_2(t), ..., x_n(t)]^T, \quad (7.3)$$

$$\mathbf{u}(t) = [u_1(t), u_2(t), ..., u_n(t)]^T, \quad (7.4)$$

$i = 1,2..n$, where n is the number of nonlinear terms. M_{i1}, M_{i2} are fuzzy sets, A_i, B_i are column vectors and $\dot{x}_i(t) = A_{ij}x(t) + B_{ij}u(t)$, $j = 1,2$, is the output from the first and the second IF-THEN rules. Given a pair of $(\mathbf{x}(t), \mathbf{u}(t))$ and take all the first linear sub-equations to form one linear subsystem and all the second linear

sub-equations to form another linear subsystem, the final output of the fuzzy system is inferred as follows:

$$\dot{\mathbf{x}}(t) = \mathbf{M}_1 \begin{bmatrix} A_1 x(t) + B_1 u(t) \\ A_2 x(t) + B_2 u(t) \\ \vdots \\ A_{i1} x(t) + B_{i1} u(t) \end{bmatrix} + \mathbf{M}_2 \begin{bmatrix} A_1 x(t) + B_1 u(t) \\ A_2 x(t) + B_2 u(t) \\ \vdots \\ A_{i2} x(t) + B_{i2} u(t) \end{bmatrix} \tag{7.5}$$

where M_1 and M_2 are diagonal matrices as following:

$$\mathrm{dia}(\mathbf{M}_1) = \begin{bmatrix} M_{11} & M_{21} & \ldots & M_{i1} \end{bmatrix}, \mathrm{dia}(\mathbf{M}_2) = \begin{bmatrix} M_{12} & M_{22} & \ldots & M_{i2} \end{bmatrix}$$

Note that for each equation i:

$$\sum_{\mathrm{j}=1}^{2} \mathrm{M}_{\mathrm{ij}}(\mathrm{z}_{\mathrm{i}}(\mathrm{t})) = 1, \tag{7.6}$$

$\mathrm{M}_{\mathrm{ij}}(\mathrm{z}_{\mathrm{i}}(\mathrm{t})) \geq 0$, i = 1, 2,…, n and j=1,2.

Via the newfangled fuzzy model, the final form of the fuzzy model becomes very simple. The new model provides a much more convenient approach for fuzzy model research and fuzzy application. The simulation results of chaotic systems are discussed in next Section.

7.3 Newfangled Fuzzy Model of Chaotic Systems

In this Section, the newfangled fuzzy models of three different chaotic systems, GKv [24] master system and extended GKv master system are shown for Model 1 and Model 2. GKM [24] slave system is shown for Model 3.

Model 1: Newfangled fuzzy model of GKv system

The GKv system is:

$$\begin{cases} \dot{x}_1 = x_2 \\ \dot{x}_2 = -\alpha_1 x_2 - x_3(\alpha_2(\alpha_3 - x_1^2) + \alpha_4 x_3) \\ \dot{x}_3 = -\alpha_5 x_3 + \alpha_6(1 - x_3^2)x_2 + \alpha_7 x_1 \end{cases} \tag{7.7}$$

with initial states (0.01, 0.01, 0.01). The parameters are $\alpha_1 = 0.08, \alpha_2 = -0.35$, $\alpha_3 =$

100.56, $\alpha_4 = -1000.02$, $\alpha_5 = 0.61$, $\alpha_6 = 0.08$, $\alpha_7 = 0.01$. The chaotic attractor of the GKv system is shown in Fig. 7.1.

If T-S fuzzy model is used for representing local linear models of GKv system, 8 fuzzy rules and 8 linear subsystems are need. The process of modeling is shown as follows:

T-S fuzzy model:

Assume that:

(1) $x_1^2 \in [-Z_1, Z_1]$ and $Z_1 > 0$

(2) $x_3 \in [-Z_2, Z_2]$ and $Z_2 > 0$

(3) $x_3^2 \in [-Z_3, Z_3]$ and $Z_3 > 0$

Then we have the following T-S fuzzy rules:

Rule 1: IF x_1^2 is M_{11} , x_3 is M_{21} and x_3^2 is M_{31} THEN $\dot{X} = A_1 X$,

Rule 2: IF x_1^2 is M_{11} , x_3 is M_{21} and x_3^2 is M_{32} THEN $\dot{X} = A_2 X$,

Rule 3: IF x_1^2 is M_{11} , x_3 is M_{22} and x_3^2 is M_{31} THEN $\dot{X} = A_3 X$,

Rule 4: IF x_1^2 is M_{11} , x_3 is M_{22} and x_3^2 is M_{32} THEN $\dot{X} = A_4 X$,

Rule 5: IF x_1^2 is M_{12} , x_3 is M_{21} and x_3^2 is M_{31} THEN $\dot{X} = A_5 X$,

Rule 6: IF x_1^2 is M_{12} , x_3 is M_{21} and x_3^2 is M_{32} THEN $\dot{X} = A_6 X$,

Rule 7: IF x_1^2 is M_{12} , x_3 is M_{22} and x_3^2 is M_{31} THEN $\dot{X} = A_7 X$,

Rule 8: IF x_1^2 is M_{12} , x_3 is M_{22} and x_3^2 is M_{32} THEN $\dot{X} = A_8 X$,

Then the final output of the GKv system can be composed by fuzzy linear subsystems mentioned above. It is obviously an inefficient and complicated work.

Newfangled fuzzy model:

By using the newfangled fuzzy model, the nonlinear terms in GKv system can be linearized as simple linear terms.

$$\begin{cases} \dot{x}_1 = x_2 \\ \dot{x}_2 = -\alpha_1 x_2 - \alpha_2 \alpha_3 x_3 + x_3 \Delta_1 \\ \dot{x}_3 = -\alpha_5 x_3 + \alpha_6 x_2 + \alpha_7 x_1 - \alpha_6 x_2 \Delta_2 \end{cases} \tag{7.8}$$

where $\Delta_1 = \alpha_2 x_1^2 - \alpha_4 x_3$ and $\Delta_2 = x_3^2$. The steps of fuzzy modeling are shown as follows:

Steps of fuzzy modeling:

Step 1:

Since no nonlinear term in first equation of Eq. (7.8), we choose $M_{11} = \frac{1}{2}$, $M_{12} = \frac{1}{2}$, M_{11} and M_{12} are fuzzy sets of the first equation of Eq. (7.8) and $M_{11} + M_{12} = 1$.

Step 2:

Assume that $\Delta_1 \in [-Z_2, Z_2]$ and $Z_2 > 0$, then the second equation of Eq. (8) can be exactly represented by newfangled fuzzy model as following:

Rule 1: IF Δ_1 is M_{21}, THEN $\dot{x}_2 = -\alpha_1 x_2 - \alpha_2 \alpha_3 x_3 + x_3 Z_2$, (7.9)

Rule 2: IF Δ_1 is M_{22}, THEN $\dot{x}_2 = -\alpha_1 x_2 - \alpha_2 \alpha_3 x_3 - x_3 Z_2$ (7.10)

where

$$M_{21} = \frac{1}{2}(1 + \frac{\Delta_1}{Z_2}), \quad M_{22} = \frac{1}{2}(1 - \frac{\Delta_1}{Z_2}),$$

and $Z_2 = 3000$ from Fig. 7.2. M_{21} and M_{22} are fuzzy sets of the second equation of Eq. (7.8) and $M_{21} + M_{22} = 1$.

Step 3:

Assume that $\Delta_2 \in [-Z_3, Z_3]$ and $Z_3 > 0$, then the third equation of Eq. (7.8) can be exactly represented by newfangled fuzzy model as following:

Rule 1: IF x_1 is M_{31}, THEN $\dot{x}_3 = -\alpha_5 x_3 + \alpha_6 x_2 + \alpha_7 x_1 - \alpha_6 x_2 Z_3$ (7.11)

Rule 2: IF x_1 is M_{32}, THEN $\dot{x}_3 = -\alpha_5 x_3 + \alpha_6 x_2 + \alpha_7 x_1 + \alpha_6 x_2 Z_3$ (7.12)

where

$$M_{31} = \frac{1}{2}(1+\frac{\Delta_2}{Z_3}), \quad M_{32} = \frac{1}{2}(1-\frac{\Delta_2}{Z_3}),$$

and $Z_3 = 18$ from Fig. 7.2. M_{31} and M_{32} are fuzzy sets of the third equation of Eq. (7.8) and $M_{31} + M_{32} = 1$.

Here, we call Eqs. (7.9) and (7.11) the first linear subsystem under the fuzzy rules, and Eqs. (7.10) and (7.12) the second linear subsystem under the fuzzy rules.

The first linear subsystem is

$$\begin{cases} \dot{x}_1 = x_2 \\ \dot{x}_2 = -\alpha_1 x_2 - \alpha_2\alpha_3 x_3 + x_3 Z_2 \\ \dot{x}_3 = -\alpha_5 x_3 + \alpha_6 x_2 + \alpha_7 x_1 - \alpha_6 x_2 Z_3 \end{cases} \tag{7.13}$$

The second linear subsystem is

$$\begin{cases} \dot{x}_1 = x_2 \\ \dot{x}_2 = -\alpha_1 x_2 - \alpha_2\alpha_3 x_3 - x_3 Z_2 \\ \dot{x}_3 = -\alpha_5 x_3 + \alpha_6 x_2 + \alpha_7 x_1 + \alpha_6 x_2 Z_3 \end{cases} \tag{7.14}$$

Via newfangled fuzzy model, the number of fuzzy rules can be greatly reduced. Just two linear subsystems are enough to express such complex chaotic behaviors. The simulation results are similar the original chaotic behavior of the GKv system as shown in Fig. 7.3.

Now we have:

$$\begin{bmatrix} \dot{x}_1 \\ \dot{x}_2 \\ \dot{x}_3 \end{bmatrix} = \begin{bmatrix} M_{11} & 0 & 0 \\ 0 & M_{21} & 0 \\ 0 & 0 & M_{31} \end{bmatrix} \begin{bmatrix} x_2 \\ -\alpha_1 x_2 - \alpha_2\alpha_3 x_3 + x_3 Z_2 \\ -\alpha_5 x_3 + \alpha_6 x_2 + \alpha_7 x_1 - \alpha_6 x_2 Z_3 \end{bmatrix} + \begin{bmatrix} M_{12} & 0 & 0 \\ 0 & M_{22} & 0 \\ 0 & 0 & M_{32} \end{bmatrix} \begin{bmatrix} x_2 \\ -\alpha_1 x_2 - \alpha_2\alpha_3 x_3 - x_3 Z_2 \\ -\alpha_5 x_3 + \alpha_6 x_2 + \alpha_7 x_1 + \alpha_6 x_2 Z_3 \end{bmatrix} \tag{7.15}$$

Eq. (7.15) can be rewritten as a simple mathematical expression:

$$\dot{\mathbf{X}}(t) = \sum_{i=1}^{2} \mathbf{\Psi}_i (\mathbf{A}_i \mathbf{X}(t) + \tilde{\mathbf{b}}_i) \tag{7.16}$$

where Ψ_i are diagonal matrices as follows:

$$dia(\boldsymbol{\Psi}_1)=\begin{bmatrix}M_{11} & M_{21} & M_{31}\end{bmatrix},\ dia(\boldsymbol{\Psi}_2)=\begin{bmatrix}M_{12} & M_{22} & M_{32}\end{bmatrix}$$

$$\mathbf{A_1}=\begin{bmatrix}0 & 1 & 0\\ \alpha_1 & 0 & -\alpha_2\alpha_3+Z_2\\ \alpha_7 & \alpha_6(1-Z_3) & -\alpha_5\end{bmatrix},\ \tilde{\mathbf{b}}_1=\begin{bmatrix}0\\0\\0\end{bmatrix}$$

$$\mathbf{A_2}=\begin{bmatrix}0 & 1 & 0\\ \alpha_1 & 0 & -\alpha_2\alpha_3-Z_2\\ \alpha_7 & \alpha_6(1+Z_3) & -\alpha_5\end{bmatrix},\ \tilde{\mathbf{b}}_2=\begin{bmatrix}0\\0\\0\end{bmatrix}$$

where $\mathbf{A_1}$, $\mathbf{A_2}$, $\tilde{\mathbf{b}}_1$, $\tilde{\mathbf{b}}_2$ are provided for the next Section to fuzzy synchronize.

Model 2: Newfangled fuzzy model of extended GKv system

The extended GKv system is:

$$\begin{cases}\dot{x}_1=x_2\\ \dot{x}_2=-\alpha_1x_2-x_3(\alpha_2(\alpha_3-x_1^2)+\alpha_4x_3-\alpha_8x_3^3)\\ \dot{x}_3=-\alpha_5x_3+\alpha_6(1-x_3^2)x_2+\alpha_7x_1\end{cases}\tag{7.17}$$

with initial states (0.01, 0.01, 0.01). The parameters are the same as that Eq. (7.7) but $-\alpha_8x_3^3$, where $\alpha_8=50$. The chaotic attractor of the extended GKv system is shown in Fig. 7.4.

If T-S fuzzy model is used for representing local linear models of extended GKv system, 16 fuzzy rules and 16 linear subsystems are needed. This T-S fuzzy system becomes too complex treat.

Newfangled fuzzy model:

By using the newfangled fuzzy model, extended GKv system can be linearized as simple linear equations.

$$\begin{cases}\dot{x}_1=x_2\\ \dot{x}_2=-\alpha_1x_2-\alpha_2\alpha_3x_3+x_3\Delta_1\\ \dot{x}_3=-\alpha_5x_3+\alpha_6x_2+\alpha_7x_1-\alpha_6x_2\Delta_2\end{cases}\tag{7.18}$$

where $\Delta_1=\alpha_2x_1^2-\alpha_4x_3+\alpha_8x_3^2$ and $\Delta_2=x_3^2$. The steps of fuzzy modeling are similar

to ***Model 1***. $Z_2 = 4000$, $Z_3 = 12$ from Fig. 7.5. And the simulation results are similar the original chaotic behavior of the extended GKv system as shown in Fig. 7.6.

Model 3: New fuzzy model of slave GKM system

The slave GKM system is:

$$\begin{cases} \dot{y}_1 = y_2 \\ \dot{y}_2 = -\beta_1 y_2 - y_1(\beta_2(\beta_3 - y_1^2) + \beta_4 y_2 y_3) \\ \dot{y}_3 = -(\beta_5 + \beta_6 y_1) y_3 + \beta_7 y_2 + \beta_8 y_1^2 \end{cases} \tag{7.19}$$

The initial conditions are chosen as (0.05, 0.05, 0.05). The parameters are $\beta_1 = -0.6, \beta_2 = 5, \beta_3 = 11, \beta_4 = 0.3, \beta_5 = 8, \beta_6 = 10, \beta_7 = 0.5, \beta_8 = 0.2$ and the GKM system model exhibits chaotic motion which is shown in Fig. 7.7.

If T-S fuzzy model is used for representing local linear models of extended GKv system, 16 fuzzy rules and 16 linear subsystems are need. This T-S fuzzy system becomes too complex treat.

By using the newfangled fuzzy model, GKM system can be linearized as simple linear equations.

$$\begin{cases} \dot{y}_1 = y_2 \\ \dot{y}_2 = -\beta_1 y_2 - \beta_2 \beta_3 y_1 + y_1 \Delta_1 \\ \dot{y}_3 = -\beta_5 y_3 + \beta_7 y_2 + y_1 \Delta_2 \end{cases} \tag{7.20}$$

where $\Delta_1 = \beta_2 x_1^2 - \beta_4 x_2 x_3$ and $\Delta_2 = -\beta_6 x_3 + \beta_6 x_1$.

New fuzzy model:

Assume that:

(1) $\Delta_1 \in [-Z_2, Z_2]$ and $Z_2 > 0$,

(2) $\Delta_2 \in [-Z_3, Z_3]$ and $Z_3 > 0$,

then we have the following new fuzzy rules:

The first equation of Eq. (7.20) is without nonlinear term, we choose $N_{11} = \frac{1}{2}$, $N_{12} = \frac{1}{2}$,

and

$$\text{Rule 1: IF } \Delta_1 \text{ is } N_{21}, \text{THEN } \dot{y}_2 = -\beta_1 y_2 - \beta_2\beta_3 y_1 + y_1 Z_2, \tag{7.21}$$

$$\text{Rule 2: IF } \Delta_1 \text{ is } N_{22}, \text{THEN } \dot{y}_2 = -\beta_1 y_2 - \beta_2\beta_3 y_1 - y_1 Z_2, \tag{7.22}$$

where

$$N_{21} = \frac{1}{2}\left(1 + \frac{\Delta_1}{Z_2}\right), \quad N_{22} = \frac{1}{2}\left(1 - \frac{\Delta_1}{Z_2}\right).$$

and

$$\text{Rule 1: IF } \Delta_2 \text{ is } N_{31}, \text{THEN } \dot{y}_3 = -\beta_5 y_3 + \beta_7 y_2 + y_1 Z_3, \tag{7.23}$$

$$\text{Rule 2: IF } \Delta_2 \text{ is } N_{32}, \text{THEN } \dot{y}_3 = -\beta_5 y_3 + \beta_7 y_2 - y_1 Z_3, \tag{7.24}$$

where

$$N_{31} = \frac{1}{2}\left(1 + \frac{\Delta_2}{Z_3}\right), \quad N_{32} = \frac{1}{2}\left(1 - \frac{\Delta_2}{Z_3}\right). \text{ In Eqs. (7.21-24), } Z_2 = 60 \text{ and } Z_5 = 300$$

from Fig. 7.8. N_{11}, N_{12}, N_{21}, N_{22}, N_{31} and N_{32} are fuzzy sets of Eq. (7.20) and $N_{11} + N_{12} = 1$, $N_{21} + N_{22} = 1$ and $N_{31} + N_{32} = 1$

Here we call Eq. (7.21) and Eq. (7.23) the first linear subsystem under the fuzzy rules and Eq. (7.22) and Eq. (7.24) the second linear subsystem under the fuzzy rules. The first linear subsystem is

$$\begin{cases} \dot{y}_1 = y_2 \\ \dot{y}_2 = -\beta_1 y_2 - \beta_2\beta_3 y_1 + y_1 Z_2 \\ \dot{y}_3 = -\beta_5 y_3 + \beta_7 y_2 + y_1 Z_3 \end{cases} \tag{7.25}$$

The second linear subsystem is

$$\begin{cases} \dot{y}_1 = y_2 \\ \dot{y}_2 = -\beta_1 y_2 - \beta_2\beta_3 y_1 - y_1 Z_2 \\ \dot{y}_3 = -\beta_5 y_3 + \beta_7 y_2 - y_1 Z_3 \end{cases} \tag{7.26}$$

The final output of the fuzzy GKM system is inferred as follows and the chaotic behavior of fuzzy system is shown in Fig. 7.9.

$$\begin{bmatrix}\dot{y}_1\\ \dot{y}_2\\ \dot{y}_3\end{bmatrix}=\begin{bmatrix}N_{11} & 0 & 0\\ 0 & N_{21} & 0\\ 0 & 0 & N_{31}\end{bmatrix}^T\begin{bmatrix}y_2\\ -\beta_1 y_2-\beta_2\beta_3 y_1+y_1 Z_2\\ -\beta_5 y_3+\beta_7 y_2+y_1 Z_3\end{bmatrix}+\begin{bmatrix}N_{12} & 0 & 0\\ 0 & N_{22} & 0\\ 0 & 0 & N_{32}\end{bmatrix}^T\begin{bmatrix}y_2\\ -\beta_1 y_2-\beta_2\beta_3 y_1-y_1 Z_2\\ -\beta_5 y_3+\beta_7 y_2-y_1 Z_3\end{bmatrix} \tag{7.27}$$

Eq. (7-27) can be rewritten as a simple mathematical expression:

$$\dot{\mathbf{Y}}(t)=\sum_{i=1}^{2}\mathbf{\Gamma}_i(\mathbf{C}_i\mathbf{Y}(t)+\tilde{\mathbf{c}}_i) \tag{7.28}$$

where

$$dia(\mathbf{\Gamma}_1)=\begin{bmatrix}N_{11} & N_{21} & N_{31}\end{bmatrix},\ dia(\mathbf{\Gamma}_2)=\begin{bmatrix}N_{12} & N_{22} & N_{32}\end{bmatrix}$$

$$\mathbf{C}_1=\begin{bmatrix}0 & 1 & 0\\ -\beta_2\beta_3+Z_2 & -\beta_1 & 0\\ Z_3 & \beta_7 & -\beta_5\end{bmatrix},\ \tilde{\mathbf{c}}_1=\begin{bmatrix}0\\ 0\\ 0\end{bmatrix}$$

$$\mathbf{C}_2=\begin{bmatrix}0 & 1 & 0\\ -\beta_2\beta_3-Z_2 & -\beta_1 & 0\\ -Z_3 & \beta_7 & -\beta_5\end{bmatrix},\ \tilde{\mathbf{c}}_2=\begin{bmatrix}0\\ 0\\ 0\end{bmatrix}$$

where $\mathbf{C}_1$, $\mathbf{C}_2$, $\tilde{\mathbf{c}}_1$, $\tilde{\mathbf{c}}_2$ are provided for the next Section to Fuzzy synchronize.

7.4 Fuzzy Synchronization Scheme

In this Section, we derive the newfangled fuzzy synchronization scheme based on our new fuzzy model to synchronize two different fuzzy chaotic systems. The following fuzzy systems as the master and slave systems are given:

master system:

$$\dot{\mathbf{X}}(t)=\sum_{i=1}^{2}\mathbf{\Psi}_i(\mathbf{A}_i\mathbf{X}(t)+\tilde{\mathbf{b}}_i) \tag{7.29}$$

slave system:

$$\dot{\mathbf{Y}}(t)=\sum_{i=1}^{2}\mathbf{\Gamma}_i(\mathbf{C}_i\mathbf{Y}(t)+\tilde{\mathbf{c}}_i)+\mathbf{B}\mathbf{U}(t) \tag{7.30}$$

Eq. (7.29) and Eq. (7.30) represent the two different chaotic systems, and in Eq. (7.30)

there is control input **U**(t). Define the error signal as $\mathbf{e}(t) = \mathbf{X}(t) - \mathbf{Y}(t)$, we have:

$$\dot{\mathbf{e}}(t) = \dot{\mathbf{X}}(t) - \dot{\mathbf{Y}}(t) = \sum_{i=1}^{2} \mathbf{\Psi}_i (\mathbf{A}_i \mathbf{X}(t) + \tilde{\mathbf{b}}_i) - \sum_{i=1}^{2} \mathbf{\Gamma}_i (\mathbf{C}_i \mathbf{Y}(t) + \tilde{\mathbf{c}}_i) - \mathbf{B}\mathbf{U}(t) \tag{7.31}$$

The fuzzy controllers are designed as follows:

$$\mathbf{U}(t) = \mathbf{u}_1(t) + \mathbf{u}_2(t) \tag{7.32}$$

where

$$\mathbf{u}_1(t) = \sum_{i=1}^{2} \mathbf{\Psi}_i \mathbf{F}_i \mathbf{X}(t) - \sum_{i=1}^{2} \mathbf{\Gamma}_i \mathbf{P}_i \mathbf{Y}(t),$$

$$\mathbf{u}_2(t) = \sum_{i=1}^{2} \mathbf{\Psi}_i \tilde{\mathbf{b}}_i - \sum_{i=1}^{2} \mathbf{\Gamma}_i \tilde{\mathbf{c}}_i$$

such that $\|\mathbf{e}(t)\| \to 0$ as $t \to \infty$. Our design is to determine the feedback gains $\mathbf{F}_i$ and $\mathbf{P}_i$.

By substituting **U**(t) into Eq.(7.31), we obtain:

$$\dot{\mathbf{e}}(t) = \sum_{i=1}^{2} \mathbf{\Psi}_i \{(\mathbf{A}_i - \mathbf{B}F_i)\mathbf{X}(t)\} - \sum_{i=1}^{2} \mathbf{\Gamma}_i \{(\mathbf{C}_i - \mathbf{B}P_i)\mathbf{Y}(t)\} \tag{7.33}$$

Theorem 1: The error system in Eq. (7.33) is asymptotically stable and the slave system in Eq. (7.30) can synchronize the master system in Eq. (7.29) under the fuzzy controller in Eq. (32) if the following conditions below can be satisfied:

$$\mathbf{G} = (\mathbf{A}_1 - \mathbf{B}\mathbf{F}_1) = (\mathbf{A}_i - \mathbf{B}\mathbf{F}_i) = (\mathbf{C}_i - \mathbf{B}\mathbf{P}_i) < 0, \ i=1\sim2. \tag{7.34}$$

Proof:

The errors in Eq. (7.33) can be exactly linearized via the fuzzy controllers in Eq. (7.32) if there exist the feedback gains F_i such that

$$(\mathbf{A}_1 - \mathbf{B}\mathbf{F}_1) = (\mathbf{A}_2 - \mathbf{B}\mathbf{F}_2) = (\mathbf{C}_1 - \mathbf{B}\mathbf{P}_1) = (\mathbf{C}_2 - \mathbf{B}\mathbf{P}_2) < 0. \tag{7.35}$$

Then the overall control system is linearized as

$$\dot{\mathbf{e}}(t) = \mathbf{G}\mathbf{e}(t), \tag{7.36}$$

where $\mathbf{G} = (\mathbf{A}_1 - \mathbf{B}\mathbf{F}_1) = (\mathbf{A}_2 - \mathbf{B}\mathbf{F}_2) = (\mathbf{C}_1 - \mathbf{B}\mathbf{P}_1) = (\mathbf{C}_2 - \mathbf{B}\mathbf{P}_2) < 0$.

As a consequence, the zero solution of the error system Eq. (7.36) linearized via the fuzzy controller Eq. (7.32) is asymptotically stable.

7.5 Simulation Results

There are two examples in this Section to investigate the effectiveness and feasibility of our new fuzzy model.

Example 1: Synchronization of Identical Master and Slave GKv systems

The fuzzy GKv system in Eq. (7.16) is chosen as the master system and the fuzzy slave GKv system, with fuzzy controllers is as follows:

$$\dot{\mathbf{Y}}(t) = \sum_{i=1}^{2} \mathbf{\Gamma}_i (\mathbf{C}_i \mathbf{Y}(t) + \tilde{\mathbf{c}}_i) + \mathbf{B}\mathbf{U}(t) \tag{7.37}$$

where $\mathbf{\Gamma}_i$ are diagonal matrices

$$dia(\mathbf{\Gamma}_1) = \begin{bmatrix} N_{11} & N_{21} & N_{31} \end{bmatrix}, \quad dia(\mathbf{\Gamma}_2) = \begin{bmatrix} N_{12} & N_{22} & N_{32} \end{bmatrix}$$

and

$$\mathbf{C}_1 = \begin{bmatrix} 0 & 1 & 0 \\ \alpha_1 & 0 & -\alpha_2\alpha_3 Z \\ \alpha_7 & \alpha_6(1-Z_3) & -\alpha_5 \end{bmatrix}, \quad \tilde{c}_1 = \begin{bmatrix} 0 \\ 0 \\ 0 \end{bmatrix}$$

$$\mathbf{C}_2 = \begin{bmatrix} 0 & 1 & 0 \\ \alpha_1 & 0 & -\alpha_2\alpha_3 Z \\ \alpha_7 & \alpha_6(1+Z_3) & -\alpha_5 \end{bmatrix}, \quad \tilde{c}_2 = \begin{bmatrix} 0 \\ 0 \\ 0 \end{bmatrix}.$$

Therefore, the error and error dynamics are:

$$\begin{bmatrix} e_1 \\ e_2 \\ e_3 \end{bmatrix} = \begin{bmatrix} x_1 - y_1 \\ x_2 - y_2 \\ x_3 - y_3 \end{bmatrix}, \tag{7.38}$$

$$\begin{bmatrix} \dot{e}_1 \\ \dot{e}_2 \\ \dot{e}_3 \end{bmatrix} = \begin{bmatrix} \dot{x}_1 - \dot{y}_1 \\ \dot{x}_2 - \dot{y}_2 \\ \dot{x}_3 - \dot{y}_3 \end{bmatrix} = \sum_{i=1}^{2} \mathbf{\Psi}_i (\mathbf{A}_i \mathbf{X}(t) + \tilde{\mathbf{b}}_i) - \sum_{i=1}^{2} \mathbf{\Gamma}_i (\mathbf{C}_i \mathbf{Y}(t) + \tilde{\mathbf{c}}_i) - \mathbf{B}\mathbf{U}(t) \tag{7.39}$$

B is chosen as an identity matrix and the fuzzy controllers in Eq. (7.32) are used:

$$\begin{bmatrix}\dot{e}_1\\ \dot{e}_2\\ \dot{e}_3\end{bmatrix}=\boldsymbol{\Psi}_1\left[\mathbf{A}_1-\mathbf{B}\mathbf{F}_1\right]_{3\times3}\begin{bmatrix}x_1\\ x_2\\ x_3\end{bmatrix}+\boldsymbol{\Psi}_2\left[\mathbf{A}_2-\mathbf{B}\mathbf{F}_2\right]_{3\times3}\begin{bmatrix}x_1\\ x_2\\ x_3\end{bmatrix}$$

$$-\boldsymbol{\Gamma}_1\left[\mathbf{C}_1-\mathbf{B}\mathbf{P}_1\right]_{3\times3}\begin{bmatrix}y_1\\ y_2\\ y_3\end{bmatrix}-\boldsymbol{\Gamma}_2\left[\mathbf{C}_2-\mathbf{B}\mathbf{P}_2\right]_{3\times3}\begin{bmatrix}y_1\\ y_2\\ y_3\end{bmatrix} \tag{7.40}$$

According to Eq. (7.34), we have $\mathbf{G}=\left[\mathbf{A}_1-\mathbf{B}\mathbf{F}_1\right]=\left[\mathbf{A}_2-\mathbf{B}\mathbf{F}_2\right]=\left[\mathbf{C}_1-\mathbf{B}\mathbf{P}_1\right]$ $=\left[\mathbf{C}_2-\mathbf{B}\mathbf{P}_2\right]<0$. $\mathbf{G}$ is chosen as:

$$\mathbf{G}=\begin{bmatrix}-1 & 0 & 0\\ 0 & -1 & 0\\ 0 & 0 & -1\end{bmatrix} \tag{7.41}$$

Thus, the feedback gains $\mathbf{F}_1$, $\mathbf{F}_2$, $\mathbf{P}_1$ and $\mathbf{P}_2$ can be determined by the following equation:

$$\mathbf{F}_1=\mathbf{B}^{-1}\left[\mathbf{A}_1-\mathbf{G}\right]=\begin{bmatrix}1 & 1 & 0\\ -0.08 & 1 & 3035.196\\ 0.01 & -1.36 & 0.39\end{bmatrix} \tag{7.42}$$

$$\mathbf{F}_2=\mathbf{B}^{-1}\left[\mathbf{A}_2-\mathbf{G}\right]=\begin{bmatrix}1 & 1 & 0\\ -0.08 & 1 & -2964.804\\ 0.01 & 1.52 & 0.39\end{bmatrix} \tag{7.43}$$

$$\mathbf{P}_1=\mathbf{B}^{-1}\left[\mathbf{C}_1-\mathbf{G}\right]=\begin{bmatrix}1 & 1 & 0\\ -0.08 & 1 & 3035.196\\ 0.01 & -1.36 & 0.39\end{bmatrix} \tag{7.44}$$

$$\mathbf{P}_2=\mathbf{B}^{-1}\left[\mathbf{C}_2-\mathbf{G}\right]=\begin{bmatrix}1 & 1 & 0\\ -0.08 & 1 & -2964.804\\ 0.01 & 1.52 & 0.39\end{bmatrix} \tag{7.45}$$

The synchronization errors are shown in Fig. 7.10.

Example 2: Synchronization of extended GKv system and GKM system.

The fuzzy extended GKv system in Eq. (7.16) is chosen as the master system and the fuzzy slave GKM system in Eq. (7.28), with fuzzy controllers is as follows:

$$\dot{\mathbf{Y}}(t)=\sum_{i=1}^{2}\mathbf{\Gamma}_i(\mathbf{C}_i\mathbf{Y}(t)+\tilde{\mathbf{c}}_i)+\mathbf{B}\mathbf{U}(t) \tag{7.46}$$

where $\mathbf{\Gamma}_i$ are diagonal matrices

$$dia(\mathbf{\Gamma}_1)=\begin{bmatrix}N_{11} & N_{21} & N_{31}\end{bmatrix},\ dia(\mathbf{\Gamma}_2)=\begin{bmatrix}N_{12} & N_{22} & N_{32}\end{bmatrix}$$

Therefore, the error and error dynamics are:

$$\begin{bmatrix}e_1\\e_2\\e_3\end{bmatrix}=\begin{bmatrix}x_1-y_1\\x_2-y_2\\x_3-y_3\end{bmatrix}, \tag{7.47}$$

$$\begin{bmatrix}\dot{e}_1\\\dot{e}_2\\\dot{e}_3\end{bmatrix}=\begin{bmatrix}\dot{x}_1-\dot{y}_1\\\dot{x}_2-\dot{y}_2\\\dot{x}_3-\dot{y}_3\end{bmatrix}=\sum_{i=1}^{2}\mathbf{\Psi}_i(\mathbf{A}_i\mathbf{X}(t)+\tilde{\mathbf{b}}_i)-\sum_{i=1}^{2}\mathbf{\Gamma}_i(\mathbf{C}_i\mathbf{Y}(t)+\tilde{\mathbf{c}}_i)-\mathbf{B}\mathbf{U}(t) \tag{7.48}$$

B is chosen as an identity matrix and the fuzzy controllers in Eq. (7.32) are used:

$$\begin{bmatrix}\dot{e}_1\\\dot{e}_2\\\dot{e}_3\end{bmatrix}=\mathbf{\Psi}_1\left[\mathbf{A}_1-\mathbf{B}\mathbf{F}_1\right]_{3\times3}\begin{bmatrix}x_1\\x_2\\x_3\end{bmatrix}+\mathbf{\Psi}_2\left[\mathbf{A}_2-\mathbf{B}\mathbf{F}_2\right]_{3\times3}\begin{bmatrix}x_1\\x_2\\x_3\end{bmatrix}$$

$$-\mathbf{\Gamma}_1\left[\mathbf{C}_1-\mathbf{B}\mathbf{P}_1\right]_{3\times3}\begin{bmatrix}y_1\\y_2\\y_3\end{bmatrix}-\mathbf{\Gamma}_2\left[\mathbf{C}_2-\mathbf{B}\mathbf{P}_2\right]_{3\times3}\begin{bmatrix}y_1\\y_2\\y_3\end{bmatrix} \tag{7.49}$$

According to Eq. (7.34), we have $\mathbf{G}=\left[\mathbf{A}_1-\mathbf{B}\mathbf{F}_1\right]=\left[\mathbf{A}_2-\mathbf{B}\mathbf{F}_2\right]=\left[\mathbf{C}_1-\mathbf{B}\mathbf{P}_1\right]$ $=\left[\mathbf{C}_2-\mathbf{B}\mathbf{P}_2\right]<0$. G is chosen as:

$$\mathbf{G}=\begin{bmatrix}-1 & 0 & 0\\0 & -1 & 0\\0 & 0 & -1\end{bmatrix} \tag{7.50}$$

Thus, the feedback gains $\mathbf{F}_1$, $\mathbf{F}_2$, $\mathbf{P}_1$ and $\mathbf{P}_2$ can be determined by the following equation:

$$F_1 = B^{-1}\left[A_1 - G\right] = \begin{bmatrix} 1 & 1 & 0 \\ -0.08 & 1 & 4035.196 \\ 0.01 & -0.88 & 0.39 \end{bmatrix} \tag{7.51}$$

$$F_2 = B^{-1}\left[A_2 - G\right] = \begin{bmatrix} 1 & 1 & 0 \\ -0.08 & 1 & -3964.804 \\ 0.01 & 1.04 & 0.39 \end{bmatrix} \tag{7.52}$$

$$P_1 = B^{-1}\left[C_1 - G\right] = \begin{bmatrix} 1 & 1 & 0 \\ 5 & 1.6 & 0 \\ 300 & 0.5 & -0.8 \end{bmatrix} \tag{7.53}$$

$$P_2 = B^{-1}\left[C_2 - G\right] = \begin{bmatrix} 1 & 1 & 0 \\ -115 & 1.6 & 0 \\ -300 & 0.5 & -0.8 \end{bmatrix} \tag{7.54}$$

The synchronization errors are shown in Fig. 7.11.

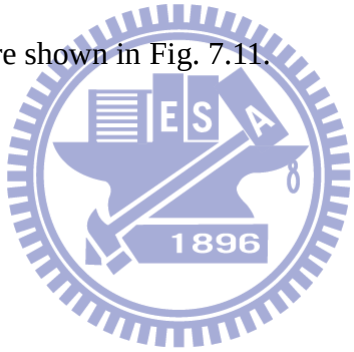

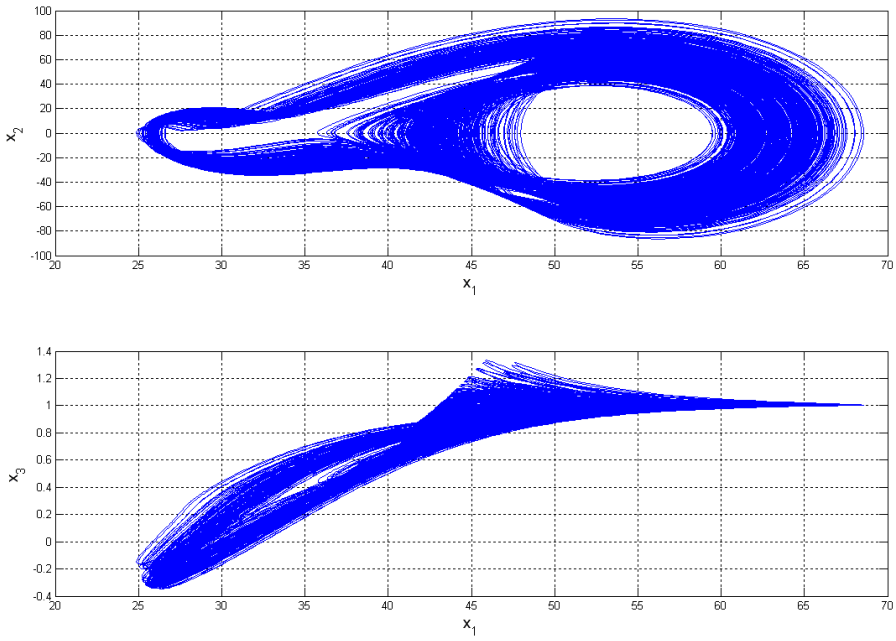

Fig. 7.1 Chaotic behavior of GKv system.

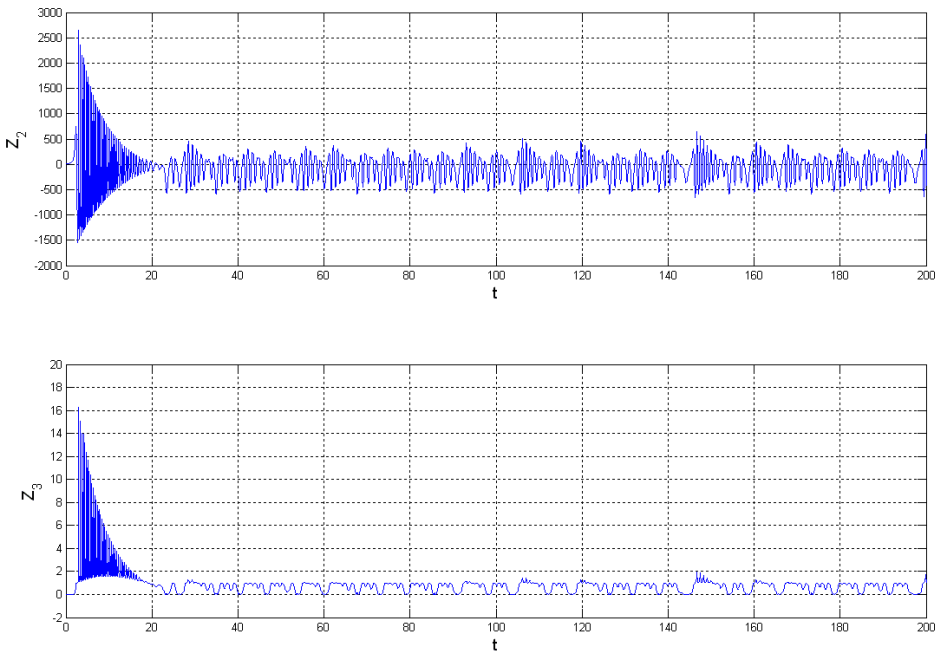

Fig. 7.2 Time histories of Z_2, Z_3 for GKv system.

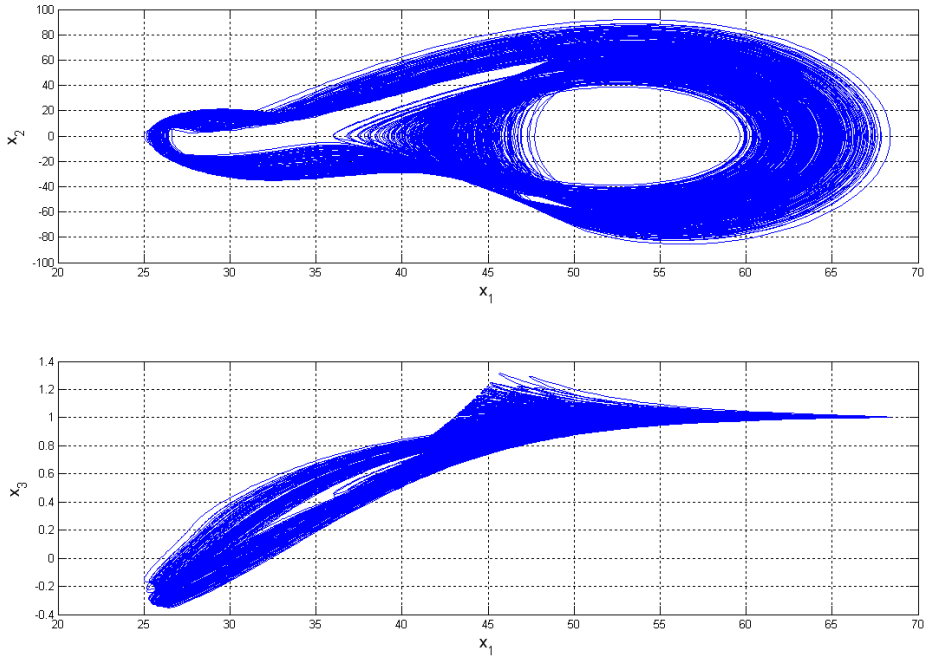

Fig. 7.3 Chaotic behavior of newfangled fuzzy GKv system.

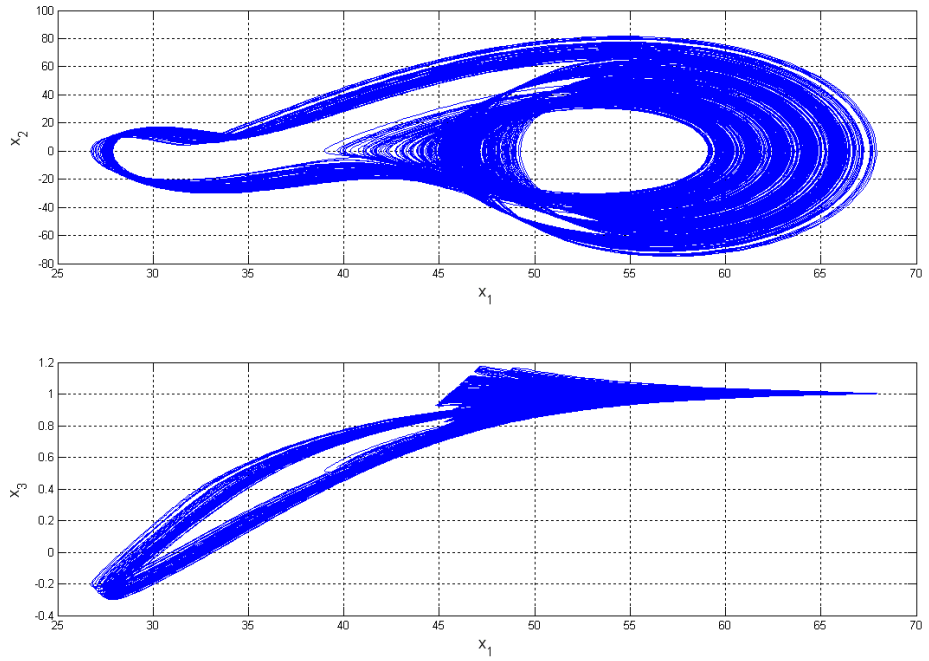

Fig. 7.4 Chaotic behavior of extended GKv system.

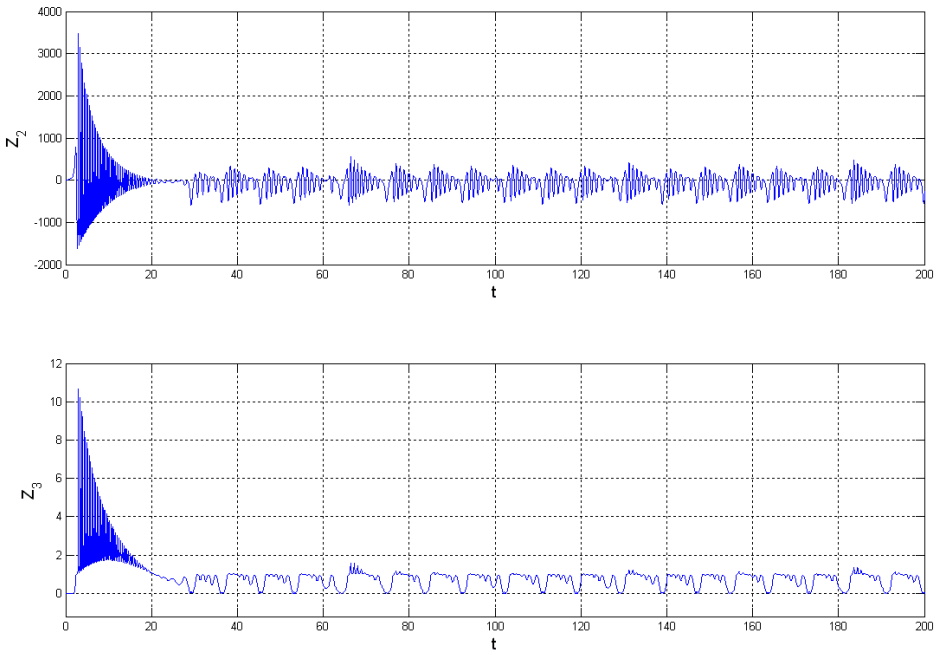

Fig. 7.5 Time histories of Z_2, Z_3 for extended GKv system.

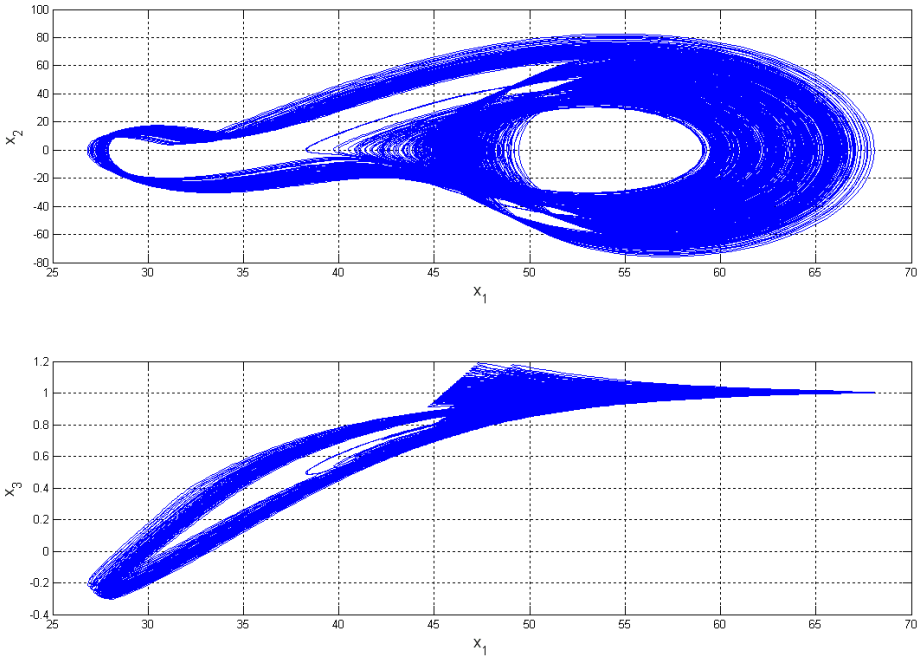

Fig. 7.6 Chaotic behavior of newfangled fuzzy extended GKv system system.

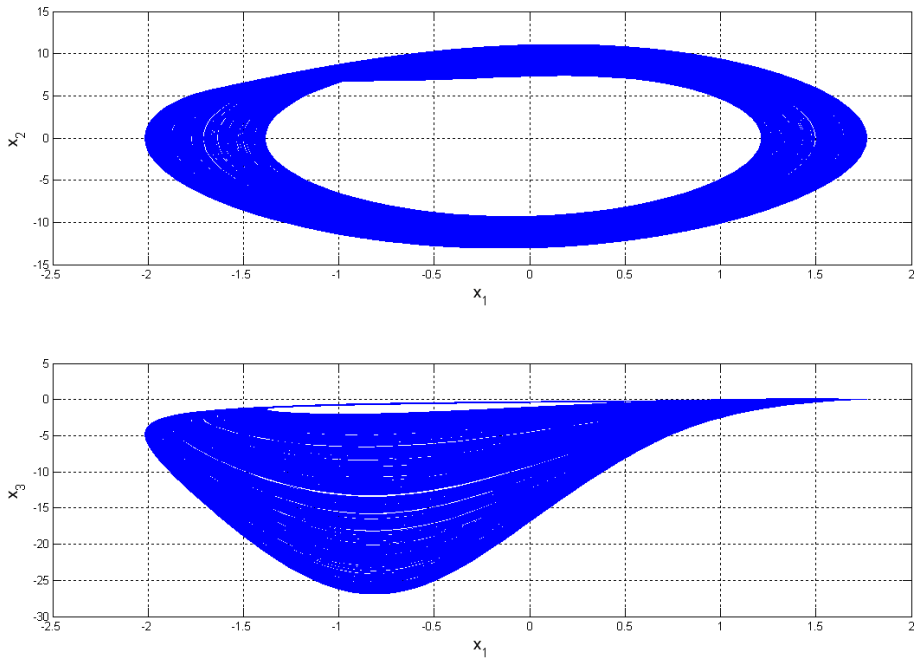

Fig. 7.7 Chaotic behavior of GKM system.

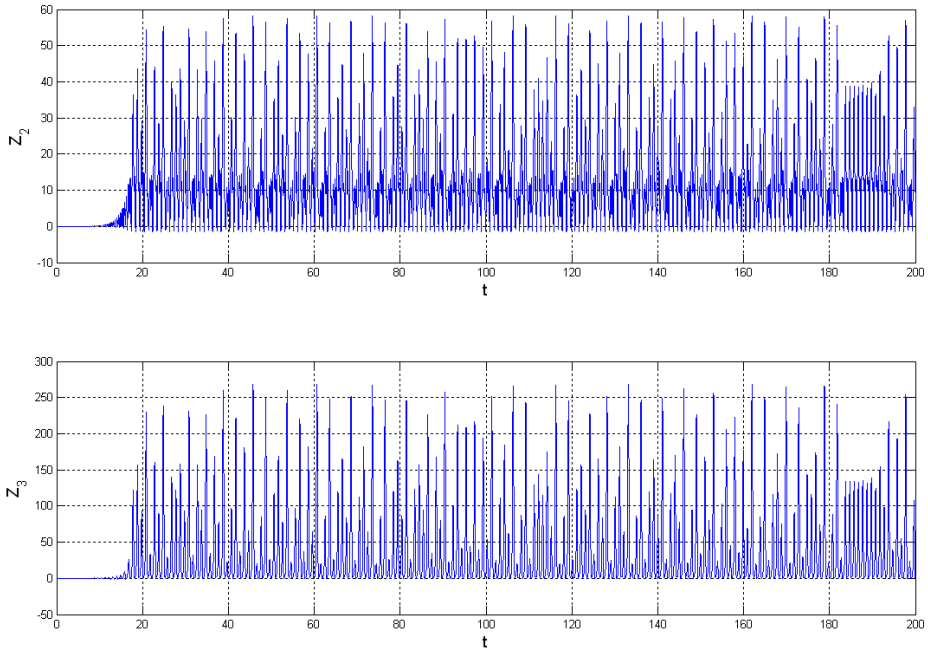

Fig. 7.8 Time histories of Z_2, Z_3 for GKM system.

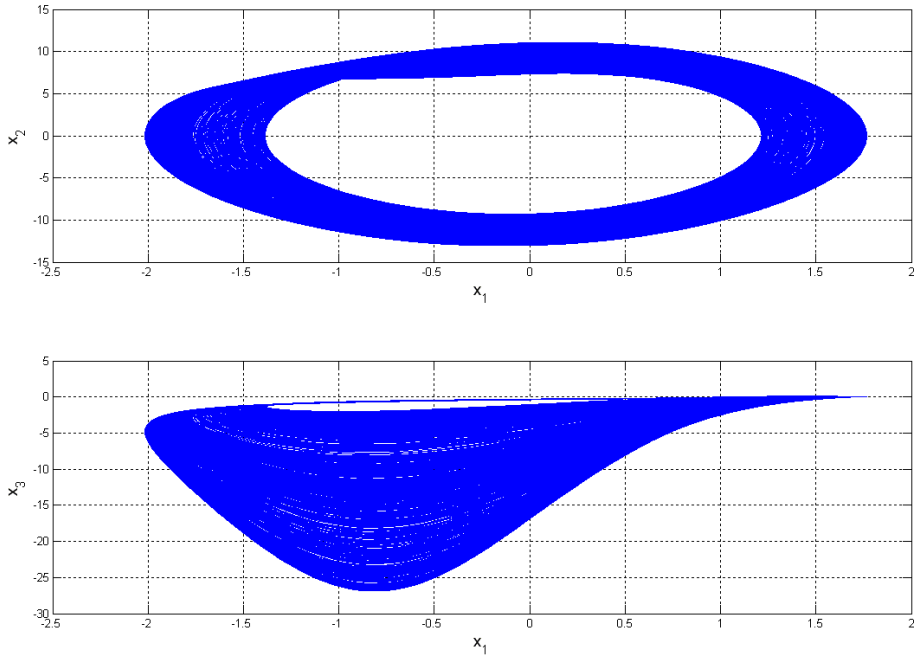

Fig. 7.9 Chaotic behavior of newfangled fuzzy GKM system.

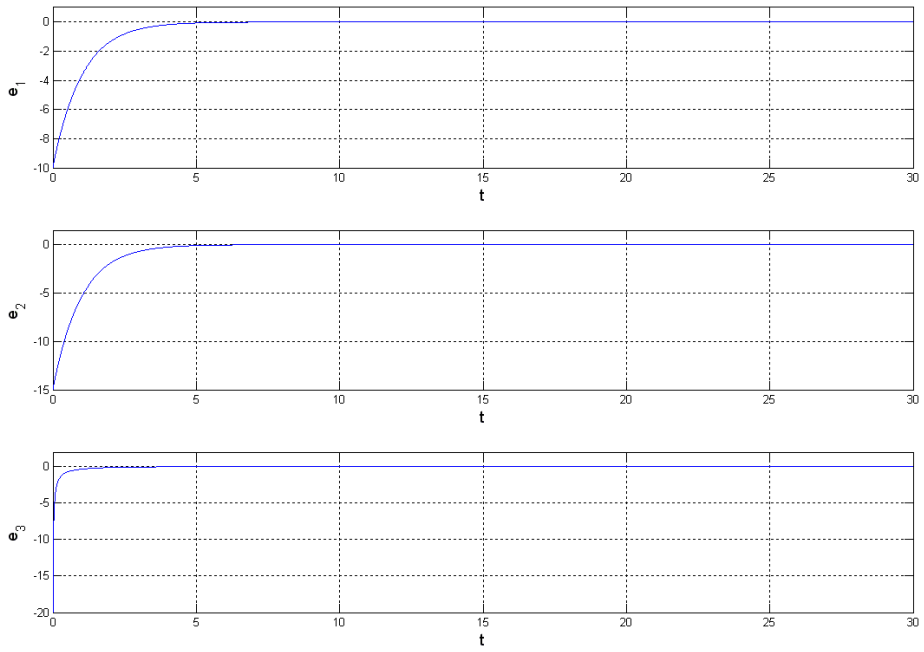

Fig. 7.10 Time histories of errors for Example 1.

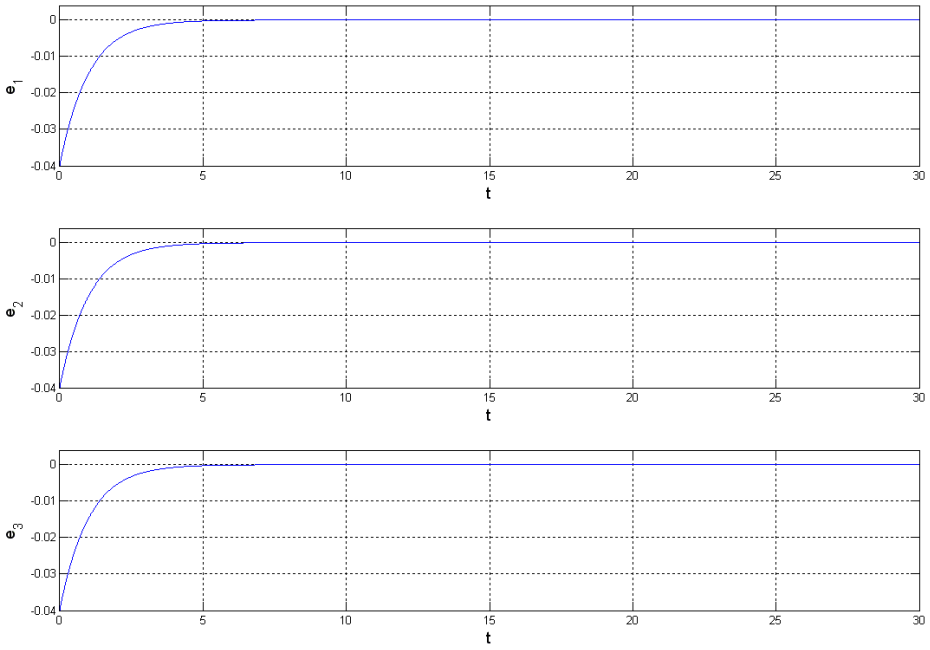

Fig. 7.11 Time histories of errors for Example 2.

Chapter 8

Conclusions

In this thesis, the chaotic behavior in new Ge-Ku-van der Pol system is studied by phase portraits, time history, Poincaré maps, Lyapunov exponent and bifurcation diagrams.

In Chapter 3, a new double symplectic synchronization of a GKv system is studied. The double symplectic synchronization is obtained by applying active control. The generalized synchronization and symplectic synchronization are special cases for the double symplectic synchronization. Two different chaotic dynamical systems, of which one is a new GKv system are in double symplectic synchronization for three cases. The Partner A are a new GKD nonlinear system, a new DGK nonlinear system and a new GKM nonlinear system respectively. The simulation results show that the proposed scheme is effective and feasible for all chaotic systems. Double symplectic synchronization of chaotic systems can be used to increase the security of secret communication.

Synchronization of real systems (expressed in real variables) has been widely explored in several problems involving physical chemical and ecological systems, human heartbeat regulation and secure communications. Yet synchronization of complex state system is firstly studied. In Chapter 4, we converted a real variable system to a complex variable system. A second-order of Ge-Ku real variable system coupled with different first-order complex state equation of complex conjugate form, and the results obtained present distinct chaotic behaviors.

Finally, synchronizations of three different chaotic systems are studied by pragmatical adaptive control method. The pragmatical asymptotical stability theorem fills the vacancy between the actual asymptotical stability and mathematical

asymptotical stability. For traditional adaptive control of chaotic motion, the Babalat's lemma is used to prove the error vector approaches zero, as time approaches infinity. But the question, why the estimated parameters also approach to the uncertain parameters, remains no answer. By the pragmatical theorem of asymptotical stability can be proved strictly that the common zero solution of error dynamics and of parameter dynamics is asymptotically stable. The conditions of the Lyapunov function for pragmatical asymptotical stability are lower than that for traditional asymptotical stability.

Our studies indicate that generalized synchronization by applying pragmatical active control is efficient and of wide applicability to synchronize chaotic system.

In Chapter 5, the different translation generalized synchronization chaotic of systems is studied by pragmatical synchronization and partial region stability theorem method. Using GYC partial region stability theorem, the Lyapunov function of pragmatical synchronization used is a simple linear homogeneous function of states and the lower order controllers are much more simple.

It is important to note that different translation k_1, k_2 are not arbitrary, two proper values must chosen to make that the error dynamics always in first quadrant, so give two more insurances are given for secret communication than other synchronization methods. This method enlarges the effective scope of chaos synchronization.

In Chapter 6, a simplest fuzzy controller (FLCC) is introduced to projective synchronization of non-autonomous chaotic systems with stochastic disturbance. Three main contributions can be concluded: (1) High performance of the convergence of error states in synchronization; (2) Good-robustness in projective synchronization of the chaotic systems with stochastic disturbance; (3) Simple constant controllers are used, which can be easily obtained.

Furthermore, due to the characters of FLCC, the mathematical models of studied systems can be even entirely unknown, all we have to do is to capture the output signals. Through the fuzzy logic rules, the strength of controllers can be adjusted via the corresponding membership functions, the well robustness and high performance in synchronization of these simplest controllers (FLCC) can be applied to various systems with various perturbations, such as neuroscience, un-model bio-systems, complicated brain network and so on.

In Chapter 7, a newfangled fuzzy model is proposed. A complicated nonlinear system can be linearized to a simple form. Most importantly, it can break the limitation of G-L fuzzy model.

Through the newfangled fuzzy model, there are two main contributions can be included: (1) all the complex nonlinear chaotic systems can be generated as two linear subsystems with their corresponding membership functions; (2) only two gain matrix are needed to synchronize the two totally different chaotic systems. The numbers of linear subsystems and gain matrix are hugely reduced and the simulation results show the great effectiveness and feasibility of our new model.

Appendix A

GYC Partial Region Stability Theory

A.1 Definition of the Stability on Partial Region

Consider the differential equations of disturbed motion of a nonautonomous system in the normal form

$$\frac{dx_s}{dt} = X_s(t, x_1, \cdots, x_n), \qquad (s = 1, \cdots, n) \tag{A.1}$$

where the function X_s is defined on the intersection of the partial region Ω (shown in Fig. A1) and

$$\sum_s x_s^2 \le H \tag{A.2}$$

and $t > t_0$, where t_0 and H are certain positive constants. X_s which vanishes when the variables x_s are all zero, is a real valued function of t, $x_1, \cdots, x_n$. It is assumed that X_s is smooth enough to ensure the existence, uniqueness of the solution of the initial value problem. When X_s does not contain t explicitly, the system is autonomous.

Obviously, $x_s = 0 \quad (s = 1, \cdots n)$ is a solution of Eq. (A.1). We are interested to the asymptotical stability of this zero solution on partial region Ω (including the boundary) of the neighborhood of the origin which in general may consist of several subregions (Fig. A1).

Definition 1:

For any given number $\varepsilon > 0$, if there exists a $\delta > 0$, such that on the closed given partial region Ω when

$$\sum_s x_{s0}^2 \le \delta, \quad (s = 1, \cdots, n) \tag{A.3}$$

for all $t \ge t_0$, the inequality

$$\sum_s x_s^2 < \varepsilon, \quad (s = 1, \cdots, n) \tag{A.4}$$

is satisfied for the solutions of Eq.(A.1) on Ω, then the disturbed motion $x_s = 0 \quad (s = 1, \cdots n)$ is stable on the partial region Ω.

Definition 2:

If the undisturbed motion is stable on the partial region Ω, and there exists a $\delta' > 0$, so that on the given partial region Ω when

$$\sum_s x_{s0}^2 \le \delta', \quad (s = 1, \cdots, n) \tag{A.5}$$

The equality

$$\lim_{t \to \infty} \left(\sum_s x_s^2 \right) = 0 \tag{A.6}$$

is satisfied for the solutions of Eq.(A.1) on Ω, then the undisturbed motion $x_s = 0 \quad (s = 1, \cdots n)$ is asymptotically stable on the partial region Ω.

The intersection of Ω and region defined by Eq.(A.5) is called the region of attraction.

Definition of Functions $V(t, x_1, \cdots, x_n)$:

Let us consider the functions $V(t, x_1, \cdots, x_n)$ given on the intersection Ω_1 of the partial region Ω and the region

$$\sum_s x_s^2 \le h, \quad (s = 1, \cdots, n) \tag{A.7}$$

for $t \ge t_0 > 0$, where t_0 and h are positive constants. We suppose that the functions are single-valued and have continuous partial derivatives and become zero when $x_1 = \cdots = x_n = 0$.

Definition 3:

If there exists $t_0 > 0$ and a sufficiently small $h > 0$, so that on partial region Ω_1 and $t \ge t_0$, $V \ge 0$ (or ≤ 0), then V is a positive (or negative) semidefinite, in general semidefinite, function on the Ω_1 and $t \ge t_0$.

Definition 4:

If there exists a positive (negative) definitive function $W(x_1 \ldots x_n)$ on Ω_1, so that on the partial region Ω_1 and $t \geq t_0$

$$V - W \geq 0 \,(or - V - W \geq 0), \tag{A.8}$$

then $V(t, x_1, \ldots, x_n)$ is a positive definite function on the partial region Ω_1 and $t \geq t_0$.

Definition 5:

If $V(t, x_1, \ldots, x_n)$ is neither definite nor semidefinite on Ω_1 and $t \geq t_0$, then $V(t, x_1, \ldots, x_n)$ is an indefinite function on partial region Ω_1 and $t \geq t_0$. That is, for any small $h > 0$ and any large $t_0 > 0$, $V(t, x_1, \ldots, x_n)$ can take either positive or negative value on the partial region Ω_1 and $t \geq t_0$.

Definition 6: Bounded function V

If there exist $t_0 > 0$, $h > 0$, so that on the partial region Ω_1, we have

$$|V(t, x_1, \ldots, x_n)| < L$$

where L is a positive constant, then V is said to be bounded on Ω_1.

Definition 7: Function with infinitesimal upper bound

If V is bounded, and for any $\lambda > 0$, there exists $\mu > 0$, so that on Ω_1 when $\sum_s x_s^2 \leq \mu$, and $t \geq t_0$, we have

$$|V(t, x_1, \ldots, x_n)| \leq \lambda$$

then V admits an infinitesimal upper bound on Ω_1.

A.2 GYC Theorem of Stability and of Asymptotical Stability on Partial Region

Theorem 1

If there can be found a definite function $V(t, x_1, \ldots, x_n)$ on the partial region for Eq. (A.1), and the derivative with respect to time based on these equations are:

$$\frac{dV}{dt} = \frac{\partial V}{\partial t} + \sum_{s=1}^{n} \frac{\partial V}{\partial x_s} X_s \tag{A.9}$$

Then, it is a semidefinite function on the paritial region whose sense is opposite to that of V, or if it becomes zero identically, then the undisturbed motion is stable on the partial region.

Proof:

Let us assume for the sake of definiteness that *V* is a positive definite function. Consequently, there exists a sufficiently large number t_0 and a sufficiently small number $h < H$, such that on the intersection Ω_1 of partial region Ω and

$$\sum_s x_s^2 \le h, \quad (s = 1, \ldots, n)$$

and $t \ge t_0$, the following inequality is satisfied

$$V(t, x_1, \ldots, x_n) \ge W(x_1, \ldots, x_n),$$

where *W* is a certain positive definite function which does not depend on *t*. Besides that, Eq. (A.9) may assume only negative or zero value in this region.

Let ε be an arbitrarily small positive number. We shall suppose that in any case $\varepsilon < h$. Let us consider the aggregation of all possible values of the quantities $x_1, \ldots, x_n$, which are on the intersection ω_2 of Ω_1 and

$$\sum_s x_s^2 = \varepsilon, \tag{A.10}$$

and let us designate by $l > 0$ the precise lower limit of the function W under this condition. By virtue of Eq. (A.8), we shall have

$$V(t, x_1, \ldots, x_n) \ge l \quad \text{for} \quad (x_1, \ldots, x_n) \quad \text{on} \quad \omega_2. \tag{A.11}$$

We shall now consider the quantities x_s as functions of time which satisfy the differential equations of disturbed motion. We shall assume that the initial values x_{s0} of these functions for $t = t_0$ lie on the intersection Ω_2 of Ω_1 and the region

$$\sum_s x_s^2 \le \delta, \tag{A.12}$$

where δ is so small that

$$V(t_0, x_{10}, \ldots, x_{n0}) < l \tag{A.13}$$

By virtue of the fact that $V(t_0, 0, \ldots, 0) = 0$, such a selection of the number δ is obviously possible. We shall suppose that in any case the number δ is smaller than ε.Then the inequality

$$\sum_s x_s^2 < \varepsilon, \tag{A.14}$$

being satisfied at the initial instant will be satisfied, in the very least, for a sufficiently small $t - t_0$, since the functions $x_s(t)$ very continuously with time. We shall show that these inequalities will be satisfied for all values $t > t_0$. Indeed, if these inequalities were not satisfied at some time, there would have to exist such an instant $t=T$ for which this inequality would become an equality. In other words, we would have

$$\sum_s x_s^2(T) = \varepsilon,$$

and consequently, on the basis of Eq. (A.11)

$$V(T, x_1(T), \ldots, x_n(T)) \ge l \tag{A.15}$$

On the other hand, since $\varepsilon < h$, the inequality (Eq.(A.7)) is satisfied in the entire interval of time [t_0, T], and consequently, in this entire time interval $\frac{dV}{dt} \le 0$. This yields

$$V(T, x_1(T), \ldots, x_n(T)) \le V(t_0, x_{10}, \ldots, x_{n0}),$$

which contradicts Eq. (A.14) on the basis of Eq. (A.13). Thus, the inequality (Eq.(A.4)) must be satisfied for all values of $t > t_0$, hence follows that the motion is stable.

Finally, we must point out that from the view-point of mathenatics, the stability

on partial region in general does not be related logically to the stability on whole region. If an undisturbed solution is stable on a partial region, it may be either stable or unstable on the whole region and vice versa. In specific practical problems, we do not study the solution starting within Ω_2 and running out of Ω.

Theorem 2

If in satisfying the conditions of Theorem 1, the derivative $\frac{dV}{dt}$ is a definite function on the partial region with opposite sign to that of V and the function V itself permits an infinitesimal upper limit, then the undisturbed motion is asymptotically stable on the partial region.

Proof:

Let us suppose that V is a positive definite function on the partial region and that consequently, $\frac{dV}{dt}$ is negative definite. Thus on the intersection Ω_1 of Ω and the region defined by Eq. (A.7) and $t \geq t_0$ there will be satisfied not only the inequality (Eq.(A.8)), but the following inequality as well:

$$\frac{dV}{dt} \leq -W_1(x_1, \ldots x_n), \tag{A.16}$$

where W_1 is a positive definite function on the partial region independent of t.

Let us consider the quantities x_s as functions of time which satisfy the differential equations of disturbed motion assuming that the initial values $x_{s0} = x_s(t_0)$ of these quantities satisfy the inequalities Eq. (A.12). Since the undisturbed motion is stable in any case, the magnitude δ may be selected so small that for all values of $t \geq t_0$ the quantities x_s remain within Ω_1. Then, on the basis of Eq. (A.16) the derivative of function $V(t, x_1(t), \ldots, x_n(t))$ will be negative at all times and, consequently, this function will approach a certain limit, as *t* increases without limit, remaining larger than this limit at all times. We shall show that this limit is equal to some positive quantity different from zero. Then for all values of $t \geq t_0$ the following

inequality will be satisfied:

$$V(t, x_1(t), \ldots, x_n(t)) > \alpha \tag{A.17}$$

where $\alpha > 0$.

Since V permits an infinitesimal upper limit, it follows from this inequality that

$$\sum_s x_s^2(t) \geq \lambda, \quad (s = 1, \ldots, n), \tag{A.18}$$

where λ is a certain sufficiently small positive number. Indeed, if such a number λ did not exist, that is , if the quantity $\sum_s x_s(t)$ were smaller than any preassigned number no matter how small, then the magnitude $V(t, x_1(t), \ldots, x_n(t))$, as follows from the definition of an infinitesimal upper limit, would also be arbitrarily small, which contradicts Eq. (A.17).

If for all values of $t \geq t_0$ the inequality Eq. (A.18) is satisfied, then Eq. (A.16) shows that the following inequality will be satisfied at all times:

$$\frac{dV}{dt} \leq -l_1,$$

where l_1 is positive number different from zero which constitutes the precise lower limit of the function $W_1(t, x_1(t), \ldots, x_n(t))$ under condition Eq. (A.18). Consequently, for all values of $t \geq t_0$ we shall have:

$$V(t, x_1(t), \ldots, x_n(t)) = V(t_0, x_{10}, \ldots, x_{n0}) + \int_{t_0}^{t} \frac{dV}{dt} dt \leq V(t_0, x_{10}, \ldots, x_{n0}) - l_1(t - t_0),$$

which is, obviously, in contradiction with Eq.(A.17). The contradiction thus obtained shows that the function $V(t, x_1(t), \ldots, x_n(t))$ approached zero as t increase without limit. Consequently, the same will be true for the function $W(x_1(t), \ldots, x_n(t))$ as well, from which it follows directly that

$$\lim_{t \to \infty} x_s(t) = 0, \quad (s = 1, \ldots, n),$$

which proves the theorem.

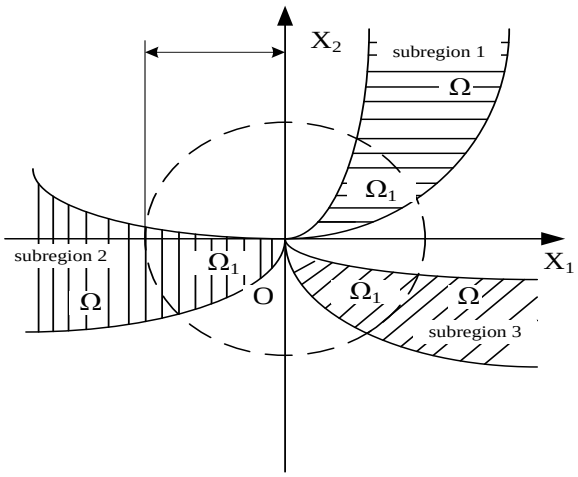

Fig. A.1. Partial regions Ω and Ω_1

Appendix B

Pragmatical Asymptotical Stability Theory

The stability for many problems in real dynamical systems is actual asymptotical stability, although may not be mathematical asymptotical stability. The mathematical asymptotical stability demands that trajectories from all initial states in the neighborhood of zero solution must approach the origin as $t \to \infty$. If there are only a small part or even a few of the initial states from which the trajectories do not approach the origin as $t \to \infty$, the zero solution is not mathematically asymptotically stable. However, when the probability of occurrence of an event is zero, it means the event does not occur actually. If the probability of occurrence of the event that the trajectries from the initial states are that they do not approach zero when $t \to \infty$, is zero, the stability of zero solution is actual asymptotical stability though it is not mathematical asymptotical stability. In order to analyze the asymptotical stability of the equilibrium point of such systems, the pragmatical asymptotical stability theorem is used.

Let X and Y be two manifolds of dimensions m and n (m<n), respectively, and φ be a differentiable map from X to Y, then $\varphi(X)$ is subset of Lebesque measure 0 of Y [61]. For an autonomous system

$$\frac{dx}{dt} = f(x_1, \cdots, x_n) \tag{B-1}$$

where $x = [x_1, \cdots, x_n]^T$ is a state vector, the function $f = [f_1, \cdots, f_n]^T$ is defined on $D \subset R^n$ and $\|x\| \le H > 0$. Let x=0 be an equilibrium point for the system (B-1). Then

$$f(0) = 0 \tag{B-2}$$

For a nonautonomous systems,

$$\dot{x} = f(x_1, ..., x_{n+1}) \tag{B-3}$$

where $x = [x_1, ..., x_{n+1}]^T$, the function $f = [f_1, ..., f_n]^T$ is define on $D \subset R^n \times R_+$,here $t = x_{n+1} \subset R_+$. The equilibrium point is

$$f(0 x_{n+1} \ni \quad . \tag{B-4}$$

Definition The equilibrium point for the system (B-1) is pragmatically asymptotically stable provided that with initial points on C which is a subset of Lebesque measure 0 of D, the behaviors of the corresponding trajectories cannot be determined, while with initial points on D－C, the corresponding trajectories behave as that agree with traditional asymptotical stability [38,39].

Theorem Let $V = [x_1, \cdots, x_n]^T$: D→R_+ be positive definite and analytic on D, where $x_1, x_2, ..., x_n$ are all space coordinates such that the derivative of V through Eq. (A-1)or(A-3), $\dot{V}$, is negative semi-definite of $[x_1, x_2, \cdots, x_n]^T$.

For autonomous system, Let X be the m-manifold consisted of point set for which $\forall x \neq 0$, $\dot{V}(x) = 0$ and D is a n-manifold. If m+1<n, then the equilibrium point of the system is pragmatically asymptotically stable.

For nonautonomous system, let X be the $m+1$-manifold consisting of point set of which $\forall x \neq 0, \dot{V}(x_1, x_2, ..., x_n) = 0$ and D is $n+1$-manifold. If $m+1+1 < n+1$, i.e. $m+1 < n$ then the equilibrium point of the system is pragmatically asymptotically stable. Therefore, for both autonomous and nonautonomous system the formula $m+1 < n$ is universal. So the following proof is only for autonomous system. The proof for nonautonomous system is similar.

Proof Since every point of X can be passed by a trajectory of Eq. (B-1), which is one- dimensional, the collection of these trajectories, A, is a (m+1)-manifold [38, 39].

If m+1＜n, then the collection C is a subset of Lebesque measure 0 of D. By the above definition, the equilibrium point of the system is pragmatically asymptotically stable.

If an initial point is ergodicly chosen in D, the probability of that the initial point falls on the collection C is zero. Here, equal probability is assumed for every point chosen as an initial point in the neighborhood of the equilibrium point. Hence, the event that the initial point is chosen from collection C does not occur actually. Therefore, under the equal probability assumption, pragmatical asymptotical stability becomes actual asymptotical stability. When the initial point falls on $D-C$, $\dot{V}(x)<0$, the corresponding trajectories behave as that agree with traditional asymptotical stability because by the existence and uniqueness of the solution of initial-value problem, these trajectories never meet C.

In Eq. (B-2-7) V is a positive definite function of n variables, i.e. p error state variables and n-p=m differences between unknown and estimated parameters, while $\dot{V}=e^{T}Ce$ is a negative semi-definite function of n variables. Since the number of error state variables is always more than one, p>1, m+1<n is always satisfied, by pragmatical asymptotical stability theorem we have

$$\lim_{t\to\infty} e=0 \qquad \text{(B-5)}$$

and the estimated parameters approach the uncertain parameters. The pragmatical adaptive control theorem is obtained. Therefore, the equilibrium point of the system is pragmatically asymptotically stable. Under the equal probability assumption, it is actually asymptotically stable for both error state variables and parameter variables.

References

[1] L.-M. Pecora and T.-L. Carroll, “Synchronization in chaotic systems”, Phys. Rev. Lett., 64(8) (1990) 821-824.

[2] N.-F. Rulkov, M.-M. Sushchik, L.-S. Tsimring and H.-D.-I. Abarbanel, “Generalized synchronization of chaos in directionally coupled chaotic systems”, Phys. Rev. E, 51 (1995) 980.

[3] G.-H. Li, “Generalized projective synchronization of two chaotic system by using active control”, Chaos, Solitons &Fractals, 30 (2006) 77-82.

[4] G.-H. Li, S.-P. Zhou and K. Yang, “Generalized projective synchronization between two different chaotic systems using active backstepping control”, Physics Letters A, 355 (2006) 326-330.

[5] M.-G. Rosenblum, A.-S. Pikovsky and J. Kurths, “Phase synchronization of chaotic oscillators”, Phys. Rev. Lett., 76 (1996) 1805.

[6] G.-H. Erjaee and S. Momani, “Phase synchronization in fractional differential chaotic systems”, Physics Letters A, 372 (2008) 2350-2354.

[7] C. Li, Q. Chen and T. Huang, “Coexistence of anti-phase and complete synchronization in coupled chen system via a single variable”, Chaos, Solitons & Fractals, 38 (2008) 461-464.

[8] M.-G. Rosenblum, A.-S. Pikovsky and J. Kurths, “From phase to lag synchronization in coupled chaotic oscillators”, Phys. Rev. Lett., 78 (1997) 4193.

[9] Y. Chen, X. Chen and S. Gu, “Lag synchronization of structurally nonequivalent chaotic systems with time delays”, Nonliner Analysis: Theory Methods & Applications, 66 (2007) 1929-1937.

[10] Z.-M. Ge and G.-H. Lin, “The complete, lag and anticipated synchronization of a BLDCM chaotic system”, Chaos, Solitons & Fractals, 34 (2007) 740-764.

[11] S.-M. Chang, M.-C. Li and W.-W. Lin, “Asymptotic synchronization of modified logistic hyper-chaotic systems and its applications”, Nonlinear Analysis: Real World Applications, 10 (2009) 869-880.

[12] G.-H. Li, “Inverse lag synchronization in chaotic systems”, Chaos, Solitons & Fractals, 40 (2009) 1076-1080.

[13] C.-S. Chen and H.-H. Chen, “Robust adaptive neural-fuzzy-network control for the synchronization of uncertain chaotic systems”, Nonliner Amalysis: Real World Applications, 10 (2009) 1466-1479.

[14] X. Meng, J. Jiao and L. Chen, “ The dynamics of an age structured predator-prey model with disturbing pulse and time delays”, Nonliner Amalysis: Real World Applications, 9 (2008) 547-561.

[15] Q. Wang and Y. Chen, “Generalized Q-S (lag, anticipated and complete) synchronization in modified Chua’s circuit and Hindmarsh-Rosw system”, Applied Mathematics and Computation, 181 (2006) 48-56.

[16] M. Hu and Z. Xu, “A general scheme for Q-S synchronization of chaotic systems”, Nonlinear Amalysis: Theory Methods & Applications, 69 (2008) 1091-1099.

[17] Y. Yang and Y. Chen, “The generalized Q-S synchronization between the generalized Lorenz canonical form and the Rossler system”, Chaos, Solitons and Fractals, 39 (2009) 2378–2385.

[18] Y.-W. Wang, Z.-H. Guan and H.-O. Wang, “LMI-based fuzzy stability and synchronization of Chen’s system”, Physics Letter A, 320 (2003) 154-159.

[19] L. Guang and A. Khajepour, “Robust control of a hydraulically driven flexible arm using backstepping technique”, Journal of Sound and Vibration, 280 (2005) 759-779.

[20] R. Mainieri and J. Rehacek, “Projective synchronization in three-dimensional chaotic systems”, Phys. Rev. Lett., 82 (1999) 3042-3045.

[21] M. Hu, Z. Xu, “Adaptive feedback controller for projective synchronization”, Nonliner Amalysis: Real World Applications, 9 (2008) 1253-1260.

[22] H.-K. Chen, “Synchronization of two different chaotic systems: a new system and each of the dynamical systems Lorenz, Chen and Lü”, Chaos, Solitons & Fractals, 25 (2005) 1049-1056.

[23] N. Vasegh and F. Khellat, “Projective synchronization of chaotic time-delayed systems via sliding mode controller”, Chaos, Solitons and Fractals, 42 (2009) 1054–1061.

[24] Z.-M. Ge and F.-N. Ku, “Stability, bifurcation and chaos of a pendulum on a rotating arm”, Jpn. J. Appl. Phys. 36 (1997) 7052-7060.

[25] Z.-M. Ge and C.-H. Yang, “Symplectic synchronization of different chaotic systems”, Chaos, Solitons and Fractals, 40 (2009) 2532–2543.

[26] H.-K. Khalil, *Nonlinear Systems*, 3rd edition, Prentice Hall, New Jersey, 2002.

[27] G. Á lvarez, S. Li, F. Montoy, Pastor, G. and Romera, M., “Breaking projective chaos synchronization secure communication using filtering and generalized synchronization”, Chaos, Solitons & Fractals, 24 (2005) 775-783.

[28] Xiao, M. and Cao, J., “Synchronization of a chaotic electronic circuit system with cubic term via adaptive feedback control”, Communications in Nonlinear Science and Numerical Simulation, 14 (2009) 3379-3388.

[29] N.-F. Rulkov, M.-M. Sushchik, L.-S. Tsimring and H.-D.-I. Abarbanel, “Generalized synchronization of chaos in directionally coupled chaotic systems”, Phys. Rev. E, 51 (1995) 980-994.

[30] G.-M. Mahmoud, T. Bountis and E.-E. Mahmoud, “Active control and global synchronization of the complex Chen and Lu systems”, International Journal of Bifurcation and Chaos, 17 (2007) 4295-4308.

[31] G.-M. Mahmoud, S.-A. Aly and A.-A. Farghaly, “On chaos synchronization of a complex two coupled dynamos system”, Chaos, Solitons and Fractals, 33 (2007) 178-187.

[32] J.-H. Park, “Adaptive synchronization of hyperchaotic chen system with uncertain parameters”, Chaos, Solitons Fractals, 26 (2005) 959-964.

[33] J.-H. Park, “Adaptive synchronization of hyperchaotic chen system with uncertain parameters”, Chaos, Solitons Fractals, 26 (2005) 959.

[34] J.-H. Park, “Adaptive synchronization of Rossler system with uncertain parameters”, Chaos, Solitons Fractals, 25 (2005) 333-338.

[35] E.-M. Elabbasy, H.-N. Agiza and M.-M. El-Desoky, “Adaptive synchronization of a hyperchaotic system with uncertain parameter”, Chaos, Solitons Fractals, 30 (2006) 1133-1142.

[36] Wu, X., Guan, Z.-H., Wu, Z. and Li, T., “Chaos synchronization between Chen system and Genesio system”, Phys. Lett. A, 364 (2007) 484-487.

[37] M.-T. Yassen, “Adaptive control and synchronization of a modified Chua’s circuit system”, Applied Mathematics and Computation, 135 (2003) 113-128.

[38] Z.-M. Ge, J.-K. Yu and Y.-T. Chen, “Pragmatical asymptotical stability theorem with application to satellite system”, Jpn. J. Appl. Phys., 38 (1999) 6178-6179.

[39] Z.-M. Ge and J.-K. Yu, “Pragmatical asymptotical stability theorem on partial region and for partial variable with applications to gyroscopic systems”, Chin. J. Mech., 16 (2000) 179-187.

[40] Y. Matsushima, *Differentiable Manifolds*, Marcel Dekker, City, 1972.

[41] Z.-M. Ge and H.-K. Chen, “Three asymptotical stability theorems on partial region with applications”, Japanese Journal of Applied Physics, 37 (1998) 2762-2773.

[42] Z.-M. Ge and S.-Y. Li, “Chaos control of new Mathieu-van der Pol systems with new Mathieu-Duffing systems as functional system by GYC partial region stability theory”, Nonlinear Analysis: Theory, Methods & Applications, 71 (2009) 4047-4059.

[43] Z.-M. Ge and C.-M. Chang, “Chaos synchronization and parameters identification of single time scale brushless DC motors”, Chaos, Solitons Fractals, 20 (2004) 883-903.

[44] T.-H.-S. Li, C.-L. Kuo and G.-N. Ren, “Design of an EP-based fuzzy sliding-mode control for a magnetic ball suspension system”, Chaos, Solitons & Fractals, 33 (2007) 1523-1531.

[45] L. A. Zadeh, “Fuzzy logic”, IEEE Comput., 21 (1998) 83-93.
[46] H.-T. Yau and C.-S. Shieh, “Chaos synchronization using fuzzy logic controller”, Nonlinear Analysis: Real World Applications, 9 (2008) 1800-1810.
[47] T. Takagi and M. Sugeno, “Fuzzy identification of systems and its applications to modelling and control,” IEEE Trans. Syst., Man., Cybern., 15 (1985) 116-132.
[48] L. Luoh, “New stability analysis of T–S fuzzy system with robust approach”, Math Comput Simul, 59 (2002) 335-340.
[49] X.-J. Wu, X.-J. Zhu, G.-Y. Cao and H.-Y. Tu, “Dynamic modeling of SOFC based on a T–S fuzzy model”, Simul Model Prac Theory, 16 (2008) 494-504.
[50] X. Liu and S. Zhong, “T–S fuzzy model-based impulsive control of chaotic systems with exponential decay rate”, Phys Lett A, 370 (2007) 260-264.
[51] J.-H. Kim, C.-W. Park, E. Kim and M. Park, “Adaptive synchronization of T–S fuzzy chaotic systems with unknown parameters”, Chaos, Solitons & Fractals, 24, (2005) 1353-1361.
[52] B. Yoo and W. Ham, “Adaptive fuzzy sliding mode control of nonlinear system”, IEEE Trans. Fuzzy Syst., 6 (1998) 315 - 321.
[53] H.-X. Li and S. Tong, “A hybrid adaptive fuzzy control for a class of nonlinear MIMO systems”, IEEE Trans. Fuzzy Syst., 11 (2003) 24 -34.
[54] C.-L. Hwang, “A novel Takagi-Sugeno-based robust adaptive fuzzy sliding-mode controller”, IEEE Trans. Fuzzy Syst., 12 (2004) 676-687.
[55] J. Wang, X. Xiong, M. Zhao and Y. Zhang, “Fuzzy stability and synchronization of hyperchaos systems”, Chaos, Solitons & Fractals, 35 (2008) 922-930.
[56] Y.-W. Wang, Z.-H. Guan and H.-O. Wang, “LMI-based fuzzy stability and synchronization of Chen's system”, Phys Lett A, 320 (2003) 154-159.
[57] H. Zhang, X. Liao and J. Yu, “Fuzzy modeling and synchronization of hyperchaotic systems”, Chaos, Solitons & Fractals, 26 (2005) 835-843.
[58] S.-W. Kau, H.-J. Lee, C.-M. Yang, C. H. Lee, L. Hong and C. H. Fang, “Robust H∞ fuzzy static output feedback control of T-S fuzzy systems with parametric uncertainties”, Fuzzy Sets Syste, 158 (2007) 135-146.
[59] Z.-M. Ge and S.-Y. Li, “Fuzzy modeling and synchronization of chaotic two-cells quantum cellular neural networks nano system via a novel fuzzy model” accepted by Journal of Computational and Theoretical Nanoscience 2009.
[60] J.-C. Sprott, “Simple chaotic systems and circuits”, Am. J. Phys., 68 (2000) 758-763.
[61] M.-Y. Chen, Z.-Z. Han and Y. Shang, “General synchronization of Genesio–Tesi system”, Int J Bifurcat Chaos, 14 (2004) 347-354.